STF25 A91028

ACTIVE FIRE PROTECTION

Extinguishment of enclosed gas fires with water sprays

Ragnar Wighus

June 1991

Norwegian Fire Research Laboratory

SINTEF REPORT

The Foundation for Scientific and Industrial
Research at the Norwegian Institute of Technology

N-7034 Trondheim, Norway

Telephone: (+ 47 7) 59 30 00
Telex: 55 620 SINTF N
Telefax: (+ 47 7) 59 24 80

Report no. STF25 A91028

Classification Unrestricted

Title of report	Date
ACTIVE FIRE PROTECTION - Extinguishment of enclosed gas fires with water sprays	1991-06-28
	No. of pages/appendices 46 + 2
Author(s) Ragnar Wighus	Divisional responsibility (sign.)
Division Norwegian Fire Research Laboratory	Project no. 251038
ISBN no.	Price group

Client/sponsor of project	Clients' ref.
Norsk Hydro, Saga Petroleum, Statoil, NTNF	

Abstract

Experiments with water spray against enclosed gas fires has been performed in a 2.5 x 2.5 x 5 [m^3] model of an offshore process module. The scale is 1:4, the fire is 1 [MW] and the enclosure is naturally ventilated through openings at floor and ceiling level. Various nozzles producing droplets of mean diameters from 0.6-1.6 [mm] has been examined, and the critical water application rate is found to extinguish this propane fire. The experimental results are presented in a form of a Spray Heat Absorption Ratio, SHAR, which is a characterisic fraction of heat absorbed by a certain spray at a certain fire/enclosure configuration. A sharp limit for extinguishment is found for the experimental conditions, and a set of scaling criteria is proposed. The effect of a water spray on the mean temperature, heat fluxes, soot production rates and heat transfer to the different sectors of the fire environment is described.

	Indexing terms: English	Norwegian
Group 1	FIRE	BRANN
Group 2	GAS	GASS
Key terms selected by author(s)	EXTINGUISHMENT	SLOKKING
	WATER	VANN
	DROPLET SIZE	DRÅPESTØRRELSE

Kjell Schmidt Pedersen

CONTENTS:

1. INTRODUCTION

Water sprays are widely used for fire fighting in industrial areas, and is used for fire protection in the process industry and on offshore oil/gas production platforms. No real quantification of the effect of water sprays as a fire fighting medium exists. The water delivery is specified through standards and regulations, which are based on industrial experience. In process areas water spray is often used in deluge systems, intended to control fires until shut down. For this purpose there is a need for quantification of the ability of a certain spray system has to remove heat from the fire, and reduce the fire load to the constructions and process equipment.

The project "Active Fire Protection" has the scope to investigate the extinguishment and control effect of various water sprays against enclosed hydrocarbon fires. To make a relevant scenario, a scaled model of a module of an offshore production platform was used in a series of experiments. This scale model is formerly used in investigations of the development of enclosed liquid hydrocarbon fires, and it is instrumented to measure heat transfer, fire development and production of soot and gases from combustion /1,2,3/. The model was modified to withstand a water spray introduced in a fire, and was equipped with a propane burner instead of the liquid pool fire.

The extinguishment of liquid pool fires by various spray systems is studied by Valtion Teknillinen Tutkimuskeskus, VTT (Technical Research Centre of Finland), and a cooperation agreement has provided the basis for mutual exchange of results between VTT and SINTEF. The experiments done by VTT has the character of full scale extinguishment tests with different liquid fuels, with standard commercial available nozzles, in a relatively large building. The influence of reduced ventilation was not studied, and the pool fires was free burning. The two research projects are complementary, and valuable experience was gained by the Finnish tests before the SINTEF experiments were designed.

The analysis of the interaction between a water spray and a fire environment is based on heat balances of water, of air flowing through the model, and for the fire compartment. A characteristic fraction, the Spray Heat Absorbtion Ratio, characterizing the effect of a certain spray/compartment configuration is presented for various sprays with different mean droplet sizes.

The project is financed by the Norwegian oil companies Norsk Hydro a.s, Saga Petroleum a.s. and Statoil a.s., and by the Royal Norwegian Council for Scientific and

Industrial Research, (NTNF).

2. THEORETICAL BASIS

2.1. Heat balance of a fire room

A major part of the heat produced in an enclosed fire is convected and radiated to the walls,ceiling and floor, and another large part is convected to the ambient through ventilation. A smaller part is radiated through openings.

In the first minutes of a fire, the internal heat accumulated in the gases of the room increases, but after this initial growth period, this part levels out. The heat absorbed by the walls, ceiling and floor is in the beginning mostly accumulated , but will gradually be conducted through the boundaries to the ambient. Steady state occurs when the heat accumulation in the boundaries goes to zero.

A graphical view of the heat balance of a fire room is shown in Figure 1.

At the moment when water spray systems usually are activated, the heat balance is dominated by the transient parts of the fire development. The water enters the room as droplets, which are heated by the hot gases they entrain. Depending of the droplet size and the flow pattern of the droplet, it may evaporate before it hits a surface, be partly evaporated or survive as a droplet. When a droplet hits a surface, it may evaporate, or form a water film which is taking heat out of the surface, or run off the surface.

The amount of heat removed by the water is dominated by the amount of water which is evaporated. The proportion of heat neccecary to bring the water from the normal tap water temperature to the boiling point to the heat of evaporation is $\approx 1/6$.

$$\Delta H_{10\text{-}100^{\circ}C} = c_{pwater} \cdot \Delta T = 4.2 \cdot 90 = 378 \text{ [kJ/kg]} \quad (1)$$

$$\Delta H_{evap} = 2257 \text{ [kJ/kg]}$$

This means that the most effective way of taking heat out of a fire room, is to evaporate the water inside the room.

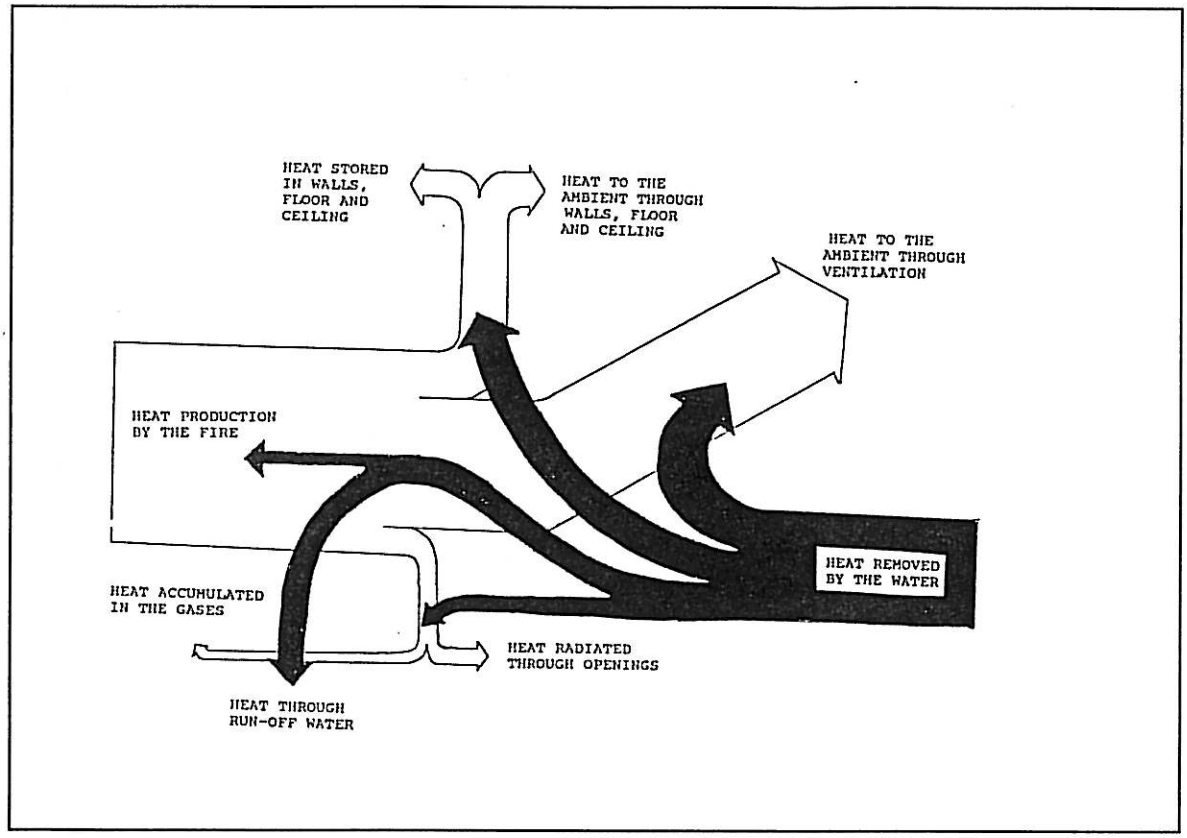

Figure 1. Heat balance of an enclosure with a fire, with water introduced for extinguishment and control.

The water may influence the heat transfer from the fire to the room and the surrounding in several ways. The water may reduce the temperature of the gases inside the room and in the effluent gases. This leads to less heat transfer to the walls, the ceiling and the floor and to objects hit by the smoke. Direct cooling of surfaces is obtained when water droplets hits them. The content of water droplets and vapour increases the absorptivity of the gases inside the fire room, and consequently this may lead to reduced radiation from the flames to surfaces.

2.2 Extinguishment of fire

The mechanisms of extinction of flames in a fire situation are several, and a successful fire fighting often depends on more than one mechanism. The main theories of extinction are grouped in four:

- Cooling of the flames to a temperature where the chemical reactions cannot be maintained.

- Reduction of oxygen concentration to a level where no combustion can be maintained.

- Speeding up flow velocity to a level where the residence time of fuel and oxygen in combustible mixture is shorter than the time scale of the chemical reactions.

- Adding components in the combustion zone which breaks the chain of chemical reactions by substitution with endothermal reactions.

The most probable mechanisms acting when water droplets are supplied in the combustion zone, is a combination of oxygen depletion by production of steam, and cooling by the evaporation of water.

In a complete mixed reactor, the critical concentration of steam for extinction appears to be $\approx$ 30 % on mole basis, /4/.

In a fire room, where the mixing is not as efficient as in a reactor, the critical mole fraction of steam which leads to extinction is assumed to be higher than 30 %, /4/.

2.3 Effect of water droplet size

The smaller the droplet diameter is, the faster it will evaporate in a hot gas environment. The residence time of a water droplet from the spray nozzle till it hits a surface or is blown out of the room, is the effective time where heat can be absorbed from the flames and the hot gases. Small droplets will evaporate in the upper part of the room, and most of the steam can follow the smoke through the exhaust opening.

The effect of evaporating water droplets will be cooling of the gases, which may

consequently lead to extincion of flames.

However, rapid evaporation of water leads to an increase of volume of the water by a factor of about 1000. This may block the air supply to the enclosure. Smoke and products from the combustion zone may be recirculated from the upper part of the enclosure. This may lead to oxygen starvation in the combustion zone, and consequently to extinction.

This transient process is very geometry dependent, and the location of the fire relative to the spray nozzle and the air supply- and outlet openings will dominate the result.

Large water droplets will survive in a hot environment, will have impact to penetrate a fire plume and will hit the fuel and the floor without being totally evaporated. The sprinkler technology utilizes this for the purpose of the cooling surfaces to prevent spread of flames. With untreated water against oil and gas fires, the profit of wetting the fuel is usually not great, except for cooling liquid pool fires to a temperature below the flash point of the liquid, /5/. The use of additives to the water to break down surface tension utilizes the wetting of liquid fuels, and the water film prevents evaporation of fuel.

The tests done by VTT in Finland examined water sprays without additives /5/. The test series of a total of 109 tests was done with 10 different liquid fuels with flash point ranging from -6 [°C] to 243 [°C]. The spray variables was obtained by 7 different nozzles, located at a distance above the fuel surface from in a range of 3 - 8 [m]. The pool size was varied from 0.4 [m^2] to 12 [m^2]. Most of the tests were done using a 1.6 [m^2] circular pool.

The main conclusions from the Finnish experiments was:

- In most cases the mechanism of extiguishment was cooling the fuel below flash point. Low flash point liquids could be extinguished only by blowing off the flame from the vicinity of the fuel surface.

- A critical flash point exists close to 60 [°C]. Liquids with higher flash point are conciderably easier to extinguish.

- Spray nozzles (high and medium velocity sprayers) did not perform better than sprinklers.

- A larger pool requires a bigger delivered water application rate.

- Delivered water application rate cannot be regarded as the only measure for dimensioning an extinguishing system. For example, a fuel with a flash point about 62 [°C] could be extinguished with a water application rate of 6.4 [l/(m^2 · min)] in one experiment, wheres in another experiment even 30 [l/(m^2 · min)] was not sufficient.

Investigations done by Underwriter's Laboratories Inc. in 1955 /6/, has shown that for small scale laboratory fires, a substantial difference in extinguishment effectiveness is found for water droplet sizes of 300 [μm]. Smaller droplets extinguished test fires with small amounts of water, as the required water discharge rates was much higher with larger droplets. This is shown in Figure 2.

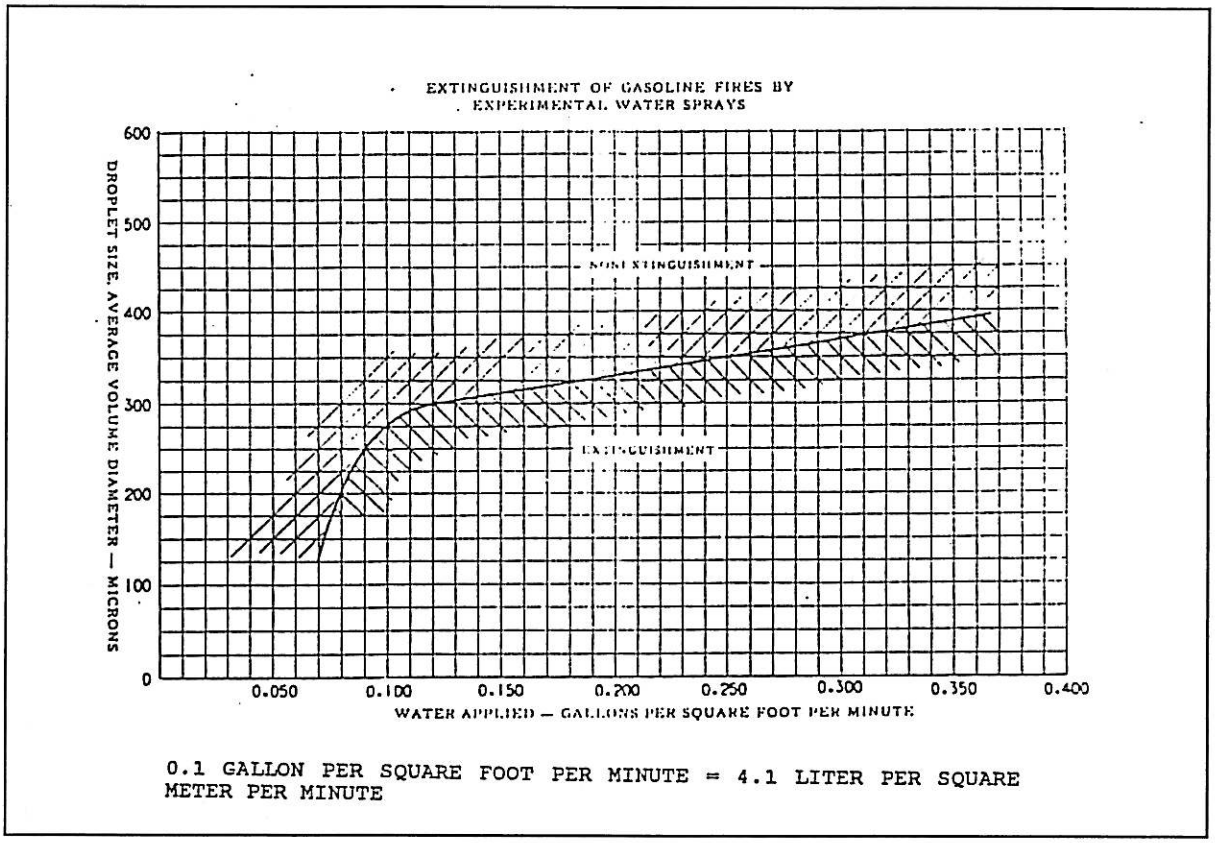

Figure 2 *Extinguishment of gasoline fires in a pool of 0.15 · 0.15 [m^2] water sprays /6/.*

Factory Mutual Research Corporation (FMRC) has done tests on hydrocarbon fires in enclosures, and extinction has been obtained with small droplets,/4/. An example of the results of various tests with Hexane fires (liquid pool fires) in a room with a single open window, is shown in Table 1.

Table 1 *Results of hexane fire extinguishment, from tests done by Factory Mutual Research Corporation /4/.*

Fuel pan diameter [m]	Sprinkler delay time [s]	Water discharge rate [g/s]	Sprinkler nozzle orifice diameter [mm] 11.0	8.36	6.69	5.57	4.17
0.914	60	1080	N	E	E		
0.914	60	707	N	N	N	E	
0.914	60	448			N	N	E
0.762	75	448		N	N	N	N

N: Not extinguished
E: Extinguished

The fuel and room parameters were kept constant in each series of tests. Various sprinkler nozzles, with different diameter of the orifice, was used, and the water pressure was increased to obtain similar water discharge rate in one series. The result of smaller orifice diameter and increased water pressure, is reduction of droplet size. A correlation for the median droplet diameter versus pressure and orifice diameter was found for the geometry of the used sprinkler nozzles, /7/:

$$d_r = (\Delta p/\Delta p_0)^{-1/3} \ (D/D_0)^{2/3} \qquad (2)$$

where

d_r : relative median droplet diameter [-]
Δp : actual pressure immediately upstream the nozzle
Δp_0 : reference pressure
D : orifice diameter
D_0 : reference orifice diameter

This correlation may be used for geometrically similar nozzles, and it gives relative median droplet diameters. To obtain the real diameters, one have to know the median diameter produced by the reference nozzle.

For the test nozzles used in the experiments at FMRC /7/, the median droplet diameter was characterized by the correlation:

$$d_m = 1.076 \cdot \Delta P^{-1/3} \cdot D^{2/3} \quad (3)$$

where

d_m : median droplet diameter in [mm]
ΔP : pressure drop over the nozzle in [kPa]
D : orifice diameter in [mm]

With the referred parameters ΔP = 17.2 [kPa] and nozzle diameter 11.2 [mm], the correlation gives a reference mean droplet diameter d_m = 0.562 [mm], or 562 [μm].

2.4 The Spray Heat Absorption Ratio

A concept for analyzing the effect of various water sprays on fires has been developed. It is based on the results of the FMRC tests /4,7/, but is adopted to the hydrocarbon fire test rig at SINTEF. The analysis is based on measuring the heat fluxes from the fire to the different parts of the fire room and its surroundings. For a fire with no spray activated, the heat release rate balances the heat losses to the walls, the ceiling and the floor, the heat convected by ventilation, the heat radiated through the openings of the room and the heat accumulated in the gases contained in the room.

A heat balance for the fire compartment with spray action adds heat loss to the water. By measuring the original heat release rate and losses, the cooling effect of the water spray may be calculated, given by:

$$SHAR = 1 - [(Q_{wall} + Q_{ceil} + Q_{floor} + Q_{vent}) / Q] \quad (4)$$

where

SHAR	:	Spray Heat Absorption Ratio
Q	:	total heat release rate
Q_{wall}	:	heat absorbed by walls
Q_{ceil}	:	heat absorbed by ceiling
Q_{floor}	:	heat absorbed by floor
Q_{vent}	:	heat convected by ventilation

The heat accumulated in the gases enclosed in the fire room, and the fraction of heat

radiated through the openings of the room are neglected in the analysis. From earlier experiments in the same fire room, and from the tests done by FMRC, it is documented that these heat fractions are in the order of 0.1 % of the total heat release.

When SHAR is calculated in fires before the activation of the spray, the result should be zero. Due to difficulties in assessment of all heat fluxes, and uncertainties in the measurement of heat release rates, this ratio will suffer from an inaccuracy of about ± 20%

Another interpretation of SHAR can be expressed directly as:

$$SHAR = Q_{water}/Q \tag{5}$$

where

Q_{water} : heat absorbed by the water

The heat absorbed by the water can be split in four parts:

- the heat necessary to bring the evaporated fraction of water from the supply temperature to the boiling point,
- the heat necessary to evaporate this fraction,
- the heat necessary to superheat the steam to the temperature of the exhaust gas
- the heat necessary to bring the run off water from the supply temperature to its final temperature

Both methods have been applied for analysis of the experiment results, but the latter method is suffering from larger uncertainties than the former.

2.5 Scaling of the fire and the spray action

2.5.1 Froude Number similarity

From scaling rules developed for fire plumes, based on Froude Number similarity, a set of scaling criteria has been developed to serve a room fire with a water spray /8,9/.

If the following criteria are fulfilled in each scale, characteristic temperature, velocity concentration of mass etc. will be similar at homologous time and coordinate:

- The fire rooms must be geometrically similar.

- The fuel burning rate is scaled with $L^{5/2}$,
  i.e.

$$m_{fuel} / L^{5/2} = \text{constant} \quad (6)$$

- The thermal properties of the walls, ceiling and the floor is preserved, expressed as:

$$\lambda \cdot T_o / (\delta \cdot L^{1/2}) = \text{constant} \quad (7)$$

and

$$t_c \cdot L / (\rho \cdot c_p \cdot \lambda \cdot T_o^2) = \text{constant} \quad (8)$$

- The flow pattern of the droplets leaving the nozzle is similar.

- The droplet velocity is scaled by:

$$u_o / L^{1/2} = \text{constant} \quad (9)$$

- The droplet diameter is scaled by:

$$d_m / L^{1/2} = \text{constant} \quad (10)$$

- The water application rate is scaled by:

$$m_{water} / L^{5/2} = \text{constant} \quad (11)$$

where:

m_{fuel}	:	fuel burning rate
L	:	characteristic lenght scale
λ	:	thermal conductivity
T_o	:	ambient temperature
δ	:	wall thickness
t_c	:	characteristic fire duration
ρ	:	density
c_p	:	specific heat capacity
u_o	:	initial droplet velocity
d_m	:	mean droplet diameter, i.e. a diameter which 50 % of the droplets are larger than, on mass basis
m_{water}	:	water discharge rate

These scaling criteria are derived from Froude number modelling of fire plumes, and are solely theoretical. Experimental verification is still lacking, but there are some evidence that is has a certain validity.

2.5.2 Scaling based on droplet size.

Kung at FMRC /4/ has in his analysis also suggested scaling of the heat absorption by the spray. The heat absorption by a spray is expected to be a function of the heat release rate, the water discharge rate, m_{water} ; the relative median droplet size, d_r; and other variables such as room geometry, fuel location and spray nozzle location.

A ratio, where the fraction of heat absorbed by the spray is in the numerator, and the total heat release rate times the maximum heat absorption by the spray is in the denominator, is suggested to be a function of relative mean droplet size only. The ratio, denoted E, is :

$$E = (Q - Q_{loss}) / \{ m_{water} \cdot [H_{evap} + c_{p\,water} \cdot (T_{evap} - T_{water})] \cdot Q\} = h(d_r) \qquad (12)$$

where:

Q	:	total heat release by the fire

Q_{loss}	:	heat loss to the room and the environment, exclusive heat loss to the water
H_{evap}	:	heat of evaporation of water
m_{water}	:	the water discharge rate,
T_{evap}	:	evaporation temperature
T_{water}	:	water supply temperature
d_r	:	the relative median droplet size

When E has the dimension [MW^{-1}], the function found by FMRC is:

$$E = 0.11 \cdot d_r^{-0.73} \quad [MW^{-1}] \tag{13}$$

where the factor 0.11 is characteristic for the experimental set-up.
From a theoretical point of view, this function could as well be

$$E = K \cdot d_r^{-1} \quad [MW^{-1}] \tag{14}$$

The total surface of the droplets is proportional to the relative droplet diameter, and K is a constant valid for the spray and the room configuration.

3. EXPERIMENTS

3.1 Parameter variation

The main variables in the experiments were the nozzle type, the water pressure and the number and location of the nozzles. These variables give a water application rate. The heat output of the burner, the preburn time before spray activation and the ventilation rate to the fire compartment are other possible variables. These are varied to make qualitative evaluations only. The model compartment itself with two openings, one air inlet at the floor level of the front wall, and an outlet at the ceiling level at the rear wall, was not altered through the experiments. A list of parameter variations, and some key numbers for identification of each test is given in Table 2.

The preburn time of the fire in the model compartment is 5 minutes in the typical experiment. Then water is applied through one or two nozzles mounted in the ceiling, heading directly at the propane burner. The nozzles produce a so called full cone spray, totally covering the burner area. After the 5 minutes free burn time the spray was activated.

The pressure of the propane tank decreases during a typical experiment, and the fire starts at about 1 [MW], and decreases to about 850 - 900 [kW] in the next 15 minutes. The fire is similar in every experiment, except for one with a longer preburn time before water application, and one with a higher effect.

A description of the experiment set up is given in Figure 3. More details about the model and the spray nozzle characteristics are given in Appendix A.

Table 2 List of experiments with key data.

Date	Name	Nozzle		Pressure	Waterappl.	Mean droplet diam.	Result	
		Type	No	bar	l/(m^2·min)	µm		
890719	H7-1-25	H7	1	2.54	4.66	1130	Exting.	
890721	H7-1-1	H7	1	0.95	2.26	1569	Control	
890906	H7-1-1	H7	1	0.99	2.31	1548	Control	Extra long preburn time
890907	H7-1-25	H7	1	2.42	3.83	1149	Exting.	
890912	H7-1-2	H7	1	1.84	3.36	1259	Control	
890913	H7-1-2	H7	1	1.87	3.48	1252	Control	
890915	G22-1-7	G22	1	7.12	1.81	547	Exting.	
891012	G22-1-6	G22	1	5.53	1.63	595	Exting.	
891013	G22-1-5	G22	1	4.58	1.46	633	Exting.	
891017	G22-1-3	G22	1	2.79	1.35	747	Control	
891019	G22-1-3+	G22	1	3+	1.4-1.8	729 v.3 bar	Control	Ext.when the pressure was increased.
891020	H4-1-3	H4	1	2.74	2.64	802	Exting.	
891020	H4-1-3	H4	1	2.75	2.65	801	Exting.	
891023	H4-1-2	H4	1	2.26	2.38	855	Exting.	
891025	H4-1-1	H4	1	1.31	1.75	1025	Control	
891026	H4-1-3+	H4	1	2.96+	1.75+	-	Control	Larger fire, 1.5 MW. extinguished when pressure was increased to ≈ 5 bar.
891027	G22-2-4	G22	2	4.17	2.84	653	Control	
891030	G22-2-5	G22	2	4.95	3.11	617	Control	

Symbols: + increasing, not constant
NA not available, due to instrument problems

Key to the table:

Date: For data file identification.

Name: First letters/number is nozzle identification, referring to producer's list /11/.(The nozzle noted GG22 is the same as HH22). Second number refers to number of nozzles. Third number refers to nominal nozzle pressure in the experiment.

Pressure: Average water pressure at the nozzle.

Waterdens: Mean delivered water application rate; it means the flow of water in litres per minute, dispersed on a floor surface approximately 12 [m^2]

Mean droplet diam: Estimated mean droplet diameter based on private communication with the producer, /10/, and by scaling rules by FMRC /7/.

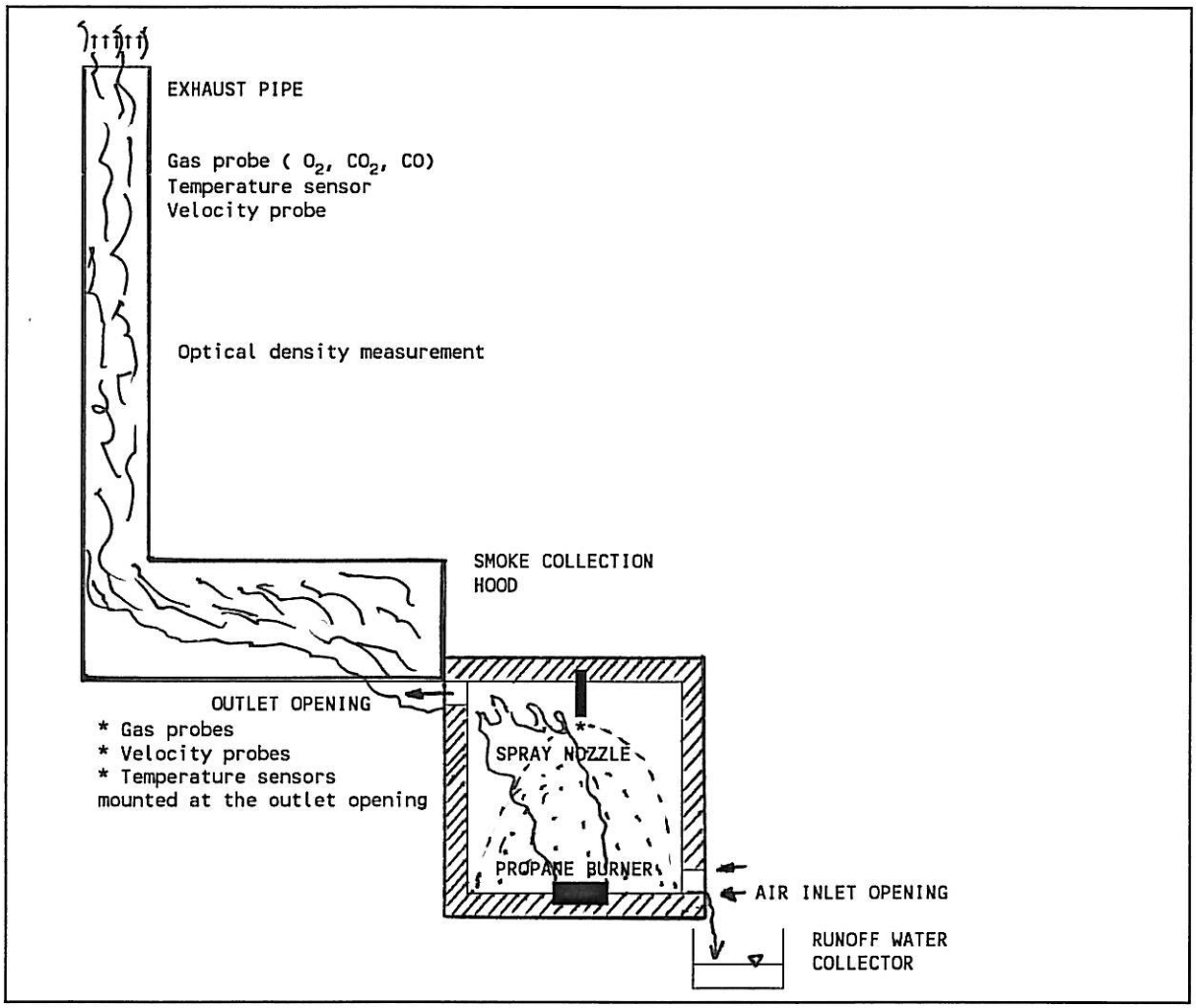

Figure 3 *Experimental set up for the water spray experiments. The enclosure is ~2.5 [m] wide, ~2.5 [m] high and ~5 [m] long.*

3.2 Extinguishment or control of the fire?

The fire in the compartment is showing two different results, depending on the characteristics of the spray. The first seconds of the spray action is very critical regarding extinguishment or not. The water spray acts at the flames from the propane burner by deflecting them, and the evaporated water enters the combustion zone. In the first critical phase there is a "fight" between the flames and the spray, where the flames become bluish and are replaced by steam. The flames may however survive in other parts of the enclosure, even burn at the outlet opening only. If the spray has an efficiency to remove the flames at the base of the burner for more than about 10 seconds, there is a good chance for permanent extinguishment of the fire. If not, the flames reenter the compartment and more or less stabilize, only influenced by the flow induced by the

spray. The fire is now controlled, but not extinguished.

The experiments were planned to find the limit for extinguishment for three nozzles producing different droplet size. To characterize the spray action in a situation without extinguishment, several heat transfer mechanisms were studied as well.

The results of the experiments are shown in Figure 4, in a diagram of water application rate and nozzle pressure.

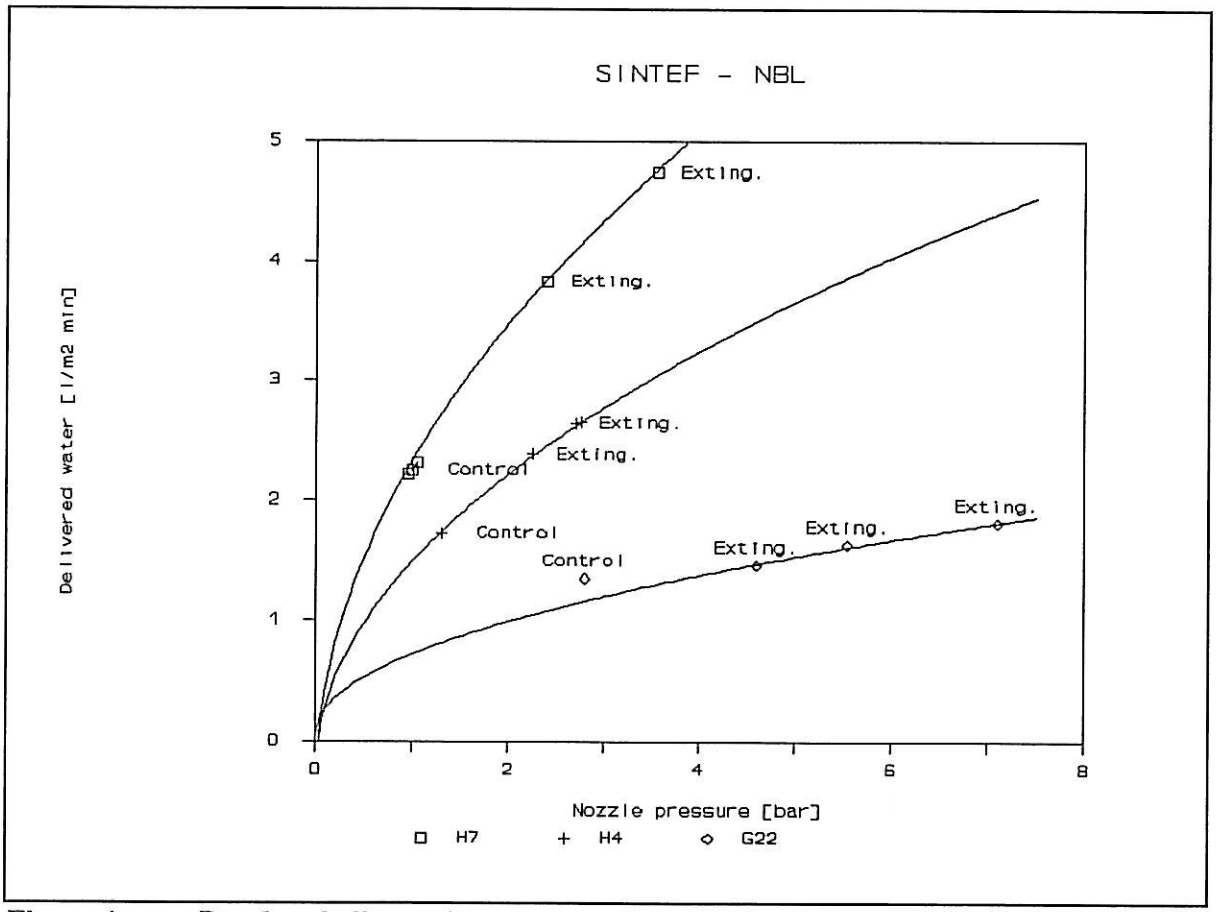

Figure 4 *Results of all experiments, denoted by Exting. - extinguished fire, and Control - not extinguished fire. The lines represent pressure - water application rate for each nozzle.*

3.3 Results from the experiment series with ~1 [MW] fire

3.3.1 Heat release rate

The heat release rate is measured in three independent ways. First, the flow of propane is measured, and the heat release is calculated from the mass flow and the heat of combustion. Next, the mass flow rate of smoke is measured by temperature and velocity measurements both in the outlet opening and in the exhaust pipe, 5-6 [m] above the top of the smoke collection hood. At the same positions the concentration of oxygen, carbon dioxide and carbon monoxide are measured. The heat release rate is calculated by the rate of oxygen consumption, by the so called oxygen depletion method, /14/. All the calculations are shown in detail in Appendix B. The heat release rate measured in three independent ways is shown in Figure 5.

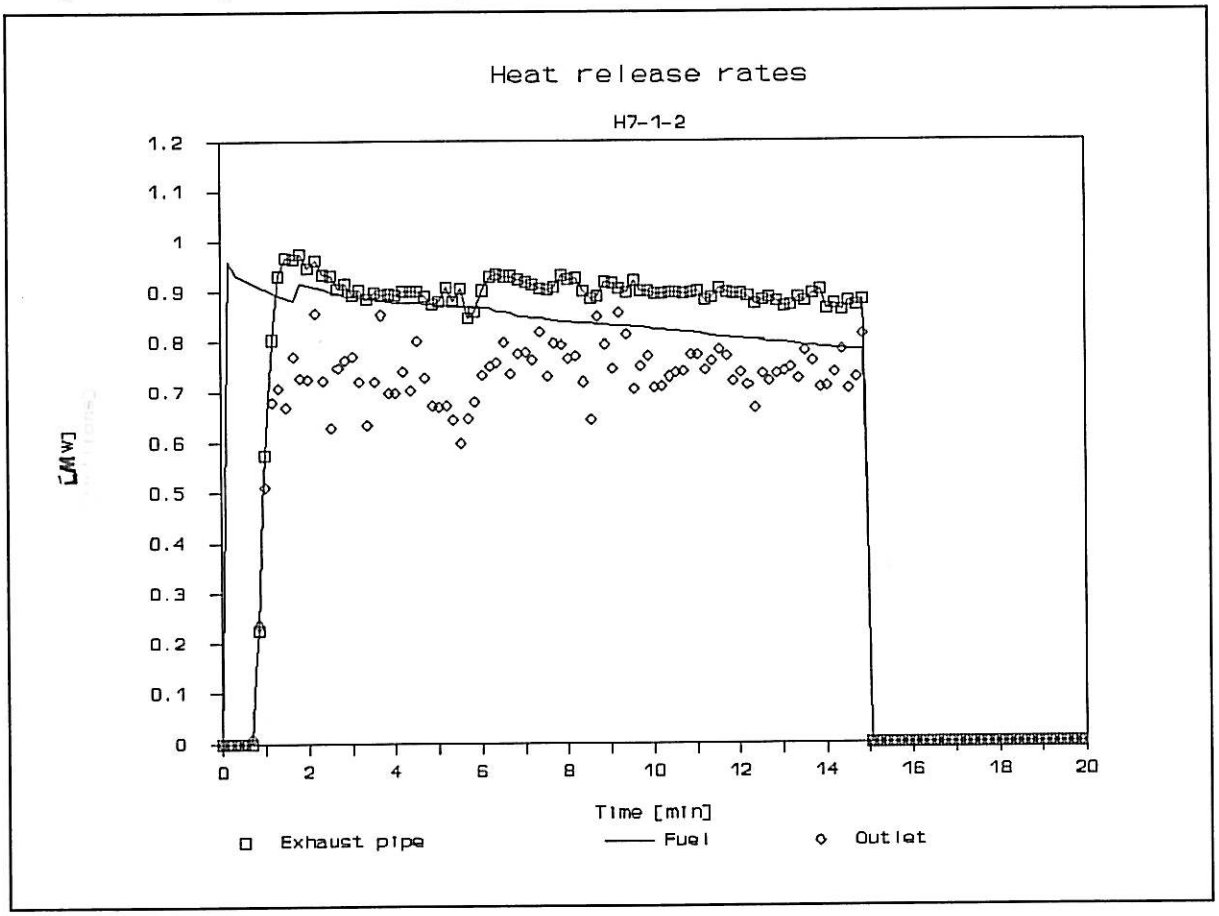

Figure 5 Heat release rate measured in three different ways.

The heat release rate based on fuel consumption and the one measured in the exhaust pipe show a good correlation in all experiments, differing within normal error bounds

only. The heat release rate measured by the oxygen consumption technique in the outlet opening is systematically underestimated in all experiments, but are presented uncompensated to be comparable to data from the earlier tests with liquid pool fires in the same model, /1,2/.

The time development of the heat release rate shows the effect of a decrease in propane tank pressure. The time delay between the graphs for fuel based and oxygen based heat release rates is due to a time delay in the gas analyzers. A small increase in the heat release rate is measured in the exhaust pipe and at the outlet, after the application of water.This may be a result of water vapour in the smoke, which is not taken into account in the calculation.

3.3.2 Water mass rates.

The water flow into and out of the model compartment is continuously measured. The inflow of water is measured by the pressure in the pipeline, at the floor level of the model compartment. The water flowing out of the model is collected in a reservoir, on top of a weighing platform. For each spray nozzle the correlation between inlet pressure and water flow is measured and is expressed by an equation. The equations are shown in Appendix B.

Figure 6 shows the water mass flow in and out of the model compartment in experiment H7-1-2.

The spray is activated 5 minutes after the fire is ignited, and the water flow is kept at a constant rate through the experiment. The water flow out of the model start about 6 minutes after ignition. The time delay of the water flow is partly due to evaporation of water, and partly due to the variation of transport time through the system and accumulation in the model itself. The time lag between opening the inlet valve and the first flow of water out of the model is measured without a fire in the model, and is 1 minute. This is compensated for in the data conversion system.

The first portion of water flowing into the model compartment hits walls and floor which has been preheated in the first 5 minutes of the fire, and almost all of it evaporates immediately. When the accumulated heat in the floor and wall linings has been used for evaporation, a fraction of the water flows through the model without being evaporated. The difference between the water flowing into and out of the model is the evaporated

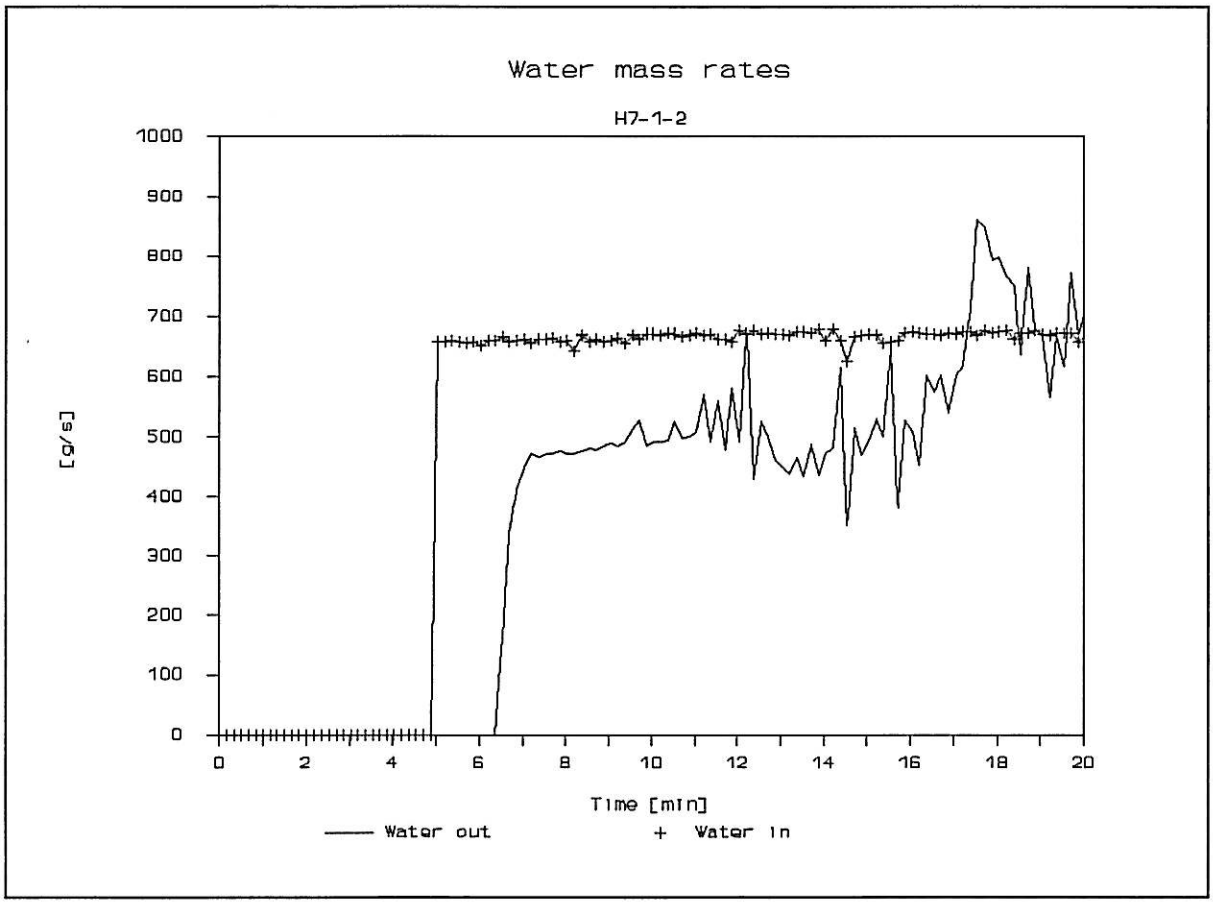

Figure 6 Water mass rates in experiment H7-1-2.

fraction, which leaves with the smoke. When the fire is stopped, 15 minutes after the start, the water flow out of the model coincidences with the flow in. This indicates that no evaporation occurs. The fluctuations in water flow out of the model is partly due to the fluctuations of the water flow, and partly to the sensitivity of the weighing cell.

In experiment H7-1-2 about 170 [g/s] water is evaporated when the fire is on. This is shown graphically in Figure 7.

3.3.3 Heat to evaporated water

The evaporation of water takes heat from the fire itself, and cools the model compartment. In the experiments where extinction was not obtained, this heat rate is calculated. The time development of this heat rate in experiment H7-1-2 is shown in Figure 8.

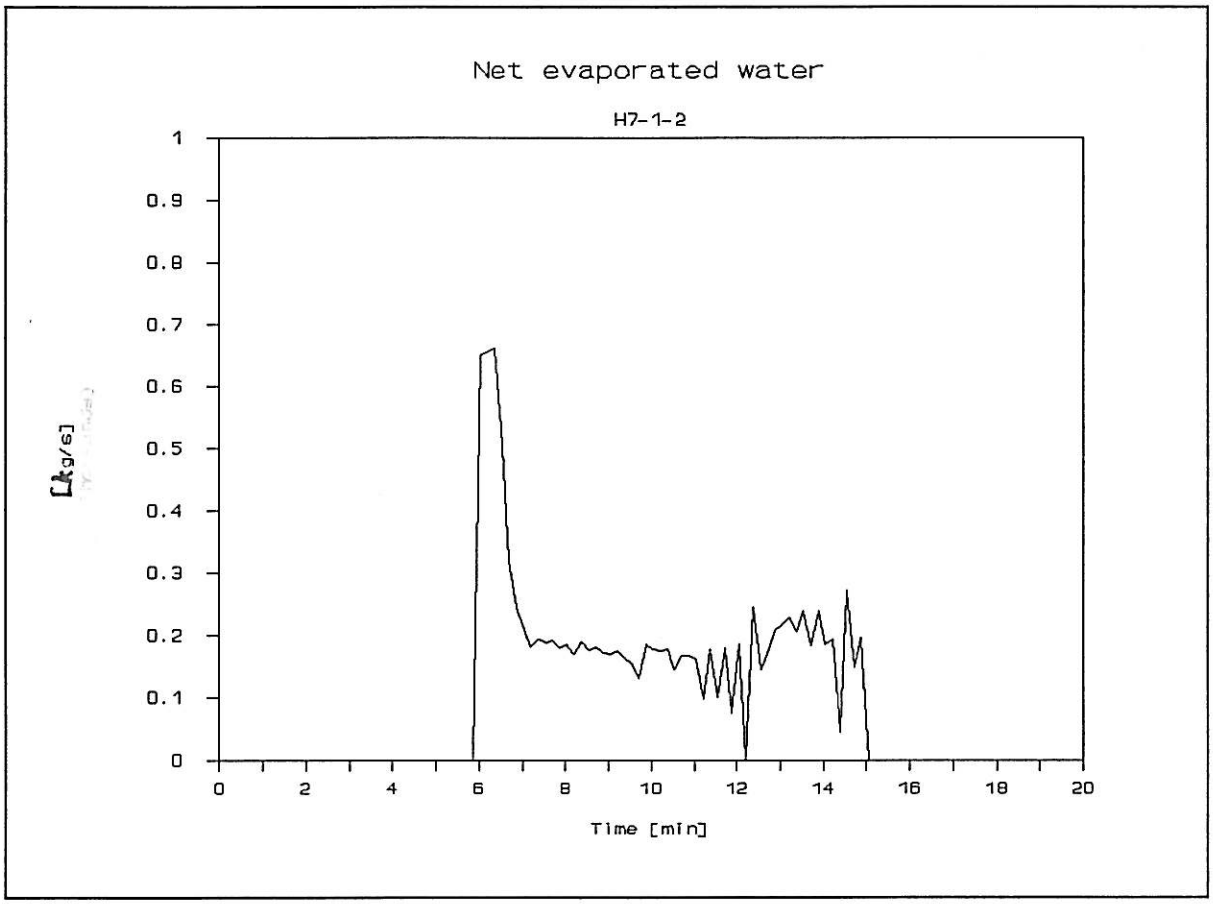

Figure 7 Rate of evaporation of water in experiment H7-1-2.

The peak heat rate of 2 [MW] at about 6-7 minutes after fire start may be unrealistic, as variations in the time lag between water flow in and out of the model makes contributions to the rate of water flow. The heat rate after 7 minutes is more realistic, showing that a heat of about 500 [kW] is taken up by evaporation of water. This represents about 55% of the heat release rate of the fire. This is a typical value for fires in this series of experiments. If the fraction of heat taken up by the water spray exceeds this level, the fire is extinguished.

3.3.4 Heat transfer to the model and its environment

The heat produced by the fire ends up partly in the model itself and is partly being transported to the surroundings. The model has thick walls constructed of insulating materials, and is so called thermally thick. The time to heat the model walls and ceiling to a equilibrium temperature, where all the heat transported into the model is convected

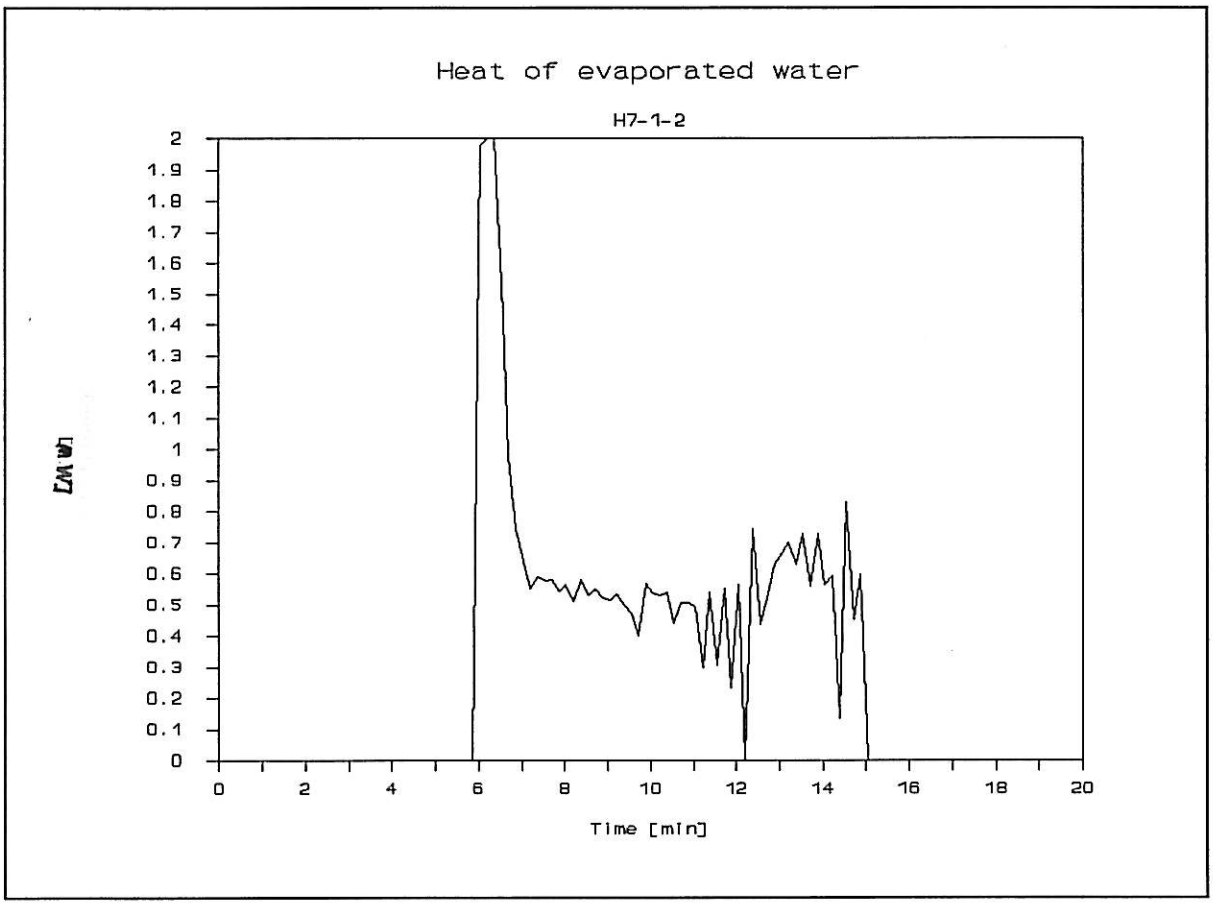

Figure 8 Heat rate by evaporation of water in experiment H7-1-2.

to the surroundings, is in the order of hours. However, the first period with rapid transients in heat transfer to the walls lasts about 5 minutes. The preburn time of the fire before water is applied is chosen to be 5 minutes, to assure equal initial conditions in every experiment. A view of heat balance for the model, as measured in the experiments, is shown in Figure 9.

A main part of the heat is leaving the model as hot smoke through the outlet opening. In experiment G22-1-3 this part is denoted ventilated heat loss, and is about 500 [kW] of the total heat release of 950 [kW] in the first 5 minutes. After activation of the spray, the fraction of heat through ventilation seem to decrease to about 400 [kW].

The next largest heat rate is to the walls and the ceiling, and then a fraction to the floor. Heat rate to the walls counts for about 300 [kW] the first 5 minutes, decreasing to about 180 [kW] after spray activation.

The heat rate to the floor is shown separately, as the steel plates of on the floor gives

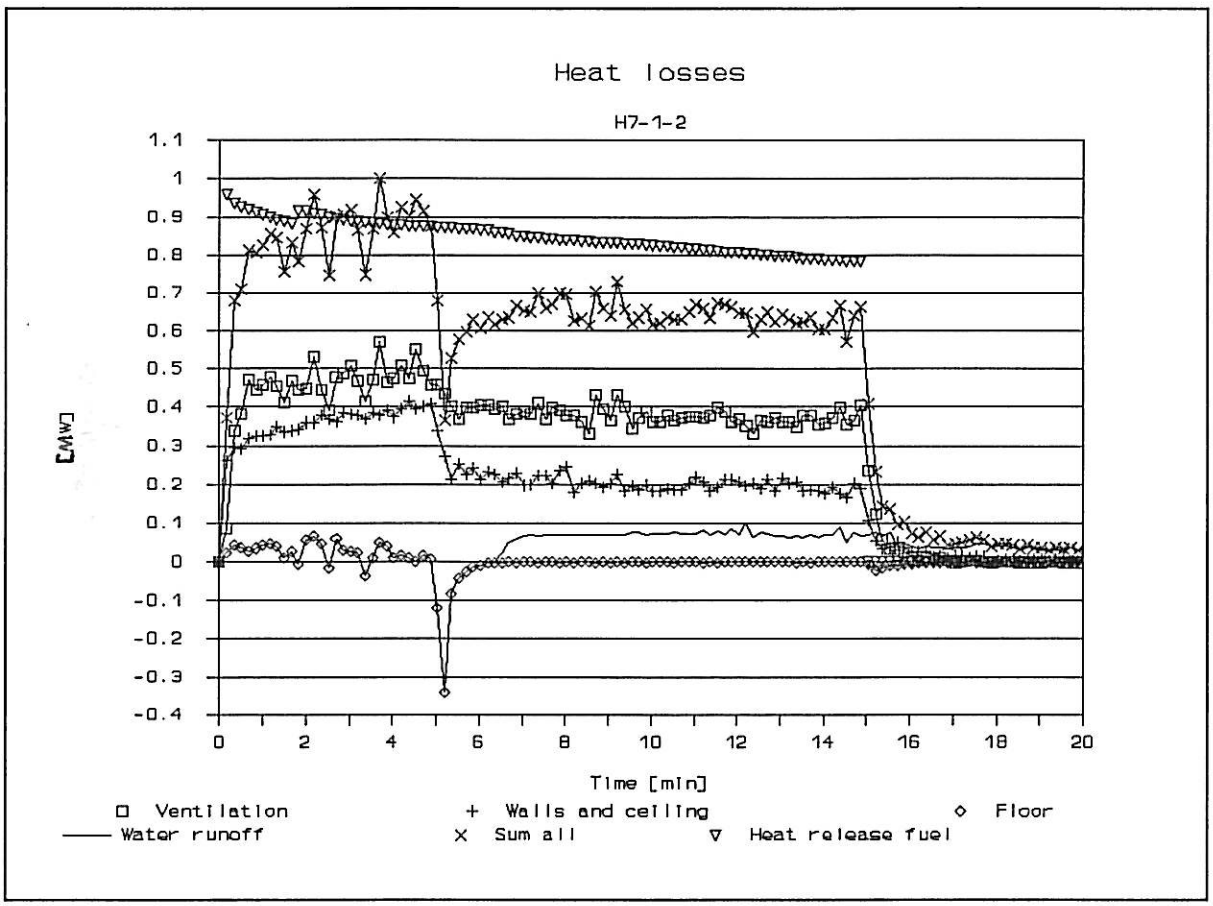

Figure 9 Heat transfer rates as measured in experiment H7-1-2.

away a large flux of heat just as the water hits the floor. This heat flux evaporates almost all the water flow in the first half minute, and is seen to be of great importance regarding instant extinction.

The heat rate through water which runs off the floor is also measured, and is a measure for the effectiveness of the water applied to the model. A large heat rate through run off water means that water has a potential to absorb heat from the fire, which is not utilized.

The sum of the heat loss through ventilation, to the walls, the ceiling and the floor, and through the run off water is shown, and can be compared with the total heat release of the fire. The difference between those is the heat rate of evaporated water.

3.3.5 SHAR - the Spray Heat Absorption Ratio

The heat absorbed by the spray is in Figure 9 shown as the difference between the heat losses to the model and its environment, and the heat release rate of the fire. To make the heat absorbed by the spray more universal, the ratio between the absorbed heat and the heat released in the fire has been calculated. This ratio is given the abbreviation SHAR - the Spray Heat Absorbtion Ratio. It is a measure for the effectiveness of a certain spray in a defined environment.

As mentioned in Chapter 2, the SHAR can be found in two ways. The most constituent way in the present experiment series is to use the heat balance of the model and the environment. The measurement of evaporated water is disturbed by accumulation in the model compartment, and the time delay between water in and water out. This makes the estimate of evaporated water uncertain in the most transient period, just after water application. The SHAR of experiments which were almost extinguished just after water application is presented in Figures 10 to 12.

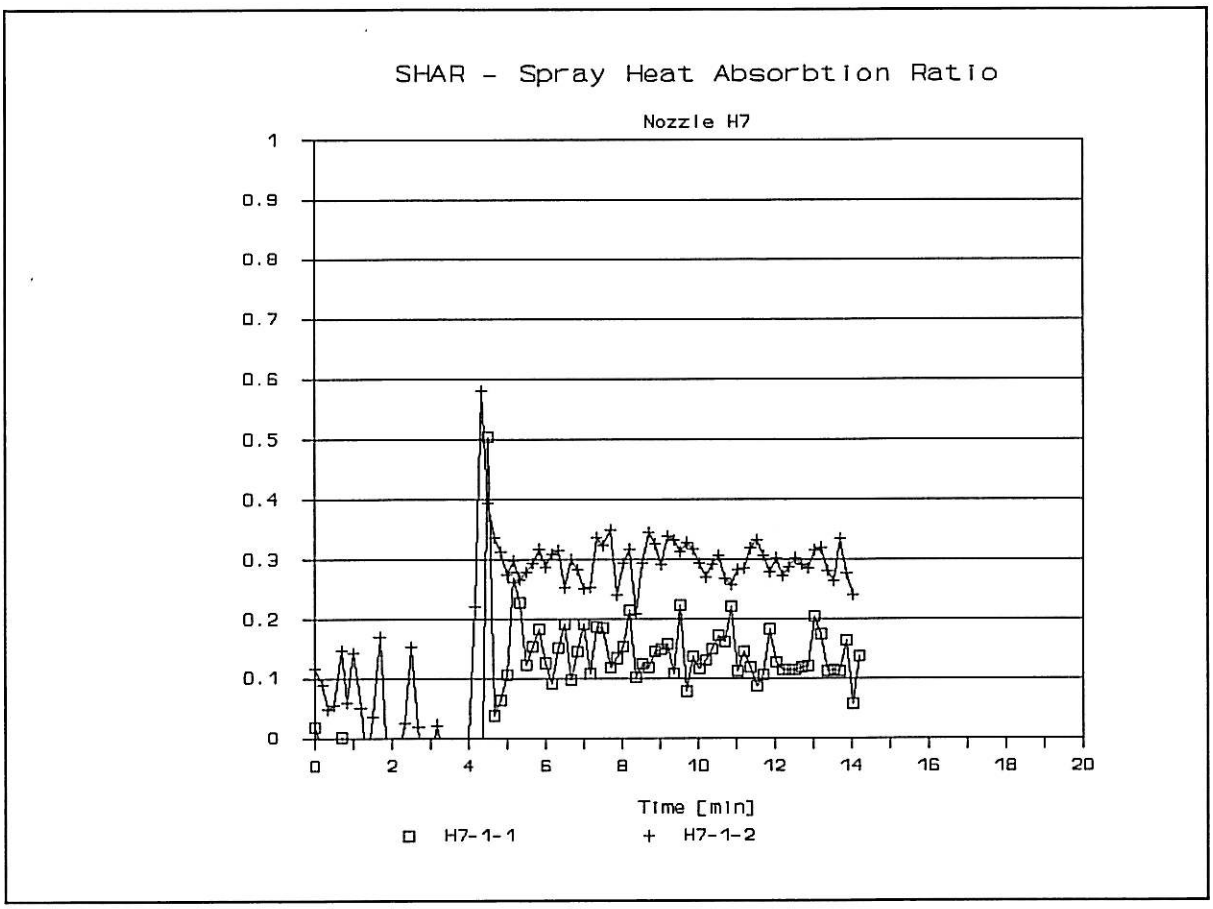

Figure 10 *SHAR - Spray Heat Absorbtion Ratio - for experiments without extinguishment, using nozzle H7.*

The two experiments with nozzle H7 presented in Figure 10 are different with respect to nozzle pressure. The higher pressure results in an increased delivered water application rate, from 2.26 [l/(m^2·min] in H7-1-1 to 3.36 [l/(m^2·min] in H7-1-2. The mean droplet diameter is reduced from 1569 [μm] to 1259 [μm].

A clear correlation is seen between the increase in nozzle pressure and SHAR. The SHAR value has a peak just at the moment of spray activation, reflecting the heat transfer to the water from the test model itself, especially the floor. The peak value is close to 0.6. with the highest nozzle pressure, and 0.5 with the lowest pressure.

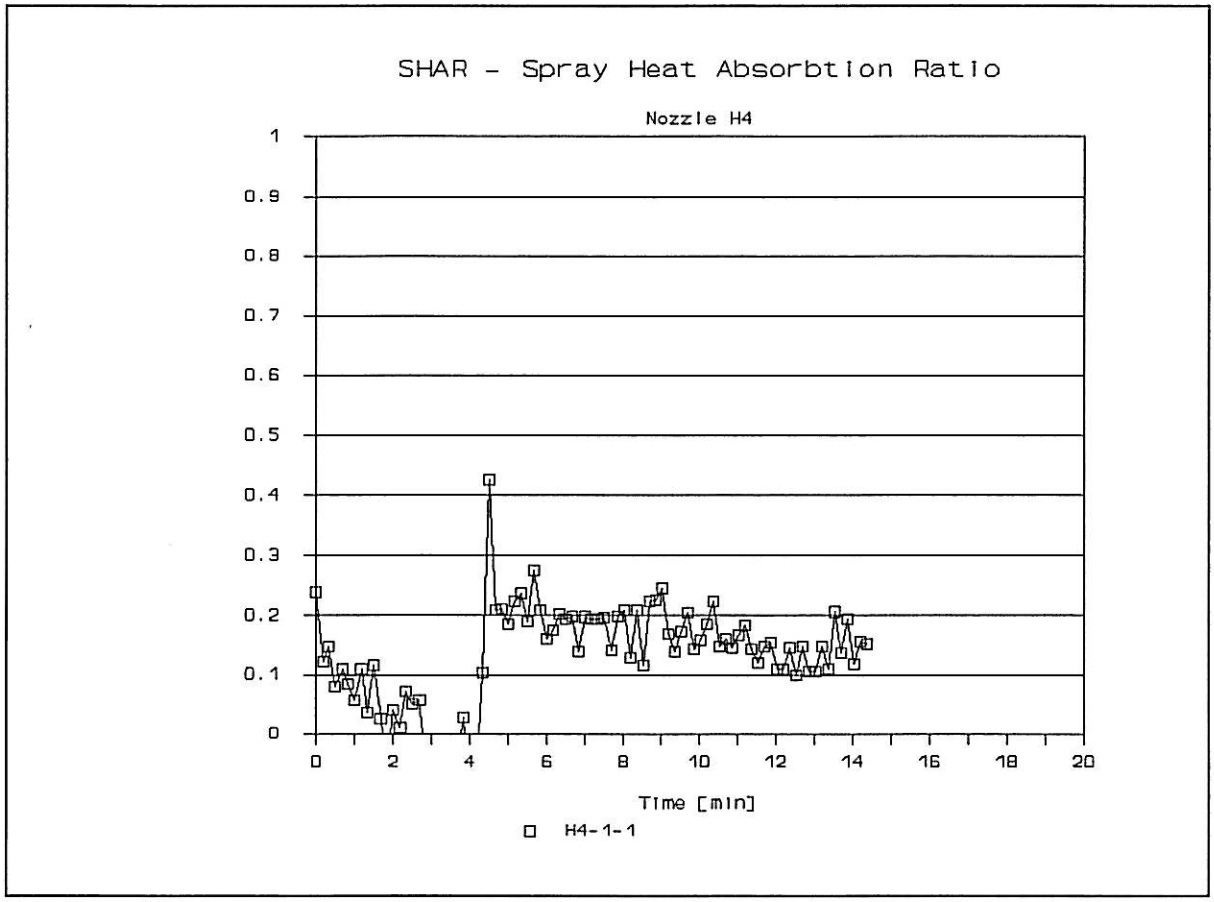

Figure 11 *SHAR - Spray Heat Absorbtion Ratio - for experiment H4-1-1.*

There is only one well documented experiment without extinguishment with nozzle H4. SHAR is about 0.2, which indicates that the water flow is somewhat off the condition for extinguishment. The peak value of SHAR just after spray activation is a little above 0.4.

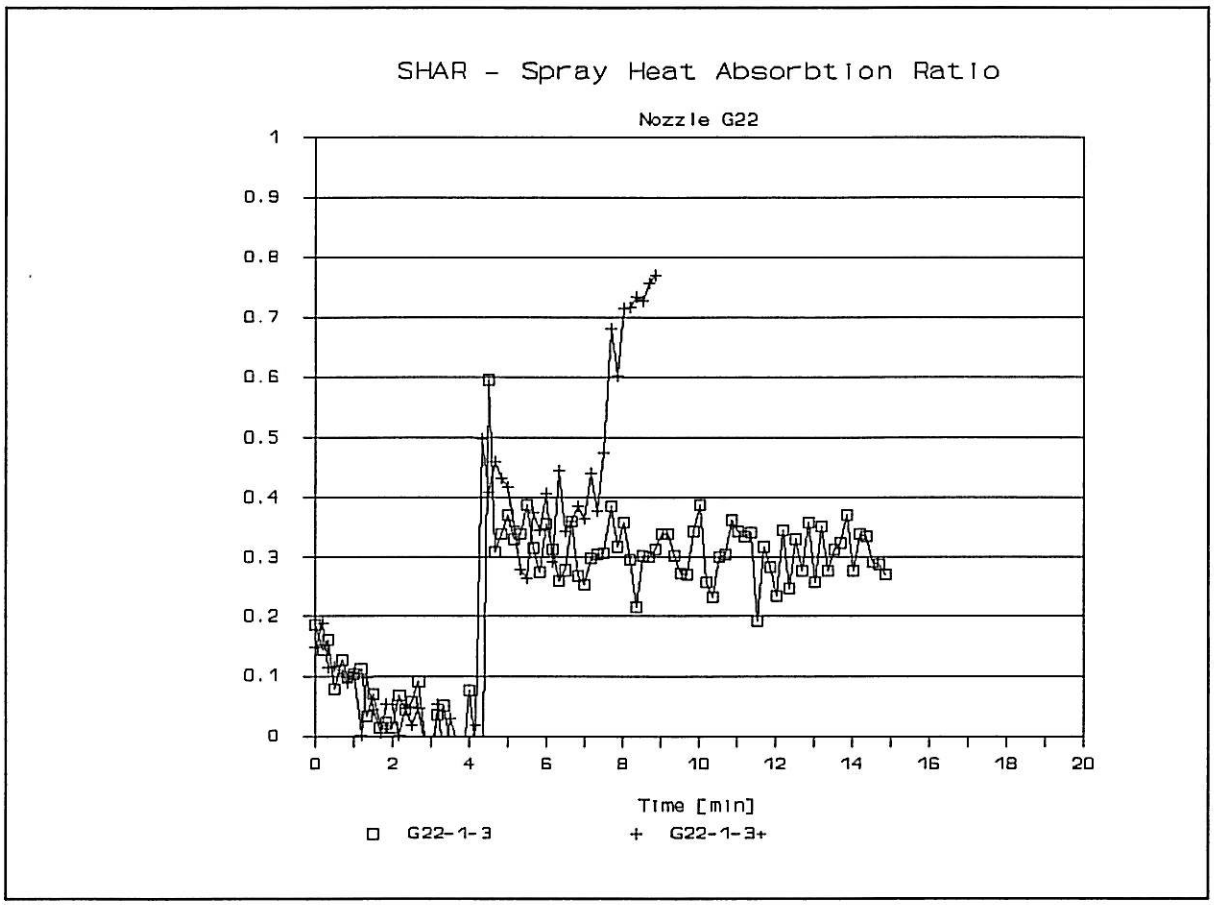

Figure 12 *SHAR - Spray Heat Absorbtion Ratio - for the experiments G22-1-3 and G22-1-3+.*

The experiments with nozzle G22 show SHAR close to 0.4 just after spray activation. The peak value just after spray activation is however not above 0.6 in either of the two experiments.

Experiment G22-1-3+ is special, as the water pressure was stepwise increased after the first spray activation. The spray was almost sufficient to extinguish the flames just after activation, but the flames survived more than the critical half minute, and recovered its original shape. The water flow was increased, the spray received more and more of the heat released by the fire, but it was still burning. When the nozzle pressure was increased to the maximum obtainable, the fire was still burning. The SHAR value was then recorded to be well above 0.7. Then the pressure was reduced a little, and then suddenly increased to its maximum. The result of this "shock" was extinguishment. A general observation is that a spray which do not absorb more than 60% of the heat released by

the fire, will fail in instant extinguishment.

If extinguishment is not obtained instantaneously, the SHAR value has to be above 0.7 to obtain extinguishment.

3.3.6 Average gas temperature

Gas temperatures are measured by 49 thermocouples inside the model compartment. The thermocouples are evenly distributed in position, and cover both the flame zone, the inflowing air and the smoke. An impression of a temperature development inside the model is shown in Figure 13. The vertical distribution of temperatures at a position close to the south end wall is shown.

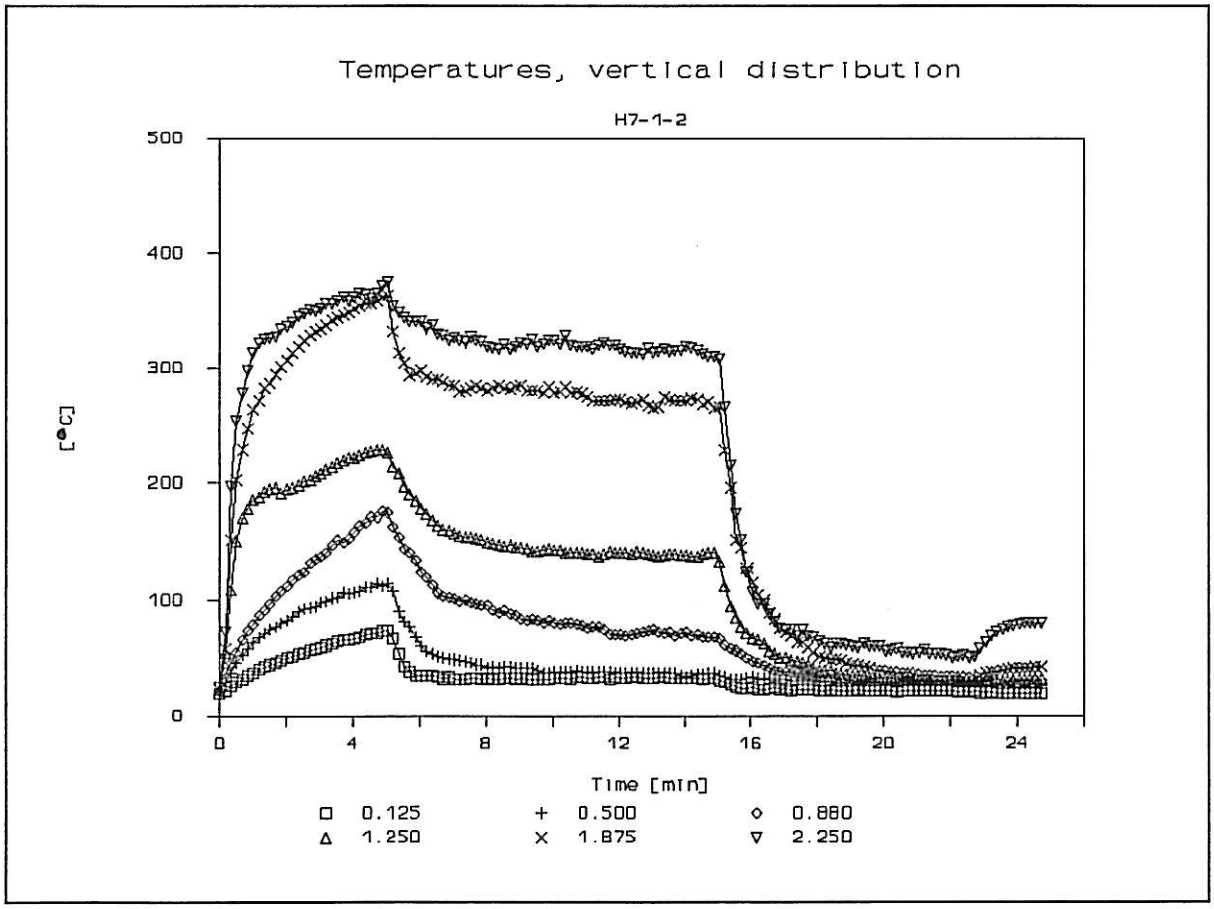

Figure 13 *Vertical temperature distribution inside the model compartment in experiment H7-1-2. The position is 0.4 [m] from south end wall, halfway between front and rear wall. Legend numbers indicate height in [m].*

The drop in temperatures after water spray activation is characteristic for all tempera-

tures inside the model, and is reflected in reduced smoke temperature at the outlet opening as well. Average temperature measured by all 49 thermocoples in the compartment is shown in Table 3. A typical drop of average temperature for a 1 [MW] experiment is from 250 to 190 [°C]. The average temperature at the outlet opening is reduced from 350 to 290 [°C].

3.3.7 Heat flux densities

The heat flux densities to surfaces inside the model compartment are measured by 8 sensors. 5 are of the Medtherm type, and 3 are steel calorimeters developed by SINTEF NBL. The steel calorimeters are described in Appendix B.4.11. The measured heat flux densities are used as input for calculation of the heat loss to the walls and the ceiling. The Medtherm flux meters are located on the front wall, on the south end wall and in the ceiling. The measured values of heat flux densities at the south end wall are presented in Figure 14.

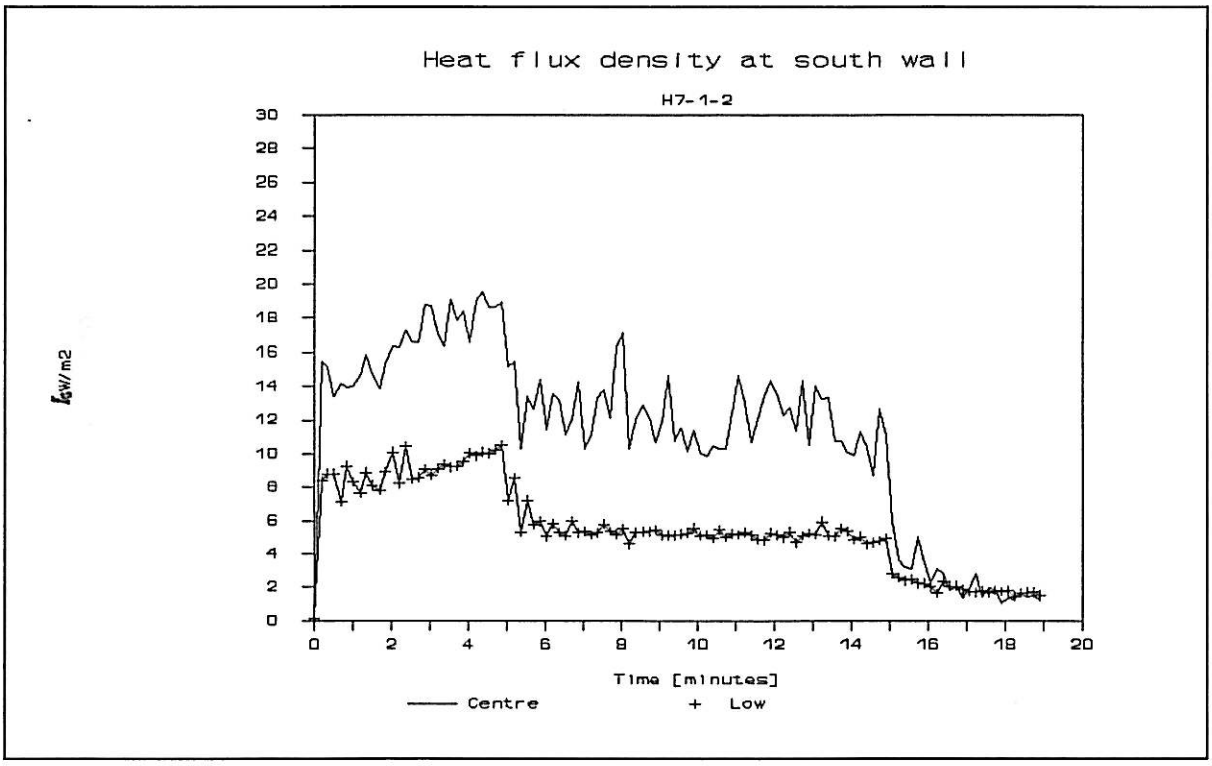

Figure 14 *Heat flux density to the south wall of the test compartment. Location of heat flux meters are 0.25 [m] (legend:low) and 1.25 [m] (legend:centre) from the floor level.*

The values of the heat flux density in the centre of the south end wall, before water spray

activation are about 18 [kW/m^2]. When the water spray is activated, the heat flux density is reduced to about 12 [kW/m^2]. The reduction is about 30 %.

The heat flux density before water spray activation, measured by a steel calorimeter at the centre of the rear wall, at a position 1.25 [m] above the floor level, is in the order of 45 [kW/m^2]. The heat flux density after spray activation is about 12 [kW/m^2]. This big reduction in heat flux density reflects that the calorimeter is directly hit by water spray in this position.

3.3.8 Soot concentration in the smoke

The soot concentration in the smoke is measured by an optical device located in the exhaust pipe, 3 [m] above the top of the smoke collection hood. Soot concentration is calculated from the obscuration of a light beam crossing the smoke flow, /15/. The soot production is calculated from the smoke flow rate and the concentration. To get a more universal measure of soot production, the ratio between the soot production rate and the fuel supply rate is calculated. The development of the soot/fuel ratio is shown in Figure 15.

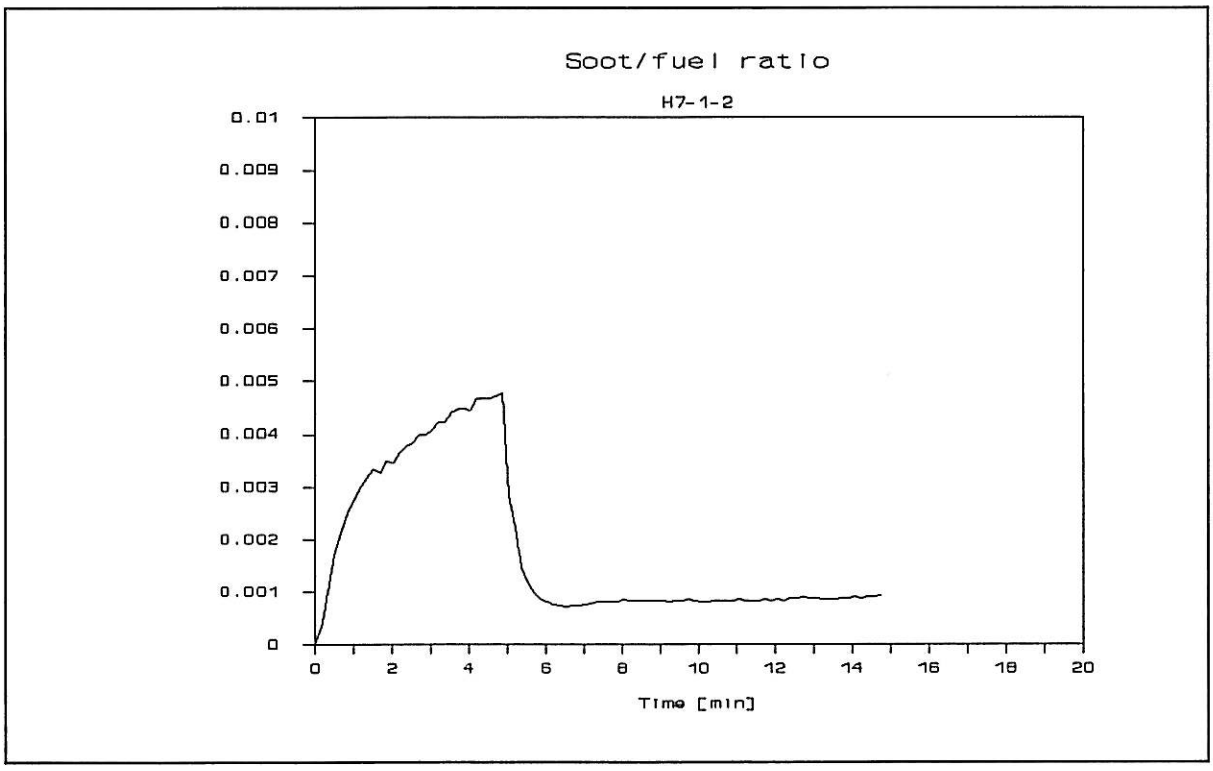

Figure 15 *Soot/fuel ratio in the experiment H7-1-2.*

The drop in soot/fuel ratio is characteristic for all experiments. A soot production of 0.5% of the fuel supply rate is normal for propane fires, but the level of 0.1% which is measured after water spray activation is very low. There is a possibility that a fraction of the soot is washed out of the smoke by the spray, and that the soot production is not influenced. The result is after all that the soot content in the smoke leaving the model compartment is significantly lower with the spray activated.

3.4 Critical parameters for extinguishment

From the theory it is well known that droplet size is a critical parameter for extinguishment of fires. Maximum heat absorbed by a single droplet of water occurs when the water is totally evaporated. To heat 1 [kg] of water from 10 - 100 [°C] takes about 380 [kJ]. To evaporate 1 [kg] of water takes 2257 [kJ]. To heat the steam further to 300 [°C] takes about 400 [kJ].

The heat transfer from hot smoke to a water droplet is depending on the temperature difference, the velocity difference between the smoke and the droplet and the total surface area. The main difference between small and large droplets in a fire environment is the surface area. For a constant water flow rate, the total surface of the droplets increases proportionally with the inverse value of the droplet radius.

Small droplets will evaporate faster than a large one, but this is not the only factor dominating the extinction of a fire. The transport of the droplets into the fire and the residence time in the hot smoke and flame zone will also influence on the heat absorption capacity of a certain water spray.

For the fire size and room configuration used in these experiments, a very sharp limit is found for instant extinguishment of the propane fire. This is shown graphically in Figure 16.

In all experiments presented in Figure 16 the spray nozzle is positioned in the centre of the ceiling, heading downwards directly at the flame base. One effect of the spray when extinguishment occurs is that the flames becomes blue, flickering about, from one part of the compartment to another for then to disappear totally. The duration of this period was less than 10 [s] in experiments with large droplets, up to 25 [s] with the smaller droplets.

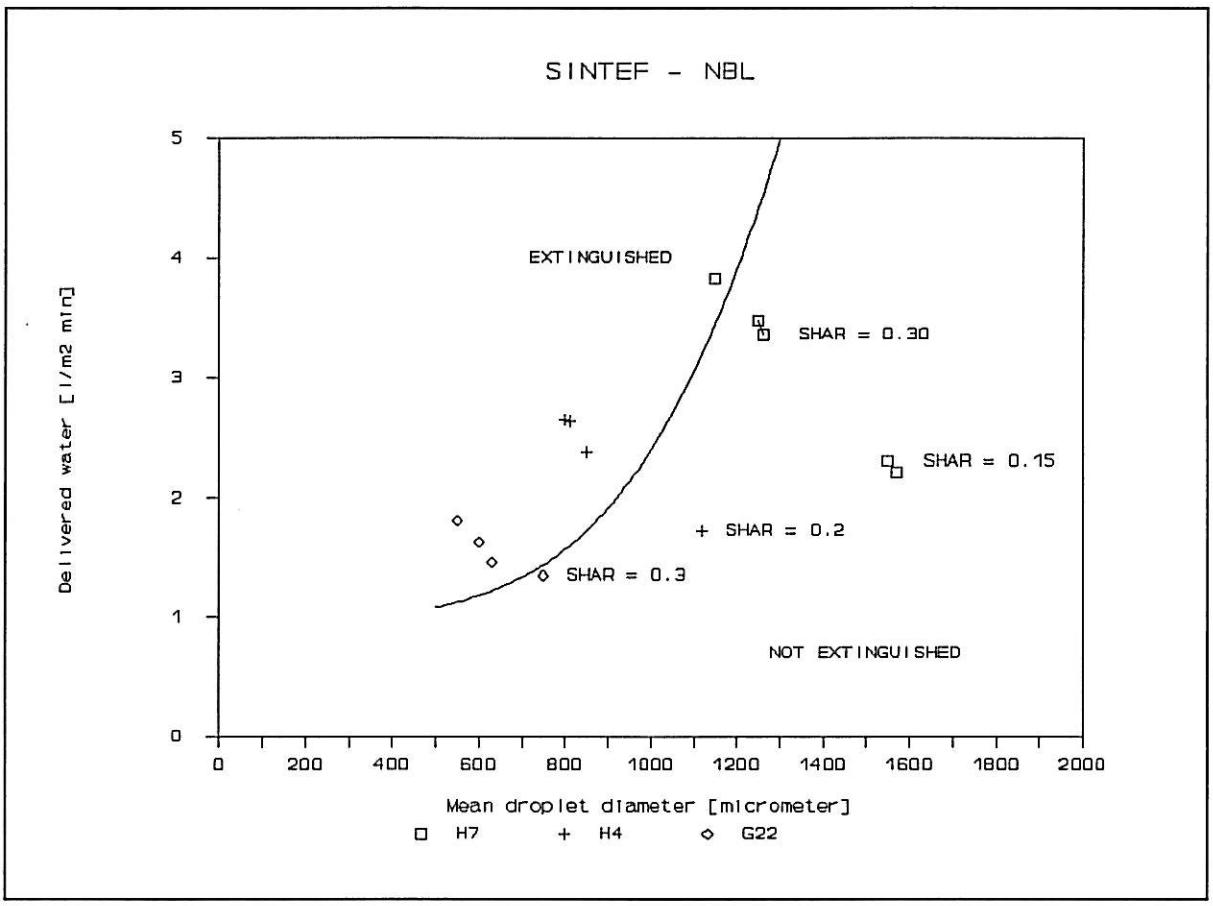

Figure 16 *Results of extinguishment tests for a propane fire about 1 [MW] in a 30 [m^3] compartment, with fire induced ventilation.*

3.5 Results from experiments with larger fire size

3.5.1 Heat release rate

Experiment H4-1-3+ is an experiment with increased fire size. The heat release rate was 4-5 [MW] about 2 minutes after ignition, decreasing to about 2 [MW] just before spray activation. This heat release rate was gradually decreasing to about 1 [MW] after 12 minutes from ignition. The spray was activated 5 minutes after ignition.

3.5.2 Temperatures

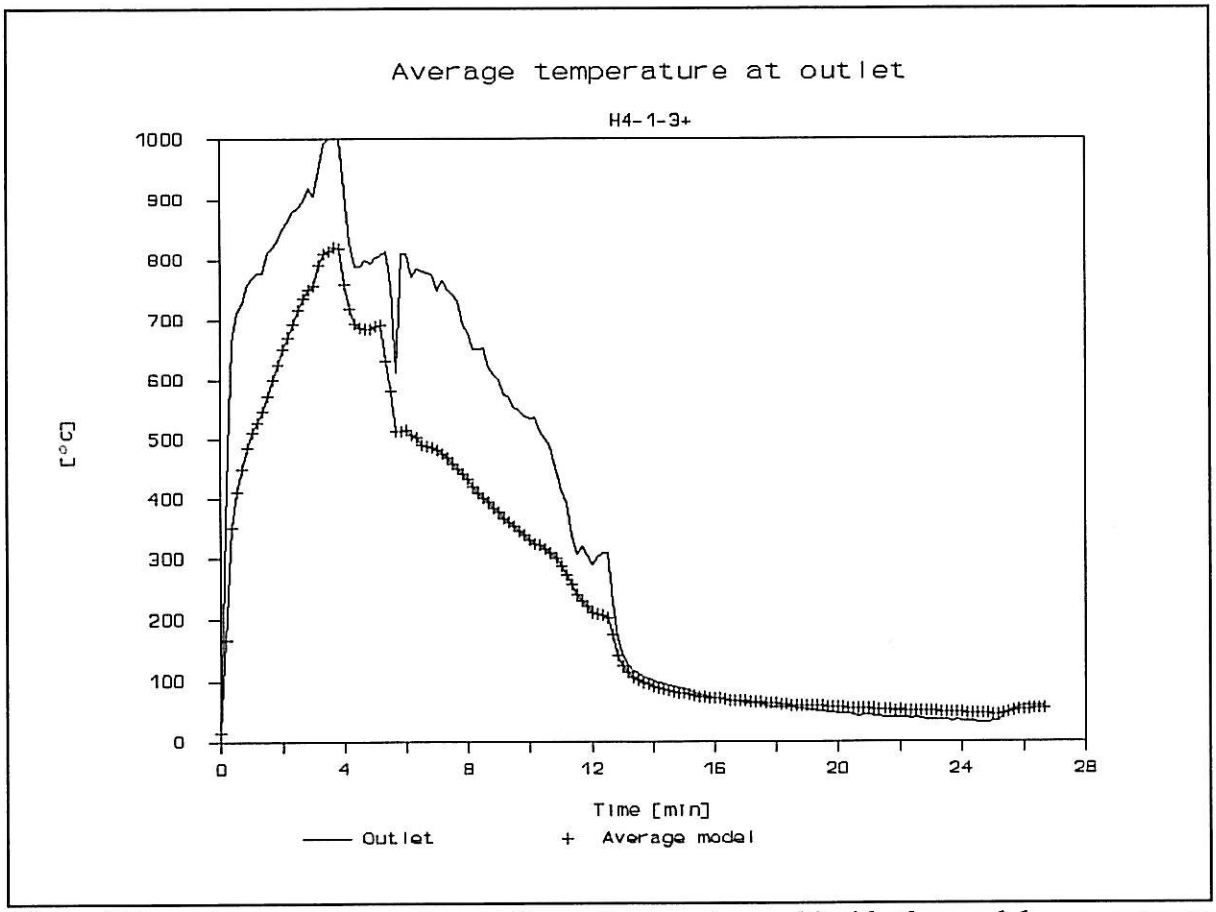

Figure 17 *Average temperature at the outlet opening and inside the model compartment in experiment H4-1-3+, with increased fire size.*

The average temperature in the compartment and at the outlet opening is shown in Figure 17. The temperature rise is high in the first minutes, and reaches 1000 [°C] at the outlet opening. In this experiment the flames were lifted off the surface of the burner

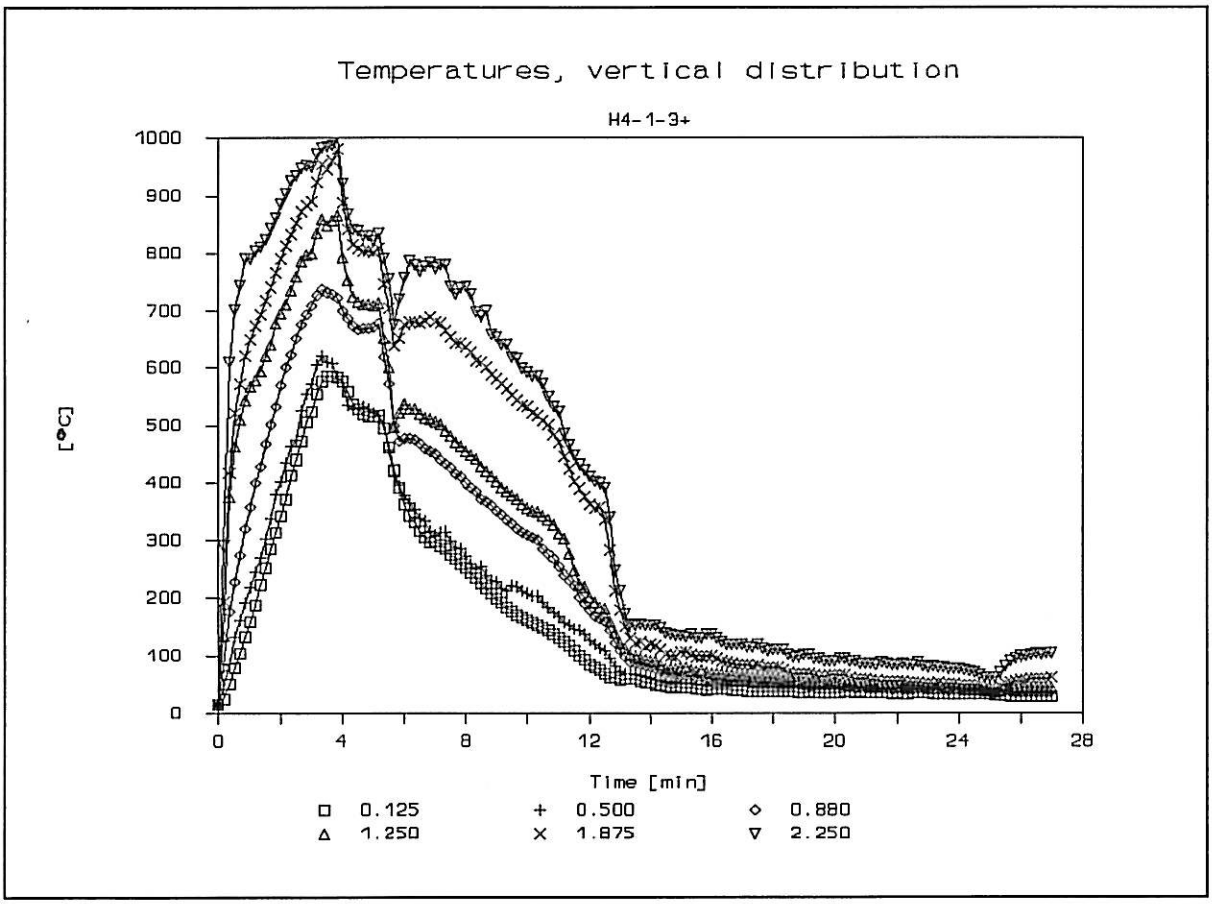

Figure 18 *Vertical temperature distribution at a position close to the south end wall of the model compartment in experiment H4-1-3+, with increased fire size. The positions are given in [m] from the floor level.*

when the spray was activated, but there were still flames out of the outlet opening. The flames were also flickering around inside the compartment. The vertical distribution of temperatures at a position close to the south end wall is shown in Figure 18.

3.5.3 Heat flux densities

The heat flux densities are measured with three different flux meters at the centre of the south end wall. The difference between the two steel calorimeters of the pilot type and a commercial type MEDTHERM heat flux meter is shown in Figure 19.

The heat flux densities are quite similar, which indicates the accuracy of the pilot probes. The measurements represent total heat flux through the probes, and are not compensated for irradiation to the compartment or variation in convective heat transfer due to different surface temperature of the probes.

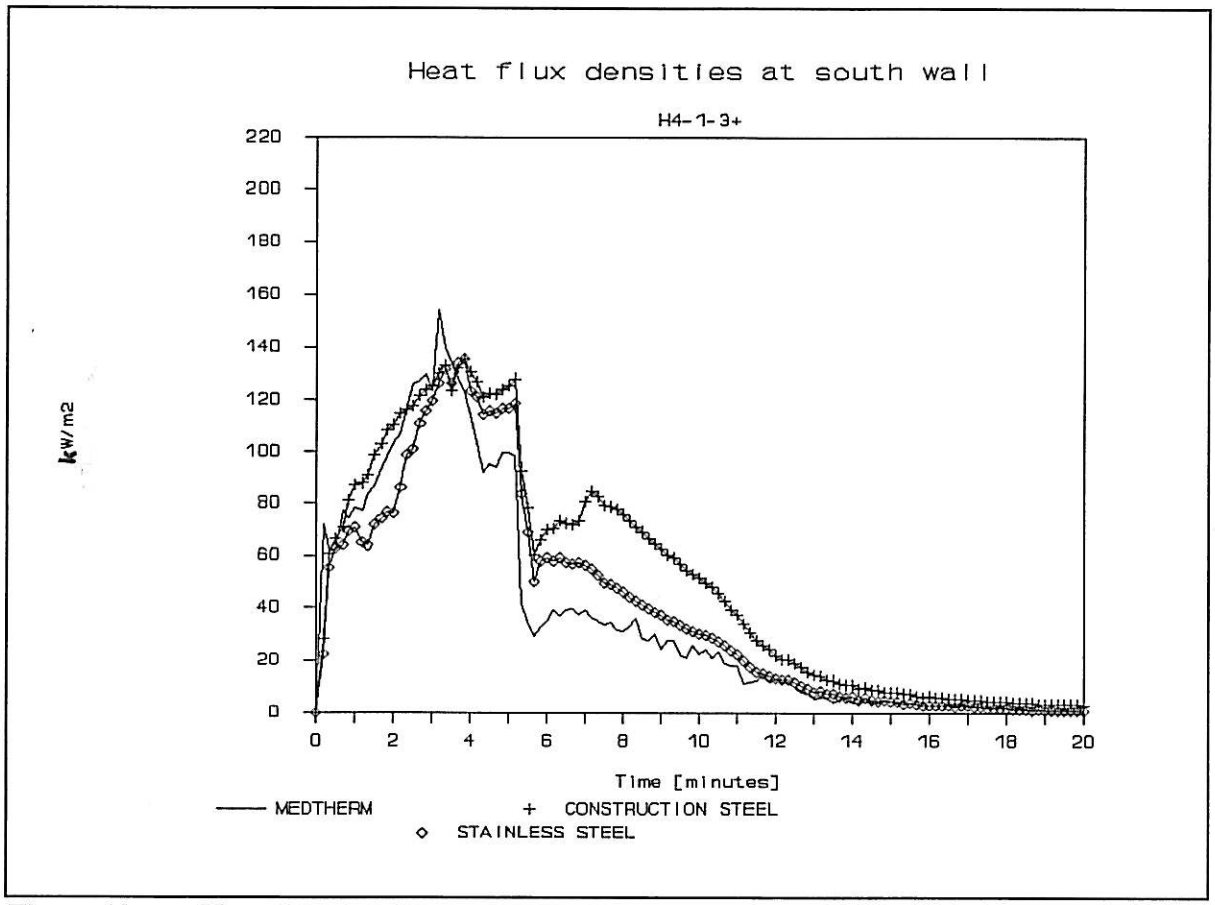

Figure 19 *Heat flux density measured at the centre of the south end wall of the model compartment.*

The heat flux density shows a significant drop just at the moment of spray action. The drop coincides with a reduction of heat release rate as well, and all the effect on heat flux can not be credited the spray action.

The heat flux density measured by a steel calorimeter of the pilot type at the rear wall, impinged by the flames, was reaching a maximum of 220 [kW/m^2] in this experiment. The maximum was reached between 3 - 4 minutes. After spray activation the heat flux was measured to 80 [kW/m^2] at this position.

3.6 Results from experiments with varied nozzle position

Two experiments were performed with two nozzles at the ceiling. The nozzles were mounted at the same height as for one nozzle, along the north-south centre line of the ceiling. The distance between the nozzles was 2.5 [m]. The results were somewhat surprising. The water flow was doubled with two nozzles, and the nominal water application rate in [l/(m^2·min)] was also doubled. The distribution of the water on the floor was different, and the sprays hit the floor in two zones between the burner and the end walls. The water distribution is shown in Appendix A, Figures A 10 and A 11. With the same water application rate which led to extinguishment with one nozzle, the fire was not extinguished with two nozzles. The flames from the burner was deflected by the two spray cones, but found its way between the cones. After a short time the fire stabilized again, and survived for the rest of the test.

3.6.1 Spray Heat Absorption Ratio

The Spray Heat Absorption Ratio for these experiments were not comparable to the other ones directly. The heat flux to the walls seems to be strongly influenced by the new locations of the spray nozzles. To compensate this, a new multiplication factor for the wall heat loss was introduced. When the same factor was applied for both tests, the resulting SHAR value before spray action was quite different. The wall heat flux was therefor multiplicated with a factor 0.5 for experiment G22-2-4, and a factor 0.8 for experiment G22-2-5. Then zero SHAR was obtained just before spray action in both experiments. The compensated values of SHAR are shown in Figure 20. There is a higher SHAR in these experiments than in experiments wich was extinguished. The reason for no extinguishment is obviously that there is no uniform mixing of the water vapour in the enclosure. This corresponds to the findings of Kung, /4/.

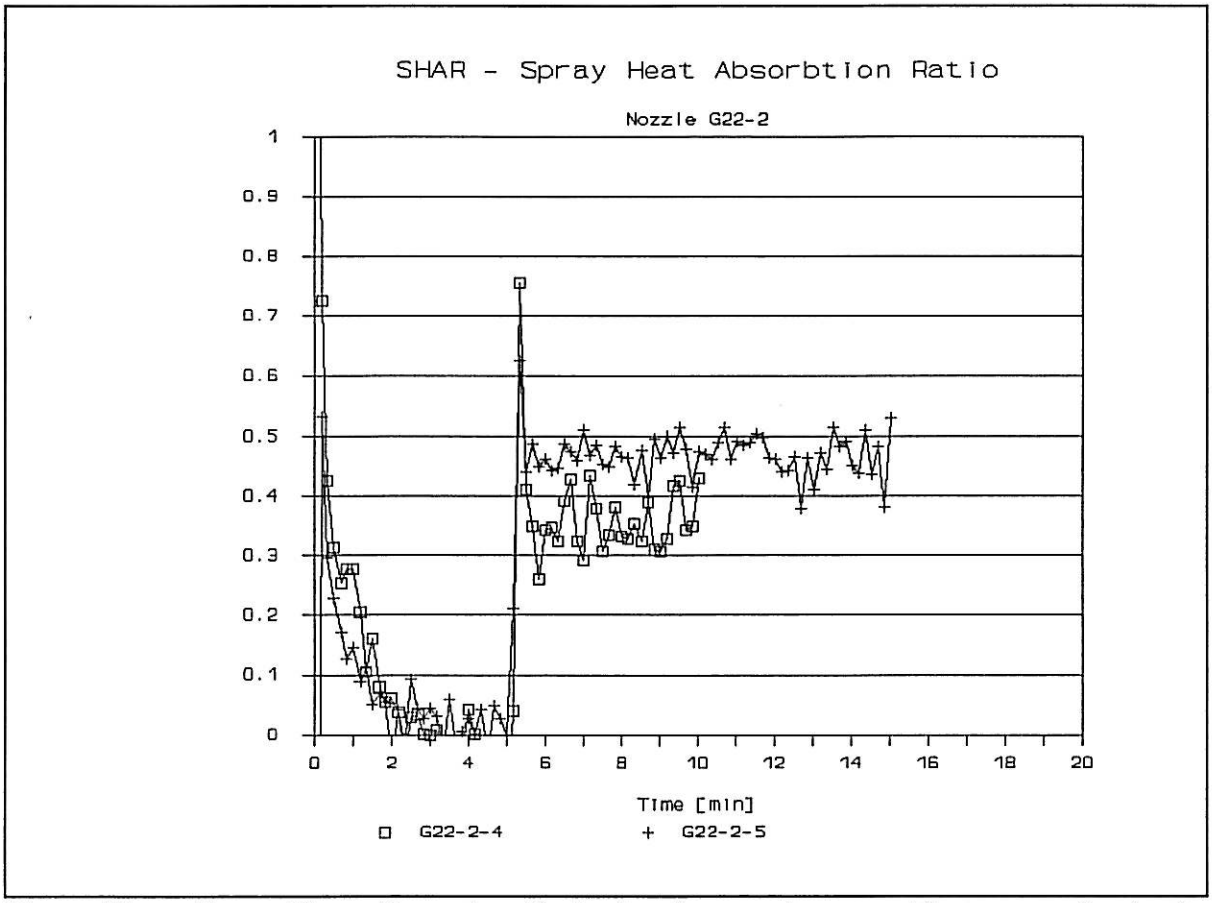

Figure 20 *Spray Heat Absorption Ratio for the experiments with two nozzles in the ceiling. The values are not calculated quite similar, but are compensated for different errors in the heat transfer to the walls.*

Table 3 *Results from all experiments. The average values represents the whole duration of the experiment, and is then an average for the fire before and after spray activation.*

Date	Name of experiment	Average heat release [kW] By fuel	At outlet	At exh. pipe	Average mass flow at outlet	Gas temperature Average	Max	Result
		[kW]	[kW]	[kW]	[g/s]	°C	°C	
890718	H7-1-3	-	-	895	-	-	570	Extinguished
890719	H7-1-3	853	370	895	781	241	567	Extinguished
890721	H7-1-1	997	787	1075	1395	212	596	
890828		307	342	311	1443	165	535	
890829		307	317	441	1402	164	477	
890904	H7-1-1	815	683	891	1469	185	599	
890906	H7-1-1X	795	732	970	1463	209	668	
890907	H7-1-2.5	893	600	812	1538	193	606	Extinguished
890911		709	601	780	1592	234	627	
890912	H7-1-2	840	689	840	1448	167	504	
890913	H7-1-2	852	723	868	1411	165	520	
890915	G22-1-7	1009	-	846	1442	211	531	Extinguished
891012	G22-1-6	974	700	872	1468	219	557	Extinguished
891013	G22-1-5	964	674	791	1420	216	546	Extinguished
891017	G22-1-3	880	775	976	1519	180	567	
891019	G22-1-3+	945	727	912	1471	184	547	
891020	H4-1-3	920	690	864	1499	216	587	Extinguished
891020	H4-1-3	924	666	843	1432	212	541	Extinguished
891023	H4-1-2	966	693	875	1436	222	547	Extinguished
891023	H4-1-1?	-	-	884	-	-	543	Extinguished
891025	H4-1-1	899	804	884	1441	199	551	
891026	H4-1-3+	-	-	-	-	-	1162	
891027	G22-2-4	795	691	747	1499	182	560	
891030	G22-2-5	967	742	769	1499	166	493	

4. DISCUSSION

The findings in this study can be compared to practice in offshore and onshore process industry. One of the most used guidelines for design of an extinguishment or fire control systems is the NFPA 15: Standard for Water Spray Fixed Systems for Fire Protection-,/17/. The standard still leaves some of the choices to the designer. An example is the choice of design water application rates, for which the standard says: *"The design density for extinguishment shall be based upon test data or knowledge concerning conditions similar to those that will apply in the actual installation. A general range of water spray application rates that will apply to most ordinary combustible solids or flammable liquids is from 8.1 [(l/min)/m^2] to 20.4 [(l/min)/m^2] of protected surface"*. The corresponding water application rate for exposure protection of vessels is 10.2 [(l/min)/m^2]. The results from this test can be compared to what is required in the NFPA 15 Standard. To do this it is necessary to scale the results to a full offshore scale.

4.1 Extinguishment of enclosed gas fires

The absorption of heat from a fire by a water spray is definitely a function of water discharge rate and mean water droplet size. In the experiment in a 30 [m^3] compartment, with ceiling mounted sprays, with full cone characteristic, with a propane fire with low exit velocity, there is a sharp limit for effective extinguishment at a droplet size about 3000 [μm] or 3 [mm]. To extinguish a fire of about 1 [MW] in this compartment, a delivered water density to the floor area of about 12 [m^2] of about
1.3 [l/(m^2· min)] is sufficient, when the mean droplet diameter is about 600 [μm].

The required water application rate for extinguishment with a spray producing droplets with a mean diameter above 1000 [μm] is more than 2.5 times larger, about
3.5 [l/(m^2· min)].

This is different from what was found in small scale experiments by Underwriter's Laboratories in 1955, /6/. The critical median droplet diameter was then 300 [μm]. This indicates that the effect of droplet size is scale dependent.

In Figure 21 the three different experiment series are compared. A best estimate on the function of water application rate neccessary to extinguish a hydrocarbon fire with various sprays producing different mean droplet size is based on information from the References /4,6 and 7/. The experiments done by Underwriters Laboratories were done with a small liquid pool fire in the open, as the tests done by Factory Mutual Research

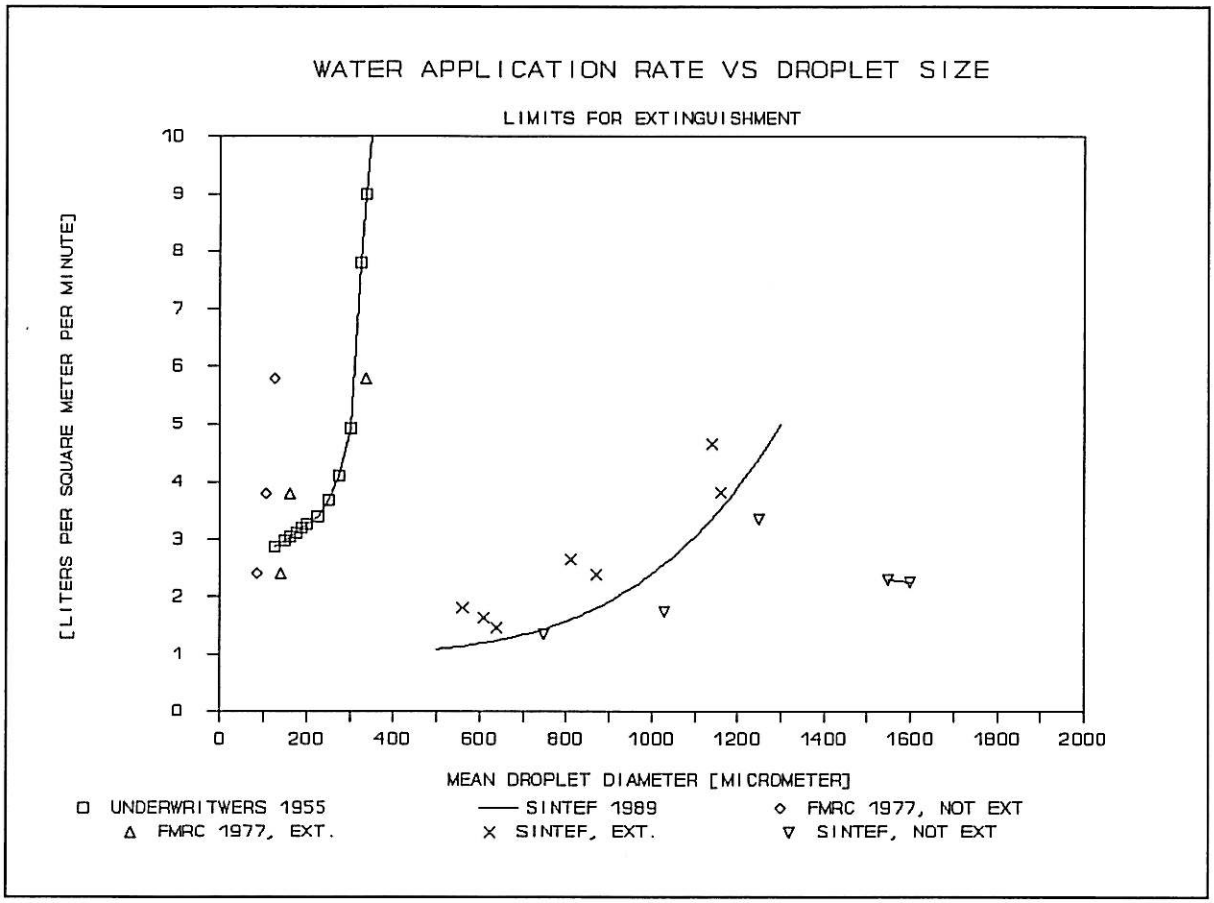

Figure 21 *Extinguishment of various enclosed hydrocarbon fires with water droplets, References /4,5,6,7/*

Corporation were performed in an enclosure about the same size as the SINTEF experiments.

The difference in critical droplet diameter for extinguishment may be explained:

- A critical droplet size for extinguishment is scale dependent.

- A critical droplet size for extinguishment is larger when the spray impinges the flame zone directly, which was the case in the SINTEF tests. In the FMRC test the flames were to some extent shielded from direct spray impingement.

- Different measurement technique for droplet size characterization may give different mean droplet size values. The test apparatus used by UL in 1955, the technique used by FMRC in 1977 and the tests done by Spraying Systems Corporation, [8,9], may well give different values.

The most effective way of extinguishment is to evaporate the water at the base of the fire. A water droplet which evaporates completely by its travel through the flame plume is optimal regarding energy transfer. The cooling effect is greatest at the base of the fire, as the mass flow rate of combustion products is low. The inerting effect by steam replacing oxygen in this zone will also most effective where the mass flow rate is low. However, a small diameter droplet follows the flow, and will not reach the base of the fire.

The optimum droplet diameter is then very dependent of the location of the spray nozzle versus the fire. A spray directly impinging the flame zone of a fire is much more effective than spray not impinging the base of the fire. However, the evaporation of water in direct contact with hot surfaces in the fire compartment may be sufficient to produce an inert atmosphere. The preburn time of the fire before spray activation will dominate the available heat accumulated in the model itself, and is in real life a function of detection or sprinkler characteristics.

A parameter which is not varied in these experiments is the air supply or ventilation rate. From the observations of the burning behaviour it is expected to have large influence, since the volume fraction of water vapour in the combustion zone seems to be critical for extinguishment.

A problem may occur if spray systems or deluge systems are activated to control a gas fire in an enclosure, and the preburn time is long enough to accumulate heat sufficient to produce an inert atmosphere inside the enclosure. Then the gas fire may be extinguished, and if the gas is still leaking, it may produce an explosive gas concentration. An explosion following a new ignition may have worse consequences than a fire controlled by the water spray.

4.2 Control of enclosed gas fires

A water spray cools the smoke from an enclosed fire, and diminishes the heat load significantly. The mean temperature inside the enclosure, and the temperature of the outflowing smoke gases are reduced. In the 1 [MW] fire, the temperature typically was reduced about 100 [°C], from a mean temperature of 200-300 [°C]. Heat flux densities to the walls and the ceiling are reduced considerably. The soot concentration in the exhaust gas is also considerably reduced with spray action.

4.3 Scaling of spray action in enclosed fires

The results from the 30 [m^3] compartment can represent a normal room, with a height of 2.5 [m]. The ventilation rate in the experiments was about 1.4 [kg/s], which was the fire induced rate with the specific geometry and fire size. The results from the experimental sprays should be representative for a room of this size, provided that the ventilation rate, wall properties and geometry are in the same order of magnitude.

From Froude Number similarity, shown in Chapter 2, the spray action in an offshore module, 4 times larger than the test model, should be as follows:

	Multiplication factor:	
Room length:	4	
Fuel burning rate:	$4^{5/2}$	= 32
Fire size:	$4^{5/2}$	= 32
Mean droplet diameter:	$4^{1/2}$	= 2
Water discharge rate:	$4^{5/2}$	= 32
Water application rate:	$4^{1/2}$	= 2
Droplet exit velocity:	$4^{1/2}$	= 2
Wall, ceiling thickness:	$(1/4)^{1/2}$	= 1/2, if the conductivity of the wall material is the same. There is no universal way of scaling wall properties, but for a specific purpose a combination of specific heat, density and conductivity may be found to represent a wall correct from one scale to another.

The scaling will provide that the temperatures and velocities are similar at homologous time and space. This means that for a certain time after ignition, the temperature at one specific coordinate in the enclosure will be the same as in another scale.

Geometry, flow pattern of the droplets in the spray and ambient temperature must be preserved.

If all these assumptions are fulfilled, the limit for extinguishment, the Spray Heat Absorption Ratio and other characteristic performances should be similar in large scale.

If the test model is scaled geometrically similar, 4 times bigger, 10 [m]·10 [m]·20 [m],

the test results indicates that a fire of 32 [MW], corresponding to a gas leakage rate of 0.7 [kg/s] of propane, may be extinguished by a water application rate of about 2.7 [l/(m^2·min)], with a full cone spray with mean droplet diameter of 1.2 [mm]. If mean droplet diameter is 2 [mm], a water application rate for extinguishment has to be about 7 [l/(m^2·min)].

Another way to use the scaling scheme is to vary other parameters than the length scale, provided that all other variables are the same. A maximum fire size which can be extinguished by a water spray with an application rate as defined by the NFPA guidelines, at a length scale 4 times bigger than the test model, can be calculated by rearranging the scaling equations:

Fire size: $L^{5/2}$

Water application rate: $L^{1/2}$

Fire size/water application rate: $L^{5/2}/L^{1/2} = L^2$

For the same length scale, 4/1, the scale of fire size to water application rate will be $1^2 = 1$.

A water application rate of 2.7 [l/(m^2·min)] is supposed to extinguish a fire of 32 [MW]. A water application rate of 10 [l/(m^2·min)] will the extinguish a fire 10/2.7 times the fire size extinguished at a water application rate of 2.7 [l/(m^2·min)], 32·10/2.7 [MW] = 119 [MW].

This corresponds to a leakage rate of propane of 2.6 [kg/s].

This scaling scheme has not been experimentally verified.

5 SUMMARY AND CONCLUSIONS

A series of experiments of fire fighting with water spray against enclosed gas fire has been done. The enclosure has a length 5 [m], width 2.5 [m] and height 2.5[m], and is ventilated through openings for air supply at the floor level, and smoke outlet at the ceiling level. The ventilation is induced by the fire itself through these openings. Three different spray nozzles producing water droplets of 0.6 - 1.6 [mm] mean diameter is tested, and a critical water application rate is found for each nozzle to extinguish a 1 [MW] propane fire.

Extinguishment of enclosed gas fires:

Gas fires can be extinguished by water sprays. The most probable mechanism of extinguishment is inerting of the fire zone with water vapour, combined with cooling of the reactants. The critical water vapour concentration seems to be about 30% locally to dilute oxygen to a concentration where combustion becomes impossible. To obtain this vapour concentration locally in the combustion zone, the critical global water vapour concentration seems to be about 40% to obtain total extinguishment in an enclosure.

In this series of experiments it is demonstrated through experiments that there is a sharp limit for instant extinguishment of gas fires in enclosures. The main factors affecting the interaction of a water spray and a fire plume is:

- the fire size and the preburn time
- the discharge rate of water
- the mean water droplet size
- ventilation rate
- location of the fuel versus the spray nozzle.

In the test enclosure of about 30 [m^3], sprays with mean water droplet diameter less than 1 [mm] are far more effective in extinguishment than sprays with larger droplet sizes.

Control of fire:

Water sprays used for control of enclosed fires works mainly by cooling the combustion products, objects and surfaces of the enclosure. The spray's ability to absorb heat is depending of some of the parameters as for extinguishment. The mean water droplet

diameter is not as important for fire control as for extinguishment, but still a spray with smaller droplets needs less water to cool the gases and surfaces than one with larger droplets. A spray with droplet size of about 0.6 [mm] controls the fire by keeping the temperature at a low level with a water application rate of 1.35 [l/(m^2·min)], as a spray with a droplet diameter of 1 [mm] uses a water application rate of 1.7 [l/(m^2·min)] to control a similar fire. The corresponding water application rate for a spray with droplets with a diameter of 1.3 [mm] is in the range of 3 [l/(m^2·min)].

The average temperature of the smoke inside a fire compartment is significantly reduced by the action of a water spray. The same is documented for the heat flux density from the fire to the walls of the fire compartment.

A reduction of soot content of the smoke leaving the fire compartment is measured during water spray action. This may be a result of the water washing out soot particles.

Scaling of fire characteristics and extinguishment:

A scaling scheme based on Froude Number similarity is proposed to be valid for water droplets in a fire. An indication based on this scaling scheme, using a 4 times larger length scale, is that a fire originating from a gas leakage of 0.7 [kg/s] of propane would be extinguished by a spray producing a water application rate of 2.7 [l/(m^2·min)], provided a water droplet diameter of 2 [mm]. This is much less than the design water application rates suggested by NFPA. The leakage rate is also among the smaller ones. If the same scaling scheme is followed to a full size offshore module (4 times bigger than the test model), a fire originating from a leakage rate of about 40 [kg/s] might be extinguished with a water application rate of 10 [l/(m^2·min)].

This has not been experimentally verified. A verification test has to be done at an increased length scale, since the wall influence on the fire development seems to be important to the time scale of evaporation of water droplets.

6. REFERENCES

1. Opstad, K.,Brandt, Ø. and Wighus, R.: Experimental Modelling of Liquid Pool Fires influenced by object, in a 1:4-scale Offshore Module. SINTEF report STF25 F89001, Trondheim, January 1989. (Restricted)

2. Opstad, K.,Brandt, Ø. and Wighus, R.: Experimental Modelling of Liquid Pool Fires in an Empty 1:4-scale Offshore Module. SINTEF report STF25 F89015, Trondheim, June 1989. (Restricted)

3. J.P.Stensaas, P.J.Hovde,and B.F.Magnussen: Physical Modelling of Enclosed Pool Fires - Development of Empirical Correlations. Proceedings of the Second International Symposium on Fire Safety Science, Tokyo 1988, Hemisphere Publishing Corporation, 1989. ISBN 0-89116-864-8

4. Hsiang-Cheng Kung: Cooling of Room Fires by Sprinkler Spray. Journal of Heat Transfer Vol. 99, August 1977

5. Kokkala, M., Andsten, T. and Björkman, J.: Extinguishment of liquid fires with sprinklers and water sprays. VTT, Technical Research Centre of Finland, Research Reports 593, Espoo, 1989, ISBN 0358-3384-4

6. Braidech, M.M, and Neale, J.A.: The Mechanism of Extinguishment of Fire by Finely Divided Water. Underwrighter's Laboratories Inc. USA, 1955

7. Hong-Zeng You, Hsiang-Cheng Kung, Zhanxian Han: Spray cooling in room fires. Factory Mutual Research Corporation, Technical report FMRC J.I.0J0N9.-RA, March 1986

8. Gunnar Heskestad: Physical modeling of fire. Journal of Fire & Flammability, Vol. 6, July 1975

9. Gunnar Heskestad: Private communications, Trondheim 1986

10. Particle size vs. volume percentage for fulljet nozzles. Spraying Systems Co., Private communications 1991.

11. Spraying nozzles & accessories, Spraying Systems Co. Industrial catalog 50 M, 1987

12. McCaffrey, B.J., Heskestad, G.: A Robust Bidirectional Low-Velocity Probe for Flames and Fire Application. Combustion and Flame 26, 125-127 (1976)

13. Andreassen, Håvie, Krogstad, Nørsett, Aasen: Numeriske metoder (Numerical methods) Tapir, Trondheim 1980

14. Surface products: Room fire tests in full scale. NORDTEST method NT FIRE 025, Approved 1986.

15. Newman, J.F., Steciak, J.: Characterization of Particulates from Diffusion Flames. Combustion and Flame 67, 55-64, 1987

16. Pehlke, R.D., Jeyarajan, A. and Wada, H.: Summary of thermal properties for casting alloys and mold materials. University of Michigan, Department of Materials and Metallurgical Engineering, Ann Arbor, USA, 1982.

APPENDIX A EXPERIMENTAL SET-UP

A 1 THE TEST HALL AND THE SMOKE COLLECTION HOOD

The tests are performed in the large fire test hall at SINTEF - NBL. The dimensions of the hall are 18 ·36 [m^2] floor area and a height of 25 [m] at maximum. The hall has a displacement ventilation system supplying conditioned air from ducts in the floor, and extracting smoke at the ceiling level.

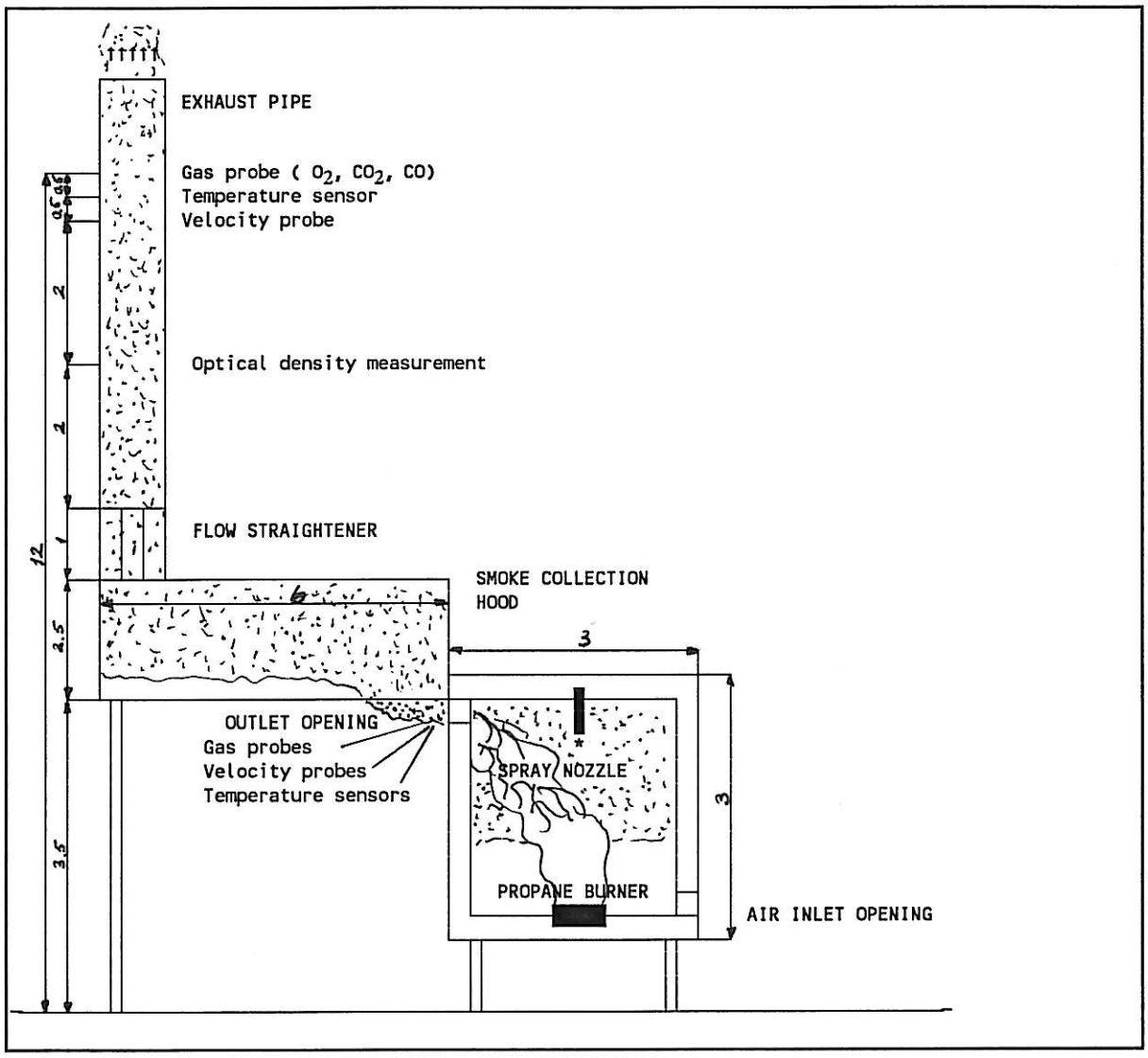

Figure A 1 Experiment set up in the water spray experiments. The enclosure is approximately 2.5 [m] wide, 2.5 [m] high and 5 [m]] long.

The enclosure where the fire and extinguishment tests are performed, is built below a smoke collection hood. The smoke leaves the collection hood by an exhaust pipe, which goes to the ambient through the ceiling. No separate fans are installed for smoke extraction from the collection hood, but the test hall is to some extent pressurized during an experiment to promote smoke flow through the exhaust pipe.

A 2 THE 1.4 SCALE MODEL OF AN OFFSHORE MODULE.

The test model compartment represents a process module of a typical offshore oilrig, at 1:4 scale. This is the same model used in projects examining the development of liquid pool fires, /1,2/. The model is modified to withstand the introduction of a water spray inside. The dimensions of the model compartment are shown in Figure A2 and A3.

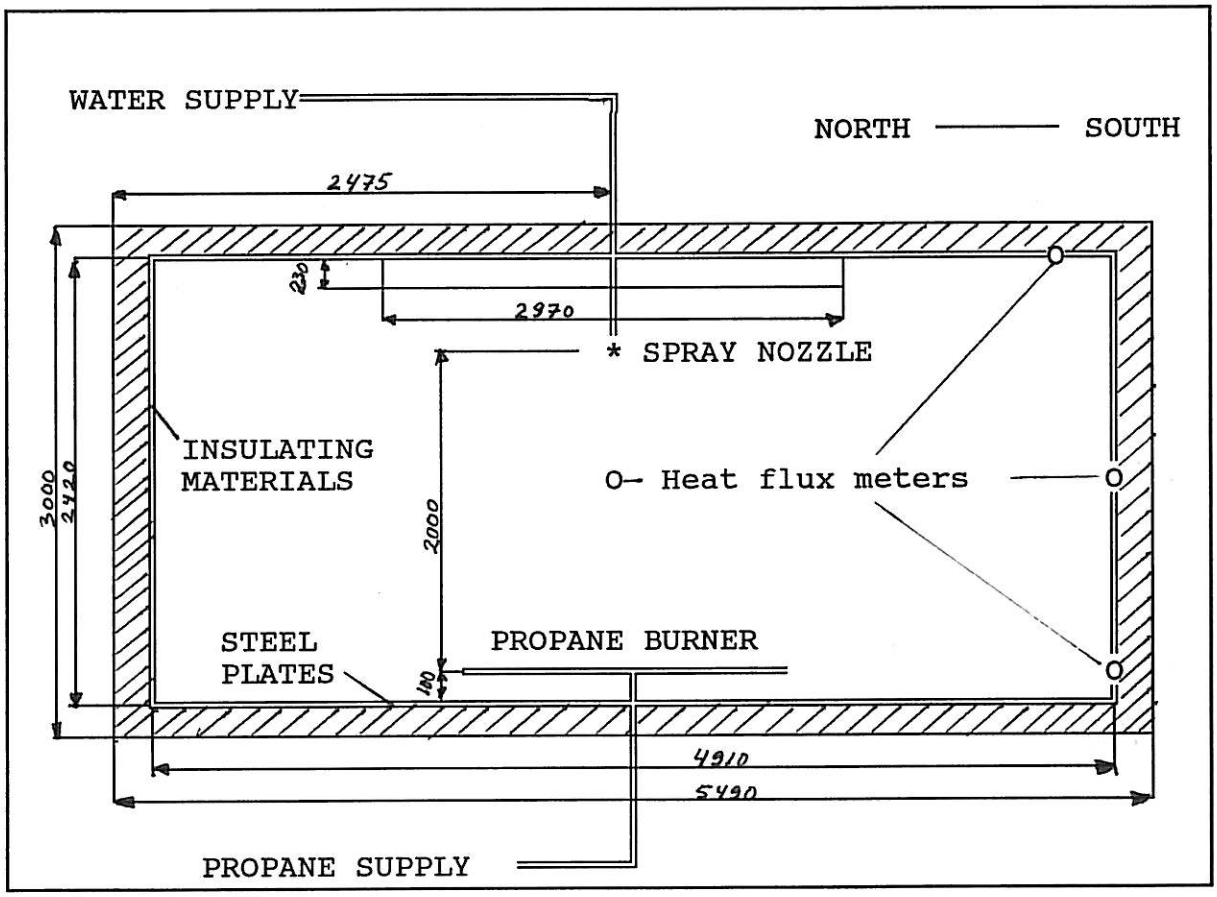

Figure A 2 *Plan view of the model compartment, central cross section. Dimensions in [mm].*

The air inlet opening covers the width of the model, and is 350 [mm] high. The outlet opening is located central at the top of the rear wall, with a width of 2970 [mm], and is 230 [mm] high.

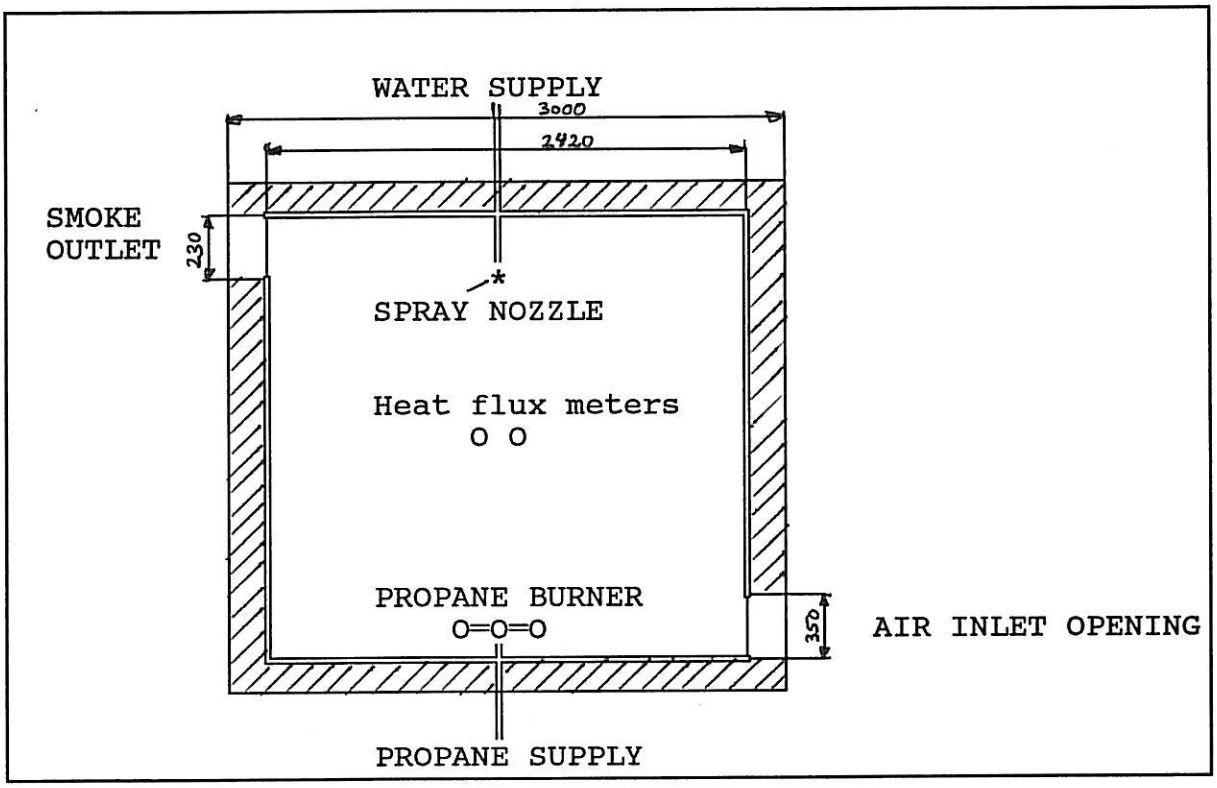

Figure A 3 *Side view of the model compartment, central cross section. Dimensions in [mm].*

The walls and the ceiling are constructed similar, with light weight concrete blocks named SIPOREX as the bearing construction, and with two layers of insulating materials as inner lining. The inner surfaces are covered with plates of the SKAMOLEX TYPE. The floor has a base of light weight concrete, then a layer of normal concrete, then a thin layer of light weight concrete, then the insulation plates of the type SKAMOLEX, and at last a cover of corrugated steel plates to catch the water. The dimensions of the wall and floor construction is shown in Figure A4.

The propane burner is constructed of three parallell 25 [mm] diameter steel pipes with closed ends, with a common central gas supply. The lenght of the pipes is 1250 [mm], and they are mounted with a centre distance of 100 [mm]. About 200 holes with 1 [mm] diameter are drilled in two lines at the upper half of the pipes' perimeter. The propane supply is then distributed evenly over a surface area 0.25 [m] · 1.25 [m], which is the same pool area as in liquid pool fire tests.

The spray nozzle is located central in the ceiling, at a level of about 250 [mm] below the

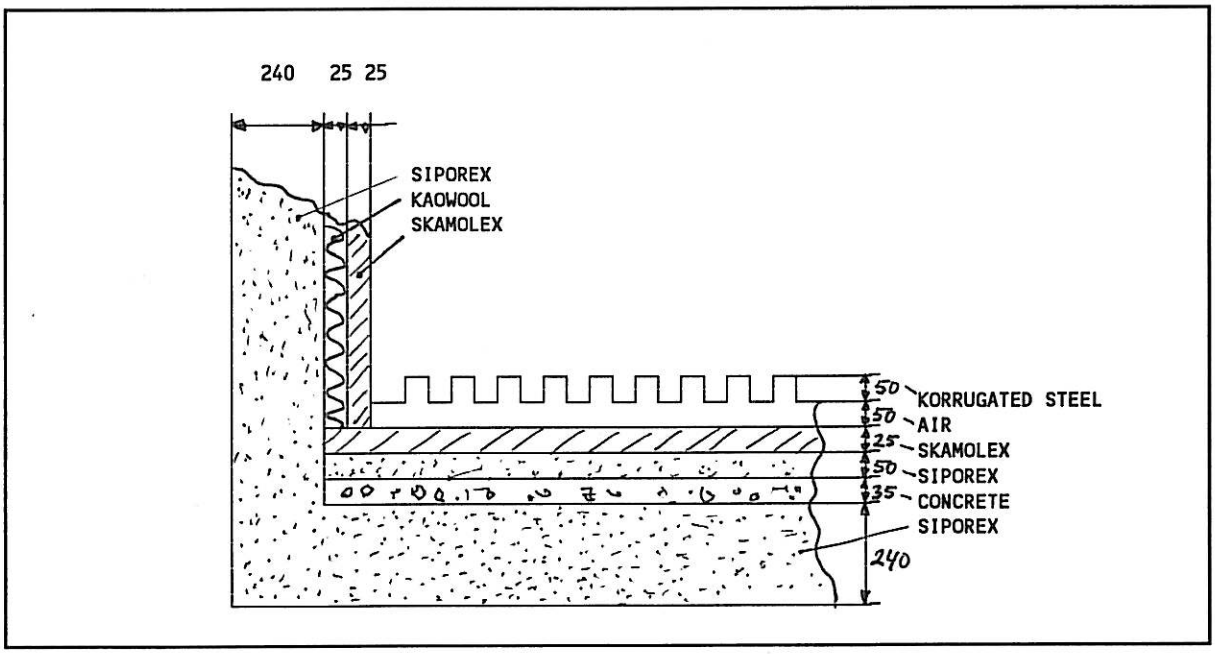

Figure A 4 *Cross-sectional view of the floor and walls of the model compartment. The ceiling construction is similar to the wall. Dimensions in [mm].*

inner lining. This is the location in all experiments with one nozzle. In the experiments with two nozzles, the distance between the nozzles is 2500 [mm], and the nozzles are located along the centre line of the north - south axis of the model.

A 3 THE SPRAY NOZZLES

The spray nozzles are chosen from commercial types, to represent nozzles used in full scale. Real deluge nozzles or sprinklers can not be used in scale experiments, since they have too large water discharge rates, or too large droplet size. The normal water application rates in full scale are typically 10 - 20 [l/(m^2 · min)], varying with the expected fire load in the actual area. The application rates scaled down to 1:4-scale, using Froude Number similarity, give rates just half of the full scale rates, which are 5 - 10 [l/(m^2 · min)]. The nozzles are chosen to give water discharge rates to give application rates in this order of magnitude. The nozzle characteristics are shown in the producer's specifications, reproduced in Figures A5, A6 and A7.

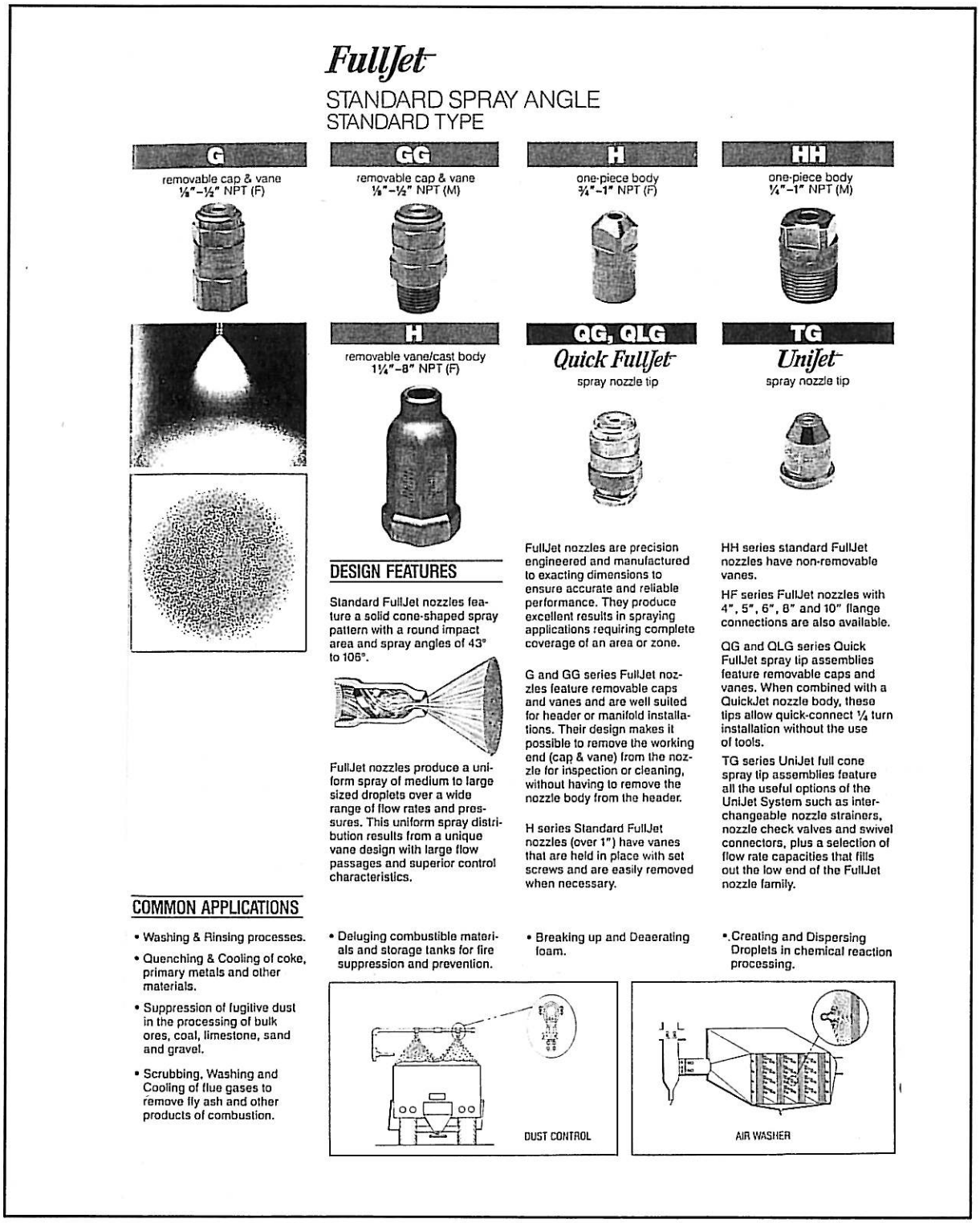

Figure A 5 Producer's description of the nozzle type used in the experiments /11/.

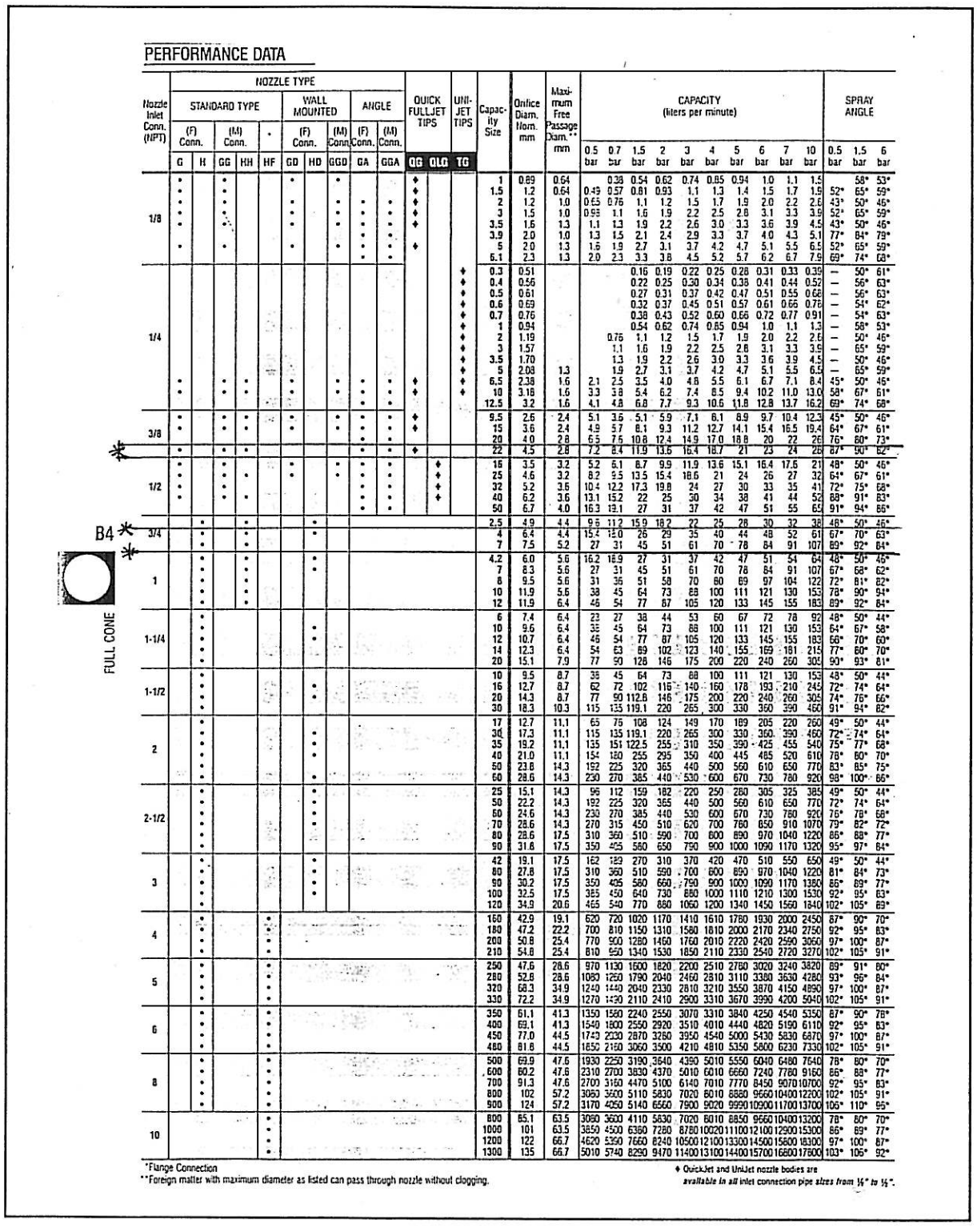

PERFORMANCE DATA

Nozzle Inlet Conn. (NPT)	NOZZLE TYPE: STANDARD TYPE (F) Conn. G	STANDARD TYPE (F) Conn. H	STANDARD TYPE (M) Conn. GG	STANDARD TYPE (M) Conn. HH	STANDARD TYPE · HF	WALL MOUNTED (F) Conn. GD	WALL MOUNTED (M) Conn. HD	ANGLE (F) Conn. GGD	ANGLE (M) Conn. GA	ANGLE (M) Conn. GGA	QUICK FULLJET TIPS QG	QUICK FULLJET TIPS QLG	UNI-JET TIPS TG	Capacity Size	Orifice Diam. Nom. mm	Maximum Free Passage Diam.** mm	CAPACITY (liters per minute) 0.5 bar	0.7 bar	1.5 bar	2 bar	3 bar	4 bar	5 bar	6 bar	7 bar	10 bar	SPRAY ANGLE 0.5 bar	1.5 bar	6 bar
1/8	•	•	•			•		•			♦			1	0.89	0.64		0.38	0.54	0.62	0.74	0.85	0.94	1.0	1.1	1.5		58°	53°
	•	•	•			•		•	•	•	♦			1.5	1.2	0.64	0.49	0.57	0.81	0.93	1.1	1.3	1.4	1.5	1.7	1.9	52°	65°	59°
	•	•	•			•		•	•	•	♦			2	1.2	1.0	0.65	0.76	1.1	1.2	1.5	1.7	1.9	2.0	2.2	2.6	43°	50°	46°
	•	•	•			•		•	•	•	♦			3	1.5	1.0	0.98	1.1	1.6	1.9	2.2	2.5	2.8	3.1	3.3	3.9	52°	65°	59°
	•	•	•			•		•	•	•	♦			3.5	1.6	1.3	1.1	1.3	1.9	2.2	2.6	3.0	3.3	3.6	3.9	4.5	43°	50°	46°
									•	•				3.9	2.0	1.0	1.3	1.5	2.1	2.4	2.9	3.3	3.7	4.0	4.3	5.1	77°	84°	79°
	•	•	•			•		•	•	•	♦			5	2.0	1.3	1.6	1.9	2.7	3.1	3.7	4.2	4.7	5.1	5.5	6.5	52°	65°	59°
									•	•				6.1	2.3	1.3	2.0	2.3	3.3	3.8	4.5	5.2	5.7	6.2	6.7	7.9	69°	74°	68°
1/4													♦	0.3	0.51				0.16	0.19	0.22	0.25	0.28	0.31	0.33	0.39	—	50°	61°
													♦	0.4	0.56				0.22	0.25	0.30	0.34	0.38	0.41	0.44	0.52	—	56°	63°
													♦	0.5	0.61				0.27	0.31	0.37	0.42	0.47	0.51	0.55	0.68	—	56°	63°
													♦	0.6	0.69				0.32	0.37	0.45	0.51	0.57	0.61	0.66	0.78	—	54°	62°
													♦	0.7	0.76				0.38	0.43	0.52	0.60	0.66	0.72	0.77	0.91	—	54°	63°
													♦	1	0.94				0.54	0.62	0.74	0.85	0.94	1.0	1.1	1.3	—	58°	53°
													♦	2	1.19			0.76	1.1	1.2	1.5	1.7	1.9	2.0	2.2	2.6	—	50°	46°
													♦	3	1.57			1.1	1.6	1.9	2.2	2.5	2.8	3.1	3.3	3.9	—	65°	59°
													♦	3.5	1.70			1.3	1.9	2.2	2.6	3.0	3.3	3.6	3.9	4.5	—	50°	46°
													♦	5	2.08	1.3		1.9	2.7	3.1	3.7	4.2	4.7	5.1	5.5	6.5	—	65°	59°
	•		•	•		•		•	•	•	♦		♦	6.5	2.38	1.6	2.1	2.5	3.5	4.0	4.8	5.5	6.1	6.7	7.1	8.4	45°	50°	46°
	•		•	•		•		•	•	•	♦		♦	10	3.16	1.6	3.3	3.8	5.4	6.2	7.4	8.5	9.4	10.2	11.0	13.0	58°	67°	61°
									•	•				12.5	3.2	1.6	4.1	4.8	6.8	7.7	9.3	10.6	11.8	12.8	13.7	16.2	69°	74°	68°
3/8	•		•	•		•		•	•	•	♦			9.5	2.6	2.4	5.1	3.6	5.1	5.9	7.1	8.1	8.9	9.7	10.4	12.3	45°	50°	46°
	•		•	•		•		•	•	•	♦			15	3.6	2.4	4.9	5.7	8.1	9.3	11.2	12.7	14.1	15.4	16.5	19.4	64°	67°	61°
									•	•				20	4.0	2.8	6.5	7.5	10.8	12.4	14.9	17.0	18.8	20	22	26	76°	80°	73°
B4 *	•		•	•					•	•	♦			22	4.5	2.8	7.2	8.4	11.9	13.6	16.4	18.7	21	23	24	28	87°	90°	82°
	•		•			•		•	•	•			♦	16	3.5	3.2	5.2	6.1	8.7	9.9	11.9	13.6	15.1	16.4	17.6	21	48°	50°	46°
	•		•	•		•		•	•	•			♦	25	4.6	3.2	8.2	9.5	13.5	15.4	18.6	21	24	26	27	32	64°	67°	61°
1/2	•		•	•					•	•			♦	32	5.2	3.6	10.4	12.2	17.3	19.8	24	27	30	33	35	41	72°	75°	68°
	•		•	•					•	•			♦	40	6.2	3.6	13.1	15.2	22	25	30	34	38	41	44	52	88°	91°	83°
									•	•				50	6.7	4.0	16.3	19.1	27	31	37	42	47	51	55	65	91°	94°	86°
3/4 *		•		•			•							2.5	4.9	4.4	9.8	11.2	15.9	18.2	22	25	28	30	32	38	46°	50°	46°
		•		•			•							4	6.4	4.4	15.4	18.0	26	29	35	40	44	48	52	61	67°	70°	63°
		•		•			•							7	7.5	5.2	27	31	45	51	61	70	78	84	91	107	89°	92°	84°
FULL CONE *		•		•			•							4.2	6.0	5.6	16.2	18.9	27	31	37	42	47	51	54	64	48°	50°	46°
1		•		•			•							7	8.3	5.6	27	31	45	51	61	70	78	84	91	107	67°	68°	62°
		•		•										8	9.5	5.6	31	36	51	58	70	80	89	97	104	122	72°	81°	82°
		•		•										10	11.9	5.6	38	45	64	73	88	100	111	121	130	153	78°	90°	94°
		•		•										12	11.9	6.4	46	54	77	87	105	120	133	145	155	183	89°	92°	84°
1-1/4		•					•							6	7.4	6.4	23	27	38	44	53	60	67	72	78	92	48°	50°	44°
		•					•							10	9.6	6.4	35	45	64	73	88	100	111	121	130	153	64°	67°	58°
		•												12	10.7	6.4	46	54	77	87	105	120	133	145	155	183	66°	70°	60°
		•												14	12.3	6.4	54	63	89	102	123	140	155	169	181	215	77°	80°	70°
		•												20	15.1	7.9	77	90	128	146	175	200	220	240	260	305	90°	93°	81°
1-1/2		•					•							10	9.5	8.7	38	45	64	73	88	100	111	121	130	153	48°	50°	44°
		•					•							16	12.7	8.7	62	72	102	116	140	160	178	193	210	245	72°	74°	64°
		•												20	14.3	8.7	77	90	112.8	146	175	200	220	240	260	305	74°	76°	66°
		•												30	18.3	10.3	115	135	119.1	220	265	300	330	360	390	460	91°	94°	82°
2		•					•							17	12.7	11.1	65	75	108	124	149	170	189	205	220	260	49°	50°	44°
		•					•							30	17.3	11.1	115	135	119.1	220	265	300	330	360	390	460	72°	74°	64°
		•					•							35	19.2	11.1	135	151	122.5	255	310	350	390	425	455	540	75°	77°	68°
		•					•							40	21.0	11.1	154	180	255	295	350	400	445	485	520	610	78°	80°	70°
		•												50	23.8	14.3	192	225	320	365	440	500	560	610	650	770	83°	85°	75°
		•					•							60	28.6	14.3	230	270	385	440	530	600	670	730	780	920	98°	100°	86°
2-1/2		•					•							25	15.1	14.3	96	112	159	182	220	250	280	305	325	385	49°	50°	44°
		•					•							50	22.2	14.3	192	225	320	365	440	500	560	610	650	770	72°	74°	64°
		•					•							60	24.6	14.3	230	270	385	440	530	600	670	730	780	920	76°	78°	68°
		•												70	28.6	14.3	270	315	450	510	620	700	780	850	910	1070	79°	82°	72°
		•												80	28.6	17.5	310	360	510	590	700	800	890	970	1040	1220	86°	88°	77°
		•												90	31.8	17.5	350	405	580	650	790	900	1000	1090	1170	1320	95°	97°	84°
3		•					•							42	19.1	17.5	162	189	270	310	370	420	470	510	550	650	49°	50°	44°
		•					•							80	27.8	17.5	310	360	510	590	700	800	890	970	1040	1220	81°	84°	73°
		•					•							90	30.2	17.5	350	405	580	660	790	900	1000	1090	1170	1380	86°	89°	77°
		•					•							100	32.5	17.5	385	450	640	730	880	1000	1110	1210	1300	1530	92°	95°	83°
		•					•							120	34.9	20.6	465	540	770	880	1060	1200	1340	1450	1560	1840	102°	105°	89°
4		•			•									160	42.9	19.1	620	720	1020	1170	1410	1610	1780	1930	2000	2450	87°	90°	70°
		•			•									180	47.2	22.2	700	810	1150	1310	1580	1810	2000	2170	2340	2750	92°	95°	83°
		•			•									200	50.8	25.4	770	900	1280	1460	1760	2010	2220	2420	2590	3060	97°	100°	87°
		•			•									210	54.8	25.4	810	950	1340	1530	1850	2110	2330	2540	2720	3270	102°	105°	91°
5		•			•									250	47.6	28.6	970	1130	1600	1820	2200	2510	2760	3020	3240	3820	89°	91°	80°
		•			•									280	52.8	28.6	1080	1260	1790	2040	2460	2810	3110	3380	3630	4280	93°	96°	84°
		•			•									320	68.3	34.9	1240	1440	2040	2330	2810	3210	3550	3870	4150	4890	97°	100°	87°
		•			•									330	72.2	34.9	1270	1490	2110	2410	2900	3310	3670	3990	4200	5040	102°	105°	91°
6		•			•									350	61.1	41.3	1350	1560	2240	2550	3070	3310	3840	4250	4540	5350	87°	90°	78°
		•			•									400	69.1	41.3	1540	1800	2550	2920	3510	4010	4440	4820	5190	6110	92°	95°	83°
		•			•									450	77.0	44.5	1740	2030	2870	3260	3950	4540	5000	5430	5830	6870	97°	100°	87°
		•			•									480	81.8	44.5	1850	2160	3060	3500	4210	4810	5350	5800	6230	7330	102°	105°	91°
8		•			•									500	69.9	47.6	1930	2250	3190	3640	4390	5010	5550	6040	6480	7640	78°	80°	70°
		•			•									600	80.2	47.6	2310	2700	3830	4370	5010	6010	6660	7240	7780	9160	86°	88°	77°
		•			•									700	91.3	47.6	2700	3160	4470	5100	6140	7010	7770	8450	9070	10700	92°	95°	83°
		•			•									800	102	57.2	3060	3600	5110	5830	7020	8010	8880	9660	10400	12200	102°	105°	91°
		•			•									900	124	57.2	3170	4050	5140	6560	7900	9020	9990	10900	11700	13700	106°	110°	95°
10					•									800	85.1	63.5	3060	3600	4110	5830	7020	8010	8850	9660	10400	13200	78°	80°	70°
					•									1000	101	63.5	3850	4500	6360	7280	8780	10020	11100	12100	12900	15300	86°	89°	77°
					•									1200	122	66.7	4620	5390	7660	8240	10500	12100	13300	14500	15600	18300	97°	100°	87°
					•									1300	135	66.7	5010	5740	8290	9470	11400	13100	14400	15700	16800	17800	103°	106°	92°

*Flange Connection

**Foreign matter with maximum diameter as listed can pass through nozzle without clogging.

♦ QuickJet and UniJet nozzle bodies are available in all inlet connection pipe sizes from ⅛" to ½".

Figure A 6 *Water discharge rates at varying pressure, for the nozzle type used in the experiments /11/. The nozzles used are denoted H7, H4 and G22.*

SPRAY ANGLE AND COVERAGE

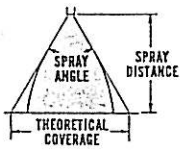

This table lists the theoretical coverage of spray patterns as calculated from the included spray angle of the spray and the distance from the nozzle orifice. These values are based on the assumption that the spray angle remains the same throughout entire spray distance. In actual practice, the tabulated spray angle does not hold for long spray distances. Write for Data Sheets on actual spray coverage.

Tabulated spray angles indicate approximate spray coverages based on water. In actual spraying, the effective spray angle varies with spray distance. If the spray coverage requirement is critical write for specific spray coverage data. Liquids more viscous than water form relatively smaller spray angles (or even a solid stream), depending upon viscosity, nozzle capacity and spraying pressure. Liquids with surface tensions lower than water will produce relatively wider spray angles than those listed for water.

Included Spray Angle	THEORETICAL COVERAGE AT VARIOUS DISTANCES (IN cm) FROM NOZZLE ORIFICE											
	5 cm	10 cm	15 cm	20 cm	25 cm	30 cm	40 cm	50 cm	60 cm	70 cm	80 cm	100 cm
5°	0.4	0.9	1.3	1.8	2.2	2.6	3.5	4.4	5.2	6.1	7.0	8.7
10°	0.9	1.8	2.6	3.5	4.4	5.3	7.0	8.8	10.5	12.3	14.0	17.5
15°	1.3	2.6	4.0	5.3	6.6	7.9	10.5	13.2	15.8	18.4	21.1	26.3
20°	1.8	3.5	5.3	7.1	8.8	10.6	14.1	17.6	21.2	24.7	28.2	35.3
25°	2.2	4.4	6.7	8.9	11.1	13.3	17.7	22.2	26.6	31.0	35.5	44.3
30°	2.7	5.4	8.0	10.7	13.4	16.1	21.4	26.8	32.2	37.5	42.9	53.6
35°	3.2	6.3	9.5	12.6	15.8	18.9	25.2	31.5	37.8	44.1	50.5	63.1
40°	3.6	7.3	10.9	14.6	18.2	21.8	29.1	36.4	43.7	51.0	58.2	72.8
45°	4.1	8.3	12.4	16.6	20.7	24.9	33.1	41.4	49.7	58.0	66.3	82.8
50°	4.7	9.3	14.0	18.7	23.3	28.0	37.3	46.6	56.0	65.3	74.6	93.3
55°	5.2	10.4	15.6	20.8	26.0	31.2	41.7	52.1	62.5	72.9	83.3	104
60°	5.8	11.6	17.3	23.1	28.9	34.6	46.2	57.7	69.3	80.8	92.4	115
65°	6.4	12.7	19.1	25.5	31.9	38.2	51.0	63.7	76.5	89.2	102	127
70°	7.0	14.0	21.0	28.0	35.0	42.0	56.0	70.0	84.0	98.0	112	140
75°	7.7	15.4	23.0	30.7	38.4	46.0	61.4	76.7	92.1	107	123	153
80°	8.4	16.8	25.2	33.6	42.0	50.4	67.1	83.9	101	118	134	168
85°	9.2	18.3	27.5	36.7	45.8	55.0	73.3	91.6	110	128	147	183
90°	10.0	20.0	30.0	40.0	50.0	60.0	80.0	100	120	140	160	200
95°	10.9	21.8	32.7	43.7	54.6	65.5	87.3	109	131	153	175	218
100°	11.9	23.8	35.8	47.7	59.6	71.5	95.3	119	143	167	191	238
110°	14.3	28.6	42.9	57.1	71.4	85.7	114	143	171	200	229	286
120°	17.3	34.6	52.0	69.3	86.6	104	139	173	208	243		
130°	21.5	42.9	64.3	85.8	107	129	172	215	257			
140°	27.5	55.0	82.4	110	137	165	220	275				
150°	37.3	74.6	112	149	187	224	299					
160°	56.7	113	170	227	284							
170°	114	229										

SPRAY DROPLET SIZE (ATOMIZATION)

Droplet size refers to the size of the individual spray droplets which comprise a nozzle's spray pattern. All of the spray droplets within a given spray are not the same size. Some of the different ways to describe droplet sizes within a spray are defined below:

(MVD) Median Volume Diameter also expressed as (VMD) Volume Median Diameter, $D_{V0.5}$ and, (MMD) Median Mass Diameter: A means of expressing droplet size in terms of the volume of liquid sprayed. The median volume diameter droplet size when measured in terms of volume (or mass) is a value where 50% of the total volume of liquid sprayed is made up of droplets with diameters larger than the median value and 50% smaller than the median value.

(SMD) Sauter Mean Diameter: A means of expressing the fineness of a spray in terms of the surface area produced by the spray. The Sauter Mean Diameter is the diameter of a droplet having the same volume to surface area ratio as the total volume of all the droplets to the total surface area of all the droplets.

(MND) Median Number Diameter: A means of expressing droplet size in terms of the number of droplets in the spray. This means that 50% of the droplets by count or number are smaller than the median diameter and 50% of the droplets are larger than the median diameter.

These droplet sizes are usually expressed in microns (micrometers). One micron equals 1/25,400 inch—or 0.001 mm. 3175 microns equals ⅛ inch.

Other than the effects of the specific material being sprayed (see pages 14 to 15), the three major factors affecting droplet size are nozzle capacity, spraying pressure, and spray pattern type. Lower spraying pressures provide larger droplet sizes, while higher spraying pressures yield smaller droplet sizes. The smallest droplet sizes are achieved by air atomizing nozzles. Generally speaking, the largest spray droplets are produced by full cone hydraulic spray nozzles. In the hydraulic spray nozzle series the smallest droplet sizes are produced by hollow cone spray nozzles, including the hydraulic atomizing type or fine spray.

Within each type of spray pattern the smallest capacities produce the smallest spray droplets, and the largest capacities produce the largest spray droplets. Because the Median Volume Diameter (MVD) is based on the volume of liquid sprayed it is a widely accepted reference and is used in the chart below.

More complete droplet size data is available on all types of spray nozzles. Contact your local Spraying Systems Co. representative for more information.

SPRAY PATTERN TYPE	0.7 bar		3 bar		7 bar	
	CAPACITY l/min	MVD MICRONS	CAPACITY l/min	MVD MICRONS	CAPACITY l/min	MVD MICRONS
AIR ATOMIZING	0.02 0.08	20 100	0.03 30	15 200	— 45	— 400
FINE SPRAY	— 0.83	— 375	0.1 1.6	110 330	0.2 2.6	110 290
HOLLOW CONE	0.19 45	360 3400	0.38 91	300 1900	0.61 144	200 1260
FLAT FAN	0.19 18.9	260 4300	0.38 38	220 2500	0.61 60	190 1400
FULL CONE	0.38 45	1140 4300	0.72 87	850 2800	1.1 132	500 1720

Based on a sampling of nozzles selected to show the wide range of possible droplet sizes available.

One Millimeter = 1000 Microns

ACTUAL DROPLET SIZES

- 500 Microns
- 1,200 Microns
- 5,500 Microns

Figure A 7 *Examples of expressions of spray droplet size, and typical water coverage characteristic for the nozzles used in the experiment. The actual nozzles are of the type Full Cone Nozzles /11/.*

A 3.1 WATER DROPLET SIZE

The water droplet size can be characterized in different ways. The most common way is to express it as Median Volume Diameter (MVD) or Median Mass Diameter (MMD).This is applied through this report. Other ways are described in Figure A 7, which is reproduced from the catalog of the spray nozzle producer, /11/.

Nozzle type	Pressure [bar]	Volume Median Diameter [μm]
HH-22	2.8	745
HH-22	7.0	550
HH-4	1.3	1200
HH-4	2.7	800
HH-7	0.7	1500
HH-7	2.5	1100

Figure A 8 Particle size distribution for various nozzles, reproduced from producer's specifications, /10/.

To obtain actual median droplet size for one special nozzle at various pressure levels, the scaling rules described by Kung, FMRC/6/, is used. The correlation is:

$$d_r = (\Delta p/\Delta p_o)^{-1/3} (D/D_o)^{2/3} \quad (2)$$

where

d_r : relative median droplet diameter [-]
Δp : actual pressure immediately upstream the nozzle
Δp_o : reference pressure
D : orifice diameter
D_o : reference orifice diameter

From the producer's product specifications, /10/, a presentation of the variation of median volume diameter versus the pressure is shown in Figure A 8. A correlation for

the mean diameter, represented by the median mass diameter, is then found for each nozzle, and the actual mean diameter is calculated for each actual pressure. The values of mean droplet diameter for the experiments are shown in Table A1.

Table A I *Calculated mean droplet diameter (Median Mass Diameter) representative for each experiment.*

Nozzle and Reference diameter	Date of experiment	Pressure at nozzle [bar]	Mean droplet diameter [micro m]	Water discharge [kg/s]
Nozzle H7	890719	2.54	1131	0.931
Ref. diam.	890721	0.95	1569	0.451
1100	890904	0.95	1569	0.441
	890906	0.99	1548	0.461
	890907	2.42	1149	0.766
	890912	1.84	1259	0.672
	890913	1.87	1252	0.696
Nozzle H4.	891020A	2.74	802	0.528
Ref. diam.	891020B	2.75	801	0.529
800	891023	2.26	855	0.475
	891025	1.31	1025	0.349
	891026	2.96		-
Nozzle G22	890915	7.12	547	0.362
Ref. diam.	891012	5.53	595	0.325
750	891013	4.58	633	0.291
	891017	2.79	747	0.269
	891019	3	729	-
	891027	4.17	653	0.568
	891030	4.95	617	0.622

A 3.2 WATER DISCHARGE RATE

The function giving water discharge rate is:

$$\dot{m}_{water} / \dot{m}_{wateref} = K \cdot (\Delta p / \Delta p_{ref})^{1/2}$$

where

$\dot{m}_{water}$	: actual water discharge rate [kg/s]
$\dot{m}_{wateref}$	: reference water discharge rate [kg/s]
K	: a proportionality constant for the actual nozzle
Δp	: actual pressure difference [bar]
Δp_{ref}	: reference pressure difference [bar]

In the experiments, the pressure is measured at the inlet to the model compartment, at the floor level. The corresponding water discharge rate is measured by collecting the run off water in a resevior, placed on a load cell. The constant K and a correction factor b is found for each nozzle during each experiment by regression analysis of different correlations between nozzle pressure and water discharge rates. The nozzle pressure is taken as the pressure measured at the floor level, minus a constant pressure difference of 0.2 [bar], due to the different level of 2.0 [m].

A list of the factors is shown in Table A2.

Table A II *Factors to be used by calculation of water discharge rate for the nozzles used in the experiments.*

Nozzle	K	b
H7	0.5517	-0.0848
H4	0.3505	-0.0521
G22	0.1313	0.0129

Function:

$$\dot{m}_{water}/\dot{m}_{water\ ref} = K \cdot (\Delta p / \Delta p_{ref})^{1/2} + b$$

A graphical presentation of the function of water application rate and nozzle pressure for the nozzles used is shown in Figure A 9.

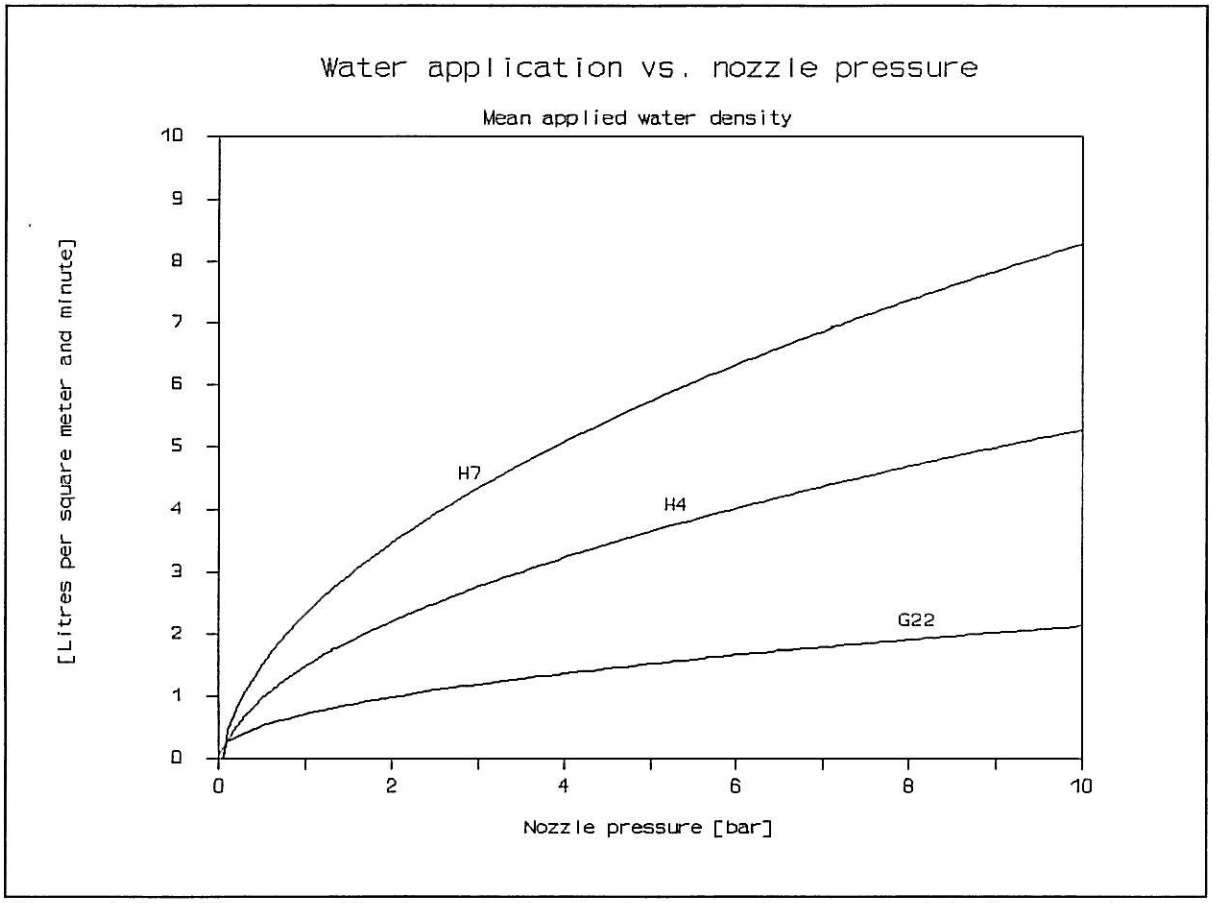

Figure A 9 Water application rate for the three nozzle types used in the experiments.

A 3.3 WATER DISTRIBUTION

The spray nozzles are specified as full cone sprays, giving a uniform distribution of water to a floor section. An study of the distribution of water was performed prior to the extinguishment experiments. A typical result is the water distribution of nozzle H7 at 3 [bar] pressure, shown in Figure A 10.

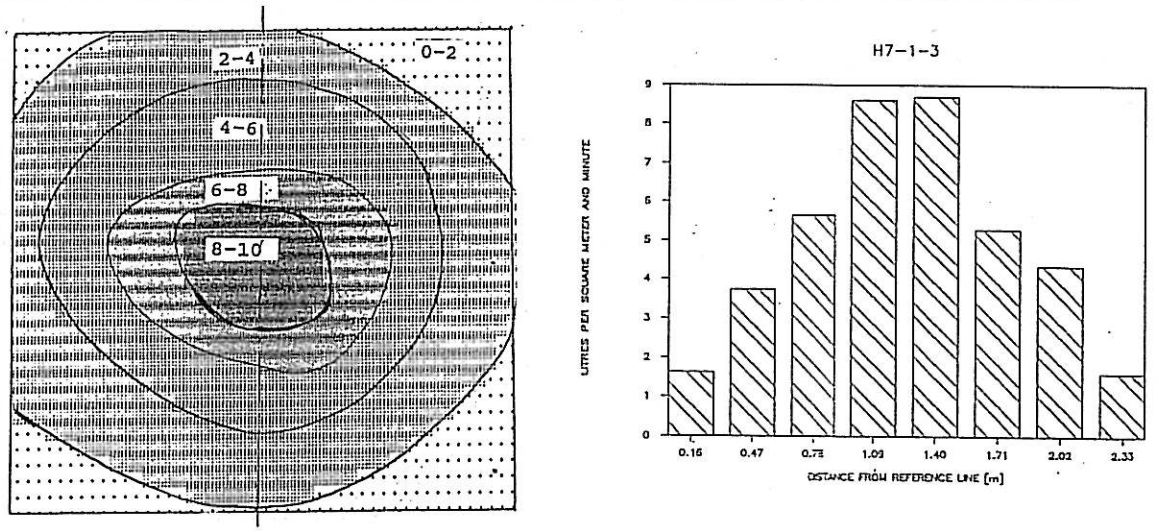

Figure A 10 *Water distribution with nozzle H7, with a pressure about 3 [bar]. Figure a) is an iso-plot made by an interpolation procedure. Figure b) represents delivered water application rate in [l/(m^2 ·min)], along the centre line.*

The actual water application rate (often denoted ADD, actual delivered density) in the centre of the area below the nozzle is almost the double of the water delivered in the outskirts of the field covered by the spray. The tests of the actual delivered water was done simply by distributing buckets at the floor, and locate the nozzle about 2 [m] above. The spray was activated and after about 5 minutes water flow, the buckets were weighed. The results are presented in Figures A10 and A11.

Figure A 11 shows the water distribution by two nozzles located with a horizontal distance 2 [m]. The overlapping zone does not give the full coverage of water at this configuration.

The test set up is shown in figure A 12.

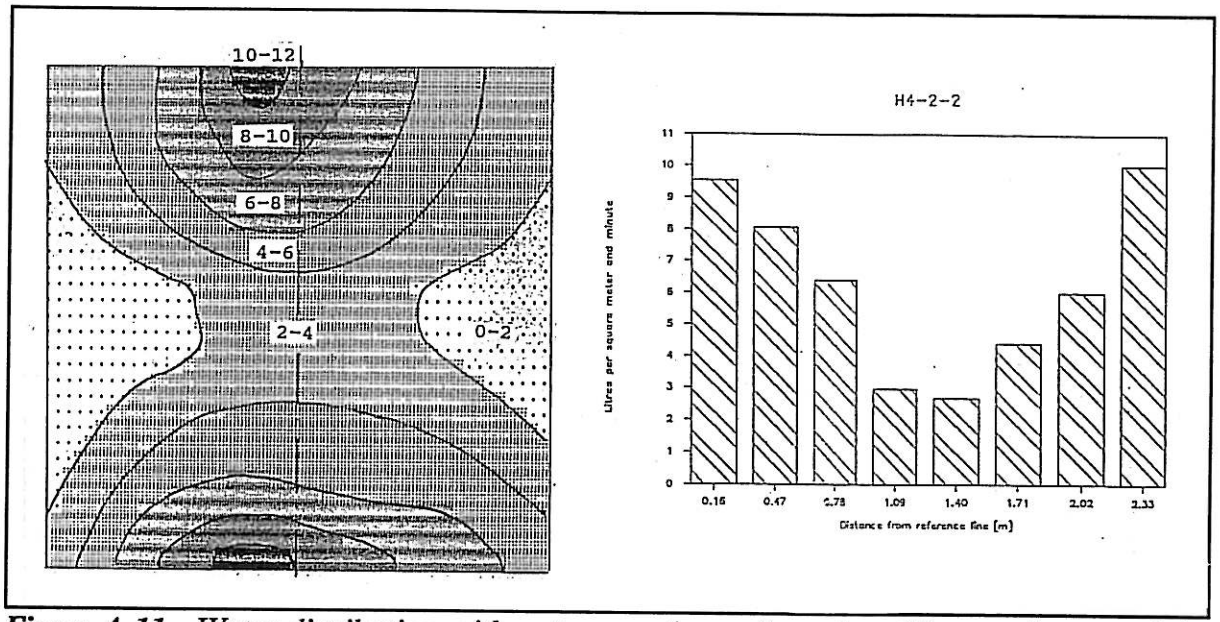

Figure A 11 *Water distribution with a two nozzle configuration. The nozzles are of the type H4, the water pressure is about 2 [bar].*

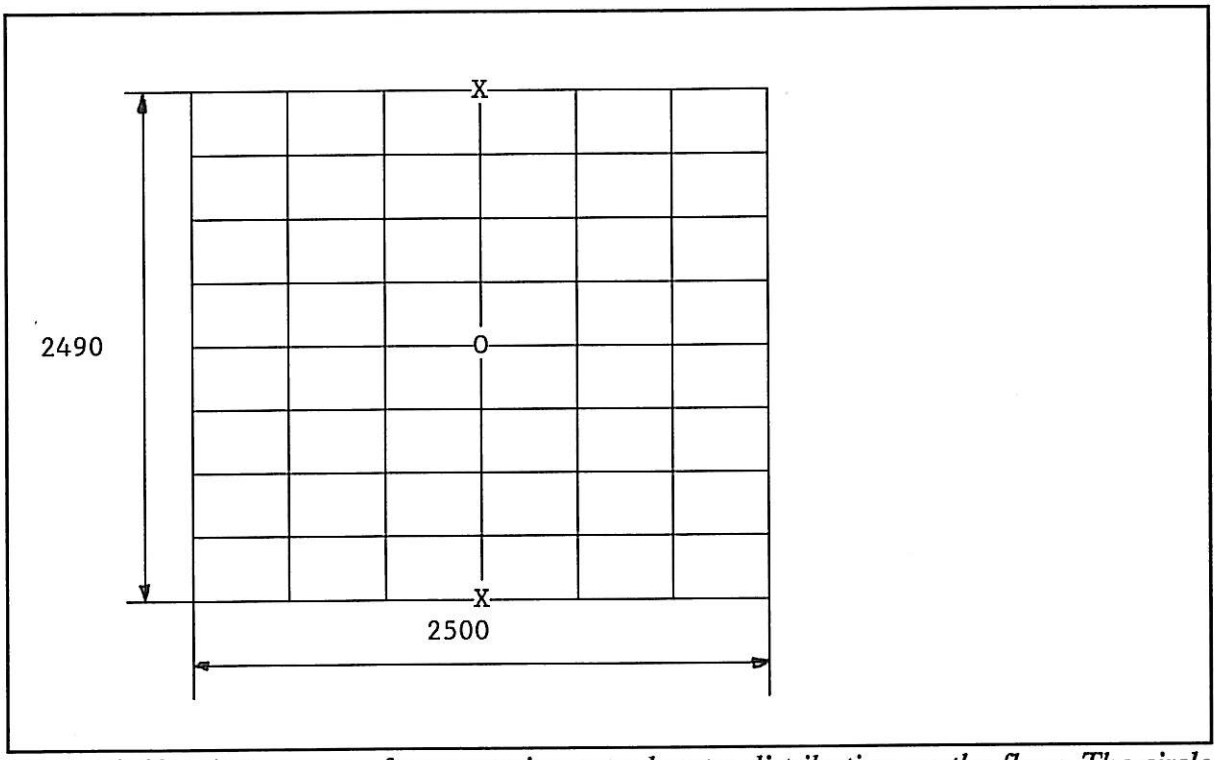

Figure A 12 *Arrangement for measuring actual water distribution on the floor. The circle in the centre indicateds a nozzle position of central positioned nozzle, as the X's represents the position when two nozzles were used. The lengths are in [mm].*

APPENDIX B DATA CONVERSION

B.1 THE EXPERIMENTAL DATA

The measured data are collected by the data acquisition system (DAS) and stored as a file at the computer. The data are calibrated by a Fortran program named M5, developed by SINTEF/NBL.

The original data are sampled every 10 second and stored as a DTA-file. The M5 program does the calculation on every time step. It is convenient to keep the amount of data as low as possible, which is done by the data compressing. The data are converted by transforming from ASCII files to binary format.

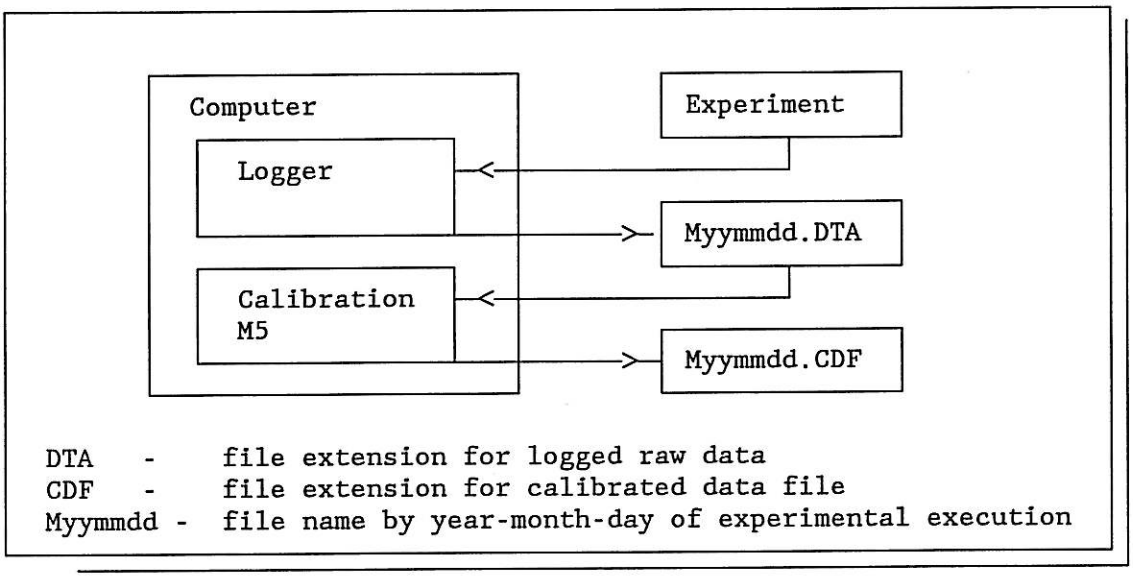

Figure B.1 Principles of the data acquisition system DAS and definition of short terms for file extensions. The data flow is indicated by the arrows.

A typical data file of DTA type is about one Kilobyte size. After the data processing it is reduced by factor of ten. A CDF file is roughly 100 kilo bytes and can be handled by common spread sheets available for personal computers.

Data files at SINTEF/NBL are available at MS-DOS formatted floppy disks.

B.2 DATA CHANNELS

The calibration program M5 is working by channel numbers, which correspond to the numbers created by the DAS system. The flow sheet in Figure B2 displays the channel numbers used in calculations, and the name of the subroutines in the program. The channel numbers are defined in Figure B3.

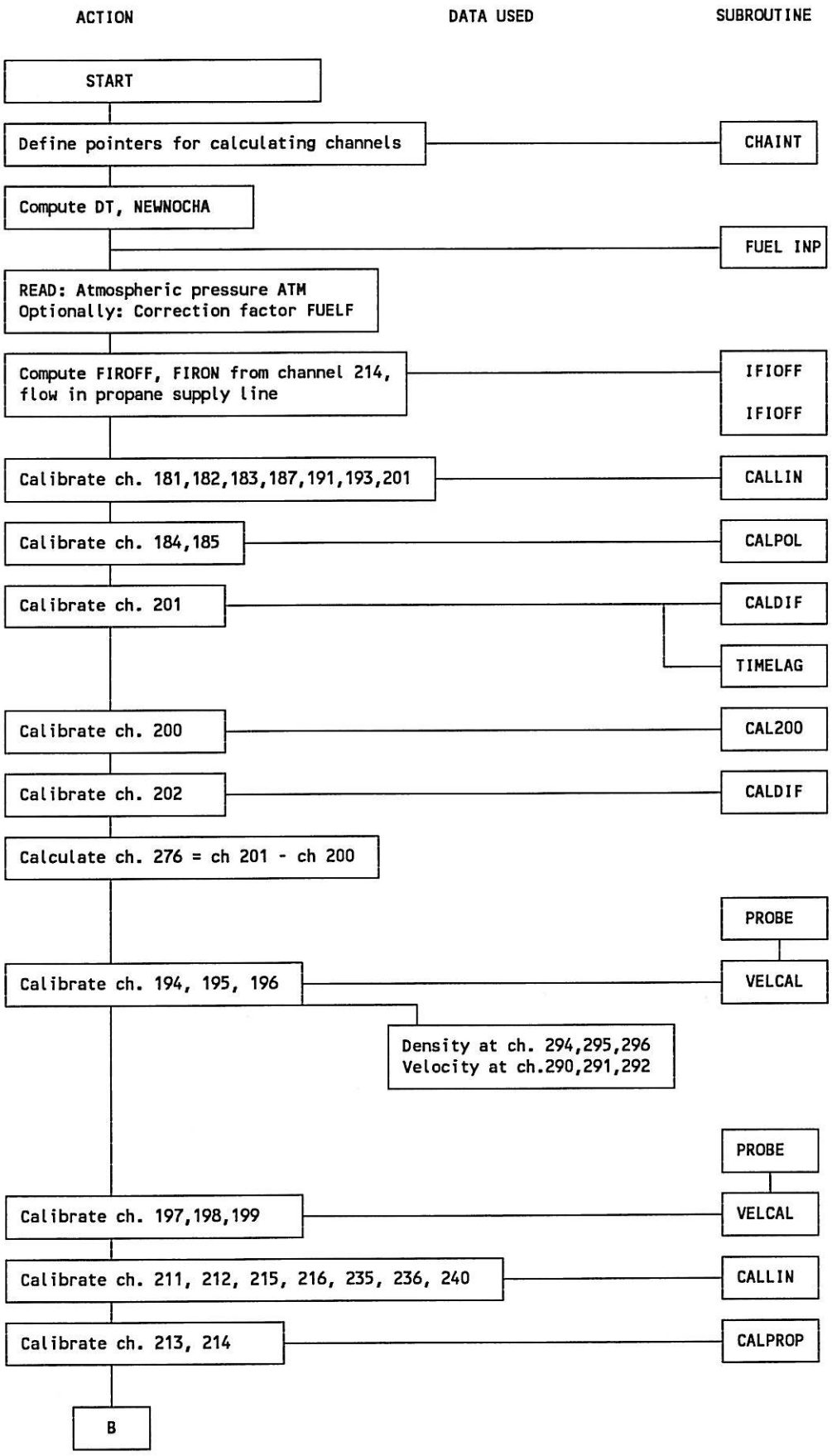
ACTION
DATA USED
SUBROUTINE
START
Define pointers for calculating channels
CHAINT
Compute DT, NEWNOCHA
FUEL INP
READ: Atmospheric pressure ATM
Optionally: Correction factor FUELF
Compute FIROFF, FIRON from channel 214,
flow in propane supply line
IFIOFF
IFIOFF
Calibrate ch. 181,182,183,187,191,193,201
CALLIN
Calibrate ch. 184,185
CALPOL
Calibrate ch. 201
CALDIF
TIMELAG
Calibrate ch. 200
CAL200
Calibrate ch. 202
CALDIF
Calculate ch. 276 = ch 201 - ch 200
PROBE
Calibrate ch. 194, 195, 196
VELCAL
Density at ch. 294,295,296
Velocity at ch.290,291,292
PROBE
Calibrate ch. 197,198,199
VELCAL
Calibrate ch. 211, 212, 215, 216, 235, 236, 240
CALLIN
Calibrate ch. 213, 214
CALPROP
B

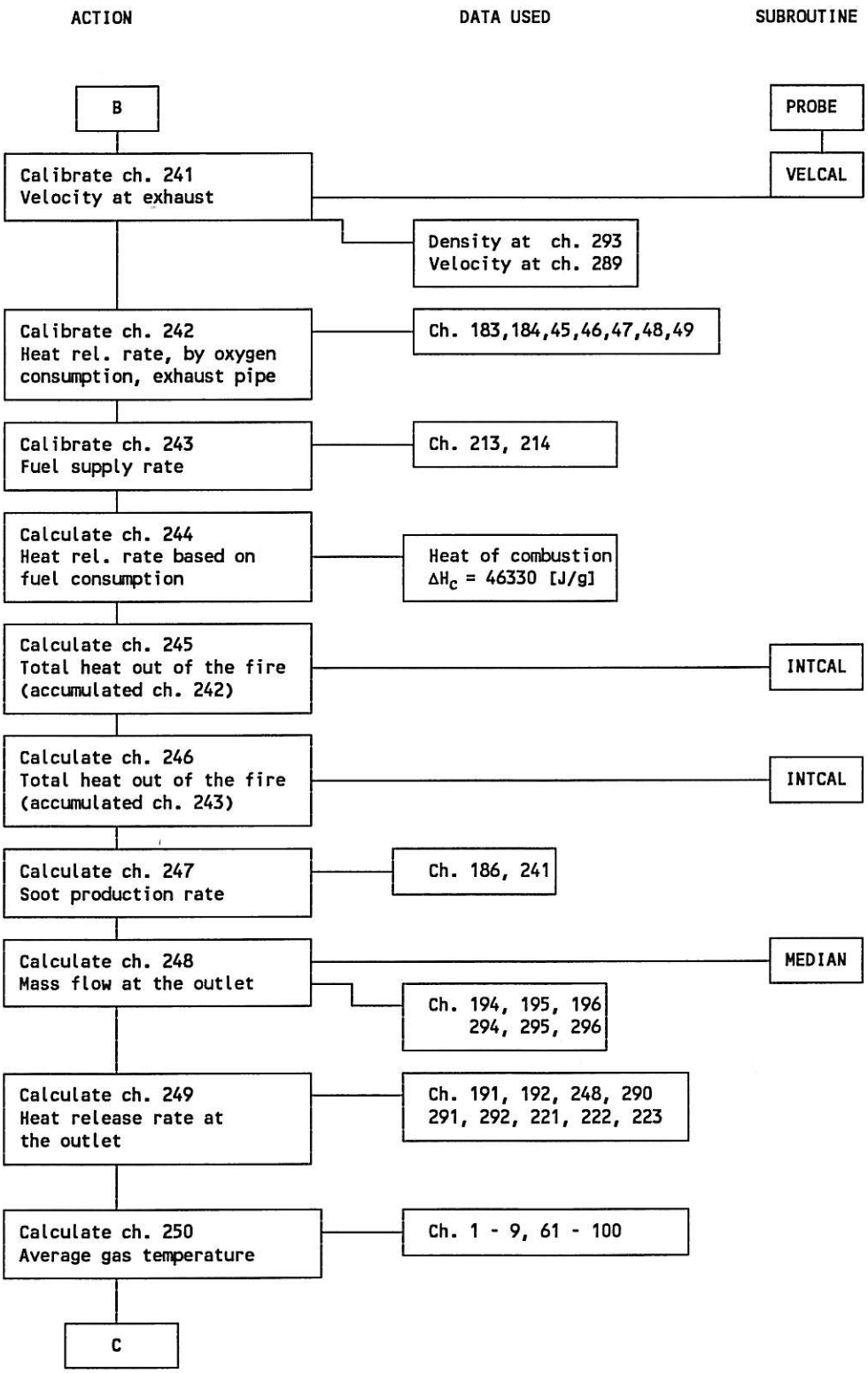
ACTION
DATA USED
SUBROUTINE
B
PROBE
Calibrate ch. 241
Velocity at exhaust
VELCAL
Density at ch. 293
Velocity at ch. 289
Calibrate ch. 242
Heat rel. rate, by oxygen
consumption, exhaust pipe
Ch. 183,184,45,46,47,48,49
Calibrate ch. 243
Fuel supply rate
Ch. 213, 214
Calculate ch. 244
Heat rel. rate based on
fuel consumption
Heat of combustion
ΔHc = 46330 [J/g]
Calculate ch. 245
Total heat out of the fire
(accumulated ch. 242)
INTCAL
Calculate ch. 246
Total heat out of the fire
(accumulated ch. 243)
INTCAL
Calculate ch. 247
Soot production rate
Ch. 186, 241
Calculate ch. 248
Mass flow at the outlet
MEDIAN
Ch. 194, 195, 196
294, 295, 296
Calculate ch. 249
Heat release rate at
the outlet
Ch. 191, 192, 248, 290
291, 292, 221, 222, 223
Calculate ch. 250
Average gas temperature
Ch. 1 - 9, 61 - 100
C

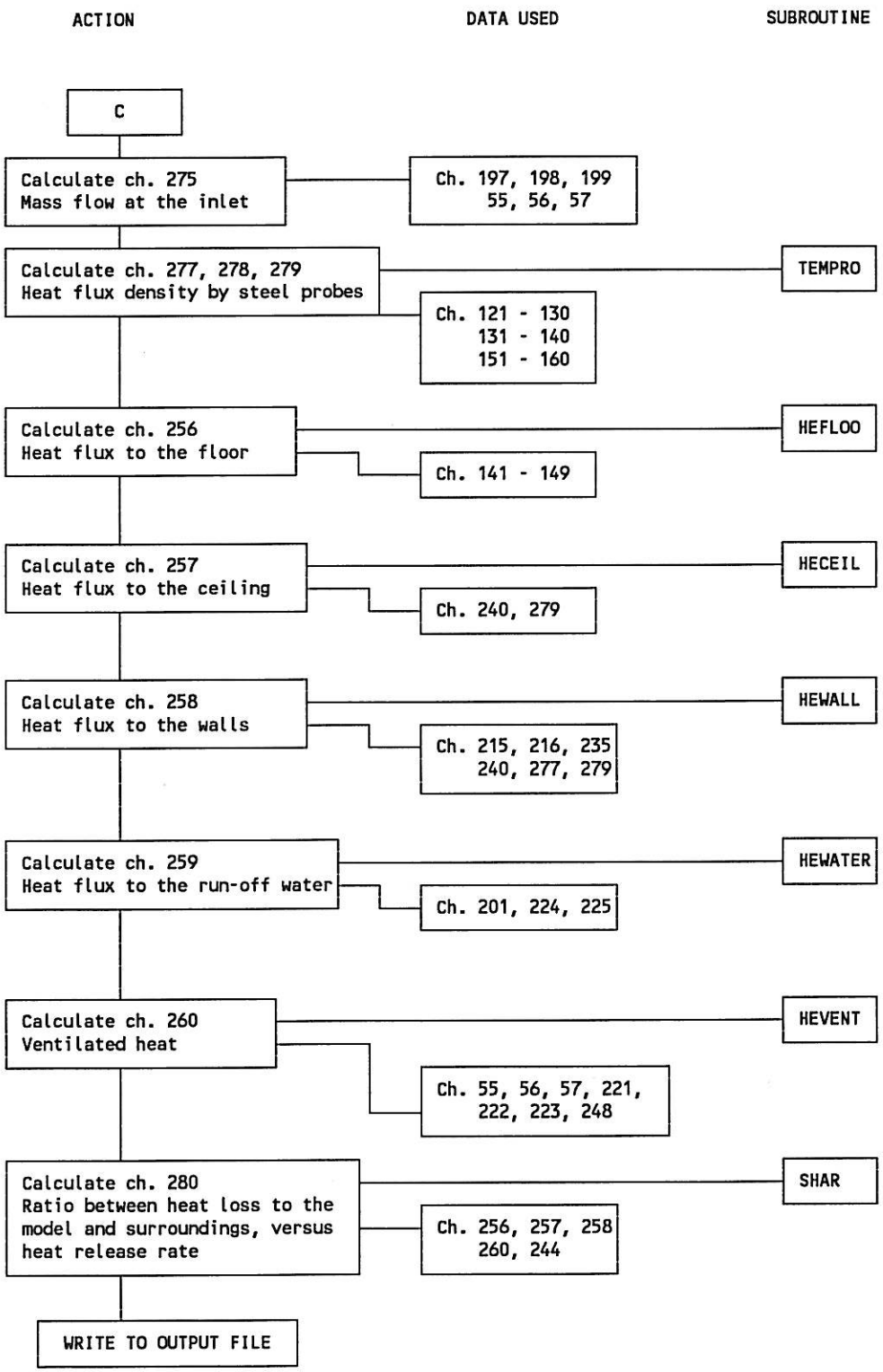

Figure B.2 *A flow sheet for the calculations done by the program M5. All channel numbers higher than 240 are created by the program. The channel numbers are defined by Figure B3. Subroutines are specific for the program M5, and are documented by the program listing.*

Table B.1 *The complete list of data channels logged and created from the experiments with water spray. The list is available as a data file. The file head gives the corresponding units to each channel. The X,Y and Z coordinates are related to the defined origo, see figure B.4. All space coordinates are in [mm]. (-1 at the X, Y and Z coordinates tells that there are no relations to origo.)*

```
@  SINTEF/NBL - KO 1988-11
@    (Experiments with water spray, M890721 - )
@  The identification (T-type) numbers are grouped in one of the
@  following numbers:
@  ____________________________________________________
@
@ -1  - unmeasured
@                                                        ┐
@  1  - temperature in gas                               │
@  2  - temperature in liquid                            │ Temperature in
@  3  - temperature in solid material                    │ Celsius degree
@  4  - temperature on surface of solid material         │ [°C]
@  5  - aspirated thermocouple                           │
@                                                        ┘
@  10 - time                [sec.]
@  11 - voltages            [volt]
@  12 - current             [amp.]
@  13 - pressure            [ Pa ]
@  14 - mass                [ g  ]
@
@  15 - velocity            [m/s   ]
@  16 - heat flux           [W/m²  ]
@  17 - mass flow           [g/s   ]
@  18 - mass flux           [g/m²·s]
@  19 - heat effect         [ W    ]
@
@  20 - Gas sampling line   [vol%]
@
@  31 - Light extinction
@  91 - Density             [kg/m3]
@  99 - No unit                                          COORDINATES
@
@ Channel no. Link no.  Comments              T        X        Y        Z
@============ ========  ====================== == ======== ======== ========
            0           Elapsed time          10       -1       -1       -1
            1       17                         1     1850      750     4500
            2       20                         1     1850     1250     4500
            3       23                         1     1850     1880     4500
            4       26                         1     1850     2380     4500
            5       15                         1     2320      250     4500
            6       18                         1     2320      750     4500
            7       21                         1     2320     1250     4500
            8       24                         1     2320     1880     4500
            9       27                         1     2320     2380     4500
           10       64                         4     2450      570     2500
           11       65                         4     2450     1250     2500
           12       66                         4     2450     2250     2500
           13       67                         3     2475     2250     2500
           14       68                         4     2450     2400     2500
           15       53                         4     2450      470     4500
           16       54                         4     2450     1250     4500
           17       55                         4     2450     2280     4500
           18       56                         3     2475     2280     4500
           19       56                         3     1250     2425     2500
           20       57                         4     1250     2400     2500
           41        1  Exhaust pipe 1         4       -1       -1       -1
           42        2  Exhaust hood 2         4       -1       -1       -1
           43        3  Exhaust hood 3         4       -1       -1       -1
           44        4  Exhaust hood 4         4       -1       -1       -1
```

45	5	Exhaust hood 5	1	-1	-1	-1
46	1	Exhaust pipe, r=500	4	-1	-1	-1
47	2	Exhaust pipe, r=400	1	-1	-1	-1
48	3	Exhaust pipe, r=250	1	-1	-1	-1
49	4	Exhaust pipe, r=000	1	-1	-1	-1
50	41		4	1250	2370	4950
51	42		4	1250	1250	4950
52	43		4	1250	250	4950
53	44		3	1250	2425	4500
54	45		4	1250	2400	4500
55		Air inlet compartment	4	-1	-1	-1
56		Air inlet compartment	4	-1	-1	-1
57	6	Air supply temperature	1	-1	-1	-1
61	41		1	2320	250	500
62	45		1	2320	1250	500
63	49		1	2320	2380	500
64	40		1	1850	250	500
65	44		1	1850	1250	500
66	48		1	1850	2380	500
67	39		1	1250	250	500
68	43		1	1250	1250	500
69	47		1	1250	2380	500
70	38		1	450	250	500
71	42		1	450	1250	500
72	46		1	450	2380	500
73	1		1	450	250	2500
74	5		1	450	1250	2500
75	9		1	450	2250	2500
76	2		1	800	250	2500
77	6		1	800	1250	2500
78	10		1	800	2250	2500
79	3		1	1250	250	2500
80	7		1	1250	1250	2500
81	11		1	1250	2250	2500
82	4		1	1850	250	2500
83	12		1	1850	2250	2500
84	8		1	1850	1250	2500
85	13		1	450	250	4500
86	16		1	450	750	4500
87	19		1	450	1250	4500
88	22		1	450	1880	4500
89	25		1	450	2380	4500
90	28		1	1250	125	4500
91	29		1	1250	250	4500
92	30		1	1250	380	4500
93	31		1	1250	500	4500
94	32		1	1250	630	4500
95	33		1	1250	750	4500
96	34		1	1250	880	4500
97	35		1	1250	1250	4500
98	36		1	1250	1875	4500
99	37		1	1250	2380	4500
100	14		1	1850	250	4500
101	46		4	50	2120	4500
102	47		4	50	1870	4500
103	48		4	50	1250	4500
104	49		4	50	250	4500
105	58		4	50	2030	2500
106	59		4	50	1250	2500
107	60		4	50	250	2500
108			1	1000	10	2500
109			4	1000	0	2500
110			3	1000	-25	2500
111	62		4	420	0	2500
112	61		4	50	0	2500
113	50		4	420	0	4500
114	52		4	1920	0	4500
115	63		4	1920	0	2500
121		Steel heat flux meter 1	4	1250	1250	4950
122		Steel heat flux meter 1	4	1250	1250	4950

123		Steel heat flux meter 1	4	1250	1250	4950
124		Steel heat flux meter 1	4	1250	1250	4950
125		Steel heat flux meter 1	4	1250	1250	4950
126		Steel heat flux meter 1	4	1250	1250	4950
127		Steel heat flux meter 1	4	1250	1250	4950
128		Steel heat flux meter 1	4	1250	1250	4950
129		Steel heat flux meter 1	4	1250	1250	4950
130		Steel heat flux meter 1	4	1250	1250	4950
131		Stainless st.heat flux meter 2	4	1250	1250	4950
132		Stainless st.heat flux meter 2	4	1250	1250	4950
133		Stainless st.heat flux meter 2	4	1250	1250	4950
134		Stainless st.heat flux meter 2	4	1250	1250	4950
135		Stainless st.heat flux meter 2	4	1250	1250	4950
136		Stainless st.heat flux meter 2	4	1250	1250	4950
137		Stainless st.heat flux meter 2	4	1250	1250	4950
138		Stainless st.heat flux meter 2	4	1250	1250	4950
139		Stainless st.heat flux meter 2	4	1250	1250	4950
140		Stainless st.heat flux meter 2	4	1250	1250	4950
141		Floor temperature	4	500	100	541
142		Floor temperature	4	1400	100	541
143		Floor temperature	4	2300	100	541
144		Floor temperature	4	500	100	1523
145		Floor temperature	4	1400	100	1523
146		Floor temperature	4	2300	100	1523
147		Floor temperature	4	500	100	2505
148		Floor temperature	4	1400	100	2505
149		Floor temperature	4	2300	100	2505
150		Floor temperature	4	1400	100	1423
151		Steel heat flux meter 3	4	50	1250	2500
152		Steel heat flux meter 3	4	50	1250	2500
153		Steel heat flux meter 3	4	50	1250	2500
154		Steel heat flux meter 3	4	50	1250	2500
155		Steel heat flux meter 3	4	50	1250	2500
156		Steel heat flux meter 3	4	50	1250	2500
157		Steel heat flux meter 3	4	50	1250	2500
158		Steel heat flux meter 3	4	50	1250	2500
159		Steel heat flux meter 3	4	50	1250	2500
160		Steel heat flux meter 3	4	50	1250	2500
181	PT 6	Velocity probe	13	-1	-1	-1
182	PT 6F	Velocity probe w/filter	13	-1	-1	-1
183		O_2 (exhaust pipe)	20	-1	-1	-1
184		CO_2 (exhaust pipe)	20	-1	-1	-1
185		CO (exhaust pipe)	20	-1	-1	-1
186		Optical density	31	-1	-1	-1
187	PT 10	Compartment pressure	13	210	100	4950
191		O_2 (outlet opening)	20	-1	-1	-1
192		CO_2 (outlet opening)	20	-1	-1	-1
193		CO (outlet opening)	20	-1	-1	-1
194	PT 3	Velocity outlet NORTH	15	-325	2285	1758
195	PT 4	Velocity outlet SOUTH	15	-325	2285	3244
196	PT 5	Velocity outlet CENTRE	15	-325	2285	2500
197	PT 7	Velocity inlet NORTH	15	2845	175	1278
198	PT 9	Velocity inlet CENTRE	15	2845	175	2505
199	PT 8	Velocity inlet SOUTH	15	2845	175	3732
200	PT 12	Water mass rate in	17	-1	-1	-1
201		Water mass rate out	17	-1	-1	-1
202		Propane mass, weight	#14	-1	-1	-1
211		Temp. propane supply	1	-1	-1	-1
212		Propane pressure	13	-1	-1	-1
213		Flow propane line 1	17	-1	-1	-1
214		Flow propane line 2	17	-1	-1	-1
215	HF 1	Heat flux SOUTH wall	16	1250	1250	4950
216	HF 2	Heat flux SOUTH wall	16	1250	250	4950
221	1	Smoke outlet NORTH	1	-325	2285	1758
222	2	Smoke outlet CENTRE	1	-325	2285	2500
223	3	Smoke outlet SOUTH	1	-325	2285	3244
224		Water supply temp.	2	-1	-1	-1
225		Water outlet temp.	2	-1	-1	-1
226		Water reservoir temp.	2	-1	-1	-1
235	HF 3	Heat flux front wall	16	2450	1250	2500

236	HF 4	Heat flux front wall	16	2450	1250	4085
240	HF 5	Heat flux ceiling	16	1250	2400	4500

@ -- Calculated and created channels by the calibration program

241	Velocity, exhaust pipe	15	-1	-1	-1
242	Heat release [O_2]	19	-1	-1	-1
243	Fuel supply rate	17	-1	-1	-1
244	Heat release [Fuel]	19	-1	-1	-1
245	Accumulated cha. 242	99	-1	-1	-1
246	Accumulated cha. 244	99	-1	-1	-1
247	Soot production	17	-1	-1	-1
248	Mass flow at the outlet	17	-1	-1	-1
249	Heat rel. at the outlet	19	-1	-1	-1
250	Average gas temperature	1	-1	-1	-1
256	Heat to floor	19	-1	-1	-1
257	Heat to ceiling	19	-1	-1	-1
258	Heat to walls	19	-1	-1	-1
259	Heat to run-off water	19	-1	-1	-1
260	Ventilated heat	19	-1	-1	-1
276	Net evaporated water	17	-1	-1	-1
277	Heat flux (121 -130)	16	1250	1250	4950
278	Heat flux (131 -140)	16	1250	1250	4950
279	Heat flux (151 -160)	16	50	1250	2500
280	1 - SHAR	99	-1	-1	-1
293	Gas density exh. pipe	91	-1	-1	-1
294	Gas density outlet N	91	-1	-1	-1
295	Gas density outlet S	91	-1	-1	-1
296	Gas density outlet C	91	-1	-1	-1

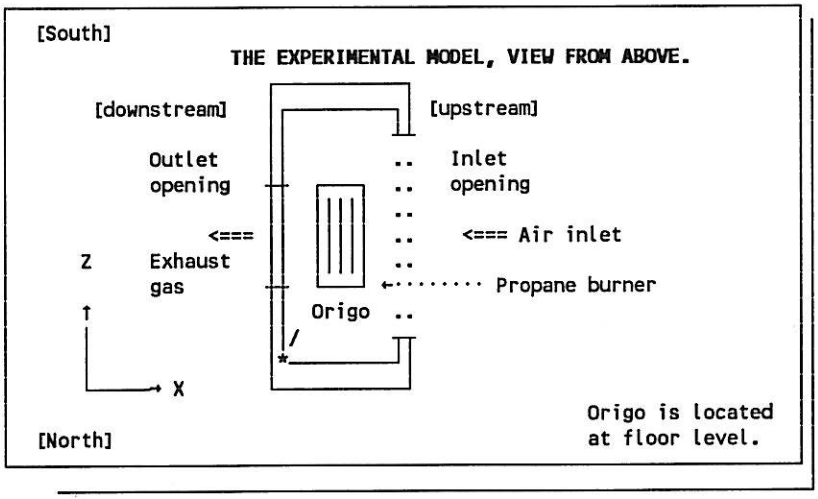

Figure B.3 *The coordinate system used to locate thermocouples and other measurement probes within the compartment. The Y - coordinate is going in the vertical direction and origo is located at the floor level. The * mark at the figure gives the location of origo in the X-Z plan. Actually, origo is placed 50 mm in the solid wall. South and north are used for directions along the Z-axes.*

B.3 FORMULAS USED

The calibration program needs the atmospheric pressure as the only environmental input for each experiment. The ambient temperature is logged by DAS. The channels are identified by a letter and a three digit number. The upper case letter C stands for channel and the three digits represent the channel number. Voltages are represented by the upper case letter E followed by the channel number. Temperatures are given as degrees Celsius by the logger. When they are used by M5, they are transformed to Kelvin degrees and symbolized by the upper case letter T, followed by the channel number. In all other cases the upper case letter is represented by its quantities.

```
C### - channel number ###
E### - voltage from measuring device, channel ###
T### - temperature in degrees Kelvin, channel ###
```

B.3.1 PRESSURE DIFFERENCES.

The velocities are measured by bidirectional probes connected to a pressure transmitter. Pressure difference is also measured between inside the model compartment and the ambient. Calibration is done by linear interpolation, by the subroutine CALLIN.
An example is shown, representing the velocity in the exhaust pipe, C_{181}.

P - pressure
g - gravitational acceleration
k_1 - calibration constant
E - voltage from pressure transmitter
k_0 - offset

$$P_{181} = (k_0 + k_1 \cdot E_{181}) \cdot g \qquad [Pa]$$

$g = 9.81$ $[m/s^2]$
$k_1 = 11.16$
$k_0 = -0.03$

Table B1 gives the calibration constants used by the subroutine CALLIN.

B.3.2 VELOCITY BASED ON BIDIRECTIONAL PROBE MEASUREMENTS.

Velocity is calculated from the pressure difference measured by a bidirectional probe and the gas density at the measurement position. An example is C_{241}, which is the velocity in the exhaust pipe. C_{241} is using the pressure calculated at C_{182} and T_{049} to predict the velocity in the exhaust pipe. The subroutine PROBE is a function defined under section B.4.3.

Table B II Calibration constants for pressure transmitters.

Channel No.	Pressure transmitter	Calibration factor	Offset
		k_1	k_0
181	PT 6	11.1625	-0.0256
182	PT 6F	11.0040	0.1492
187	PT 10	-62.9690	25.0544
194	PT 3	1.2360	-0.0131
195	PT 4	1.2500	0.0383
196	PT 5	12.0628	-0.1620
197	PT 7	1.0065	-0.0040
198	PT 9	1.0120	-0.0086
199	PT 8	1.0179	-0.0021

v - velocity
T - temperature
P_0 - atmospheric pressure

$v_{241} = \text{PROBE}(P_{182}, P_0, T_{049})$ [m/s]

B.3.3 CALCULATION OF VELOCITIES (PROBE)

Calculation of velocities is done by a subroutine named PROBE, which is based on the work done by B.J. McCaffrey and G. Heskestad, ref. /12/. The subroutine PROBE is developed by SINTEF/NBL. The subroutine uses the following algorithm:

ΔP	-	pressure across the bi-directional probe
ρ	-	gas density
v	-	velocity
Re	-	Reynolds' number
c_f	-	calibration coefficient
P_0	-	atmospheric pressure
R	-	gas constant
T	-	temperature
D	-	diameter of the bidirectional probe
$\nu(T)$	-	kinematic viscosity as a function of T

Calculation of the density ρ is given by ideal gas law.

$$\rho = P_0 / (R \cdot T)$$

$$R = 287 \quad [J/(kg \cdot K)]$$

Re is based on the diameter D equal to the diameter of the bidirectional probe.

$$Re = \frac{D \cdot v}{\nu(T)}$$

$$D = 16.0 \qquad [mm]$$

1st

When $Re < 40$,
$=> \; v = 0$

2nd When $40 \leq Re \leq 2740$,
$=>$

The absolute value of v is given by the following expressions, which are solved by Newton's equation solving method, ref. /13/.

$$\frac{\{2\Delta P/\rho\}^{1/2}}{v} = 1.533 - 1.366 \cdot 10^{-3} \; Re - 9.706 \cdot 10^{-10} \cdot \; Re^2 + 1.688 \cdot 10^{-6} \cdot Re^3$$

$$+ 2.555 \cdot 10^{-13} \cdot Re^4 - 2.484 \cdot 10^{-17} \cdot \; Re^5$$

$$v = \frac{Re \cdot \nu(T)}{D} \qquad [m/s]$$

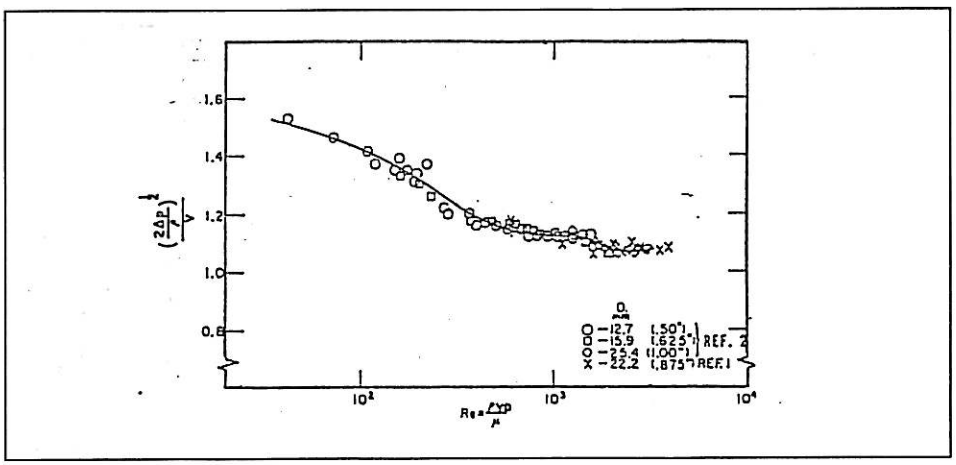

Figure B.4 The response of the bidirectional probe for various Reynolds' numbers. Ref. /11/.

3rd When Re > 2740,

=>

v is calculated by using the standard NT - FIRE 025, ref. /14/.

$$v = \left[\frac{2\,\Delta P}{\rho\, c_f} \right]^{1/2}, \quad c_f = 1.08$$

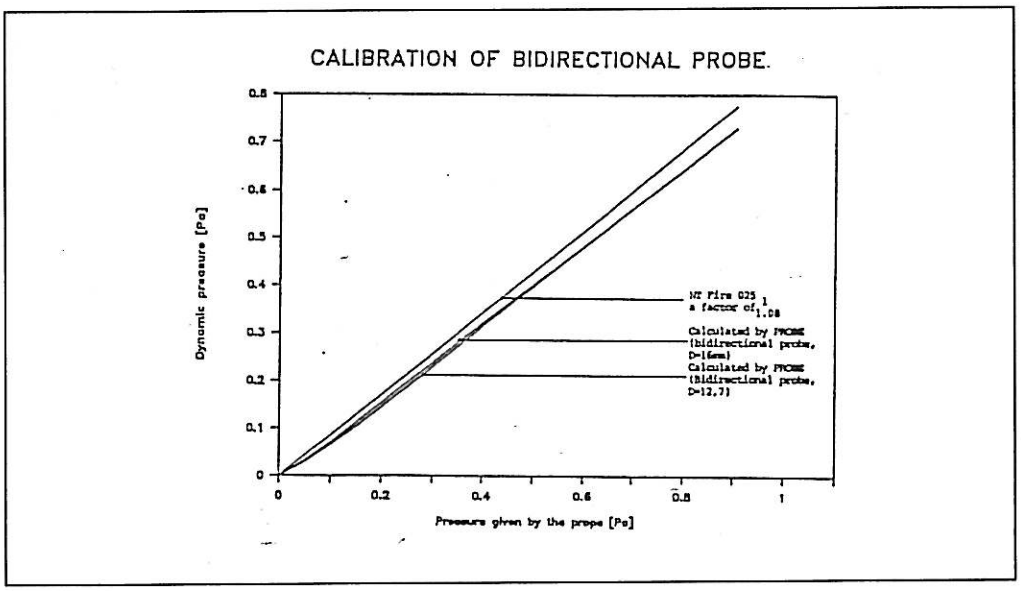

Figure B.5 The response of the PROBE function for various input pressures.

B.3.4 GAS CONCENTRATIONS

The oxygen concentration in the exhaust pipe, C_{183}, is measured by a gas analyzer, type SIEMENS OXYMAT 5T. Calibration is done by linear interpolation, by the subroutine CALLIN.

X - gas concentration
k_1 - calibration constant
k_0 - offset at ambient concentration
E - voltage measured by the gas analyzer

$$X_{183} = k_0 + k_1 \cdot E_{183} \qquad [vol.\%]$$

k_0 = 0.0251
k_1 = 8.7861

Carbon dioxide concentration in the exhaust pipe, C_{184}, is measured by a gas analyzer type URAS 7N. Calibration is done by the subroutine CALPOL, which performs a polynomial interpolation.

X - gas concentration
k_i - calibration constants
k_0 - offset at ambient concentration

$$X_{184} = k_0 + k_1 \cdot E_{184} + k_2 \cdot E_{184}^2 + k_3 \cdot E_{184}^3 \qquad [vol.\%]$$

$k_0 = -7.19 \cdot 10^{-3}$
$k_1 = 0.304$
$k_2 = 3.93 \cdot 10^{-3}$
$k_3 = 4.095 \cdot 10^{-3}$

Carbon monoxide concentration in the exhaust pipe, C_{185}, is measured by a gas analyzer type URAS 7N. Calibration is done by the subroutine CALPOL, which performs a polynomial interpolation.

X - gas concentration
k_i - calibration constants
k_0 - offset at ambient concentration

$$X_{185} = k_0 + k_1 \cdot E_{185} + k_2 \cdot E_{185}^2 \qquad [vol.\%]$$

$k_0 = 0$
$k_1 = 0.1408$
$k_2 = 0.0065$

Concentrations of oxygen at the outlet is measured by a gas analyzer of the type MAGNOS 5T. Carbon dioxide and carbon monoxide at the outlet opening are measured by gas analyzers of the type URAS 3G. Calibration is done by linear interpolation, by the subroutine CALLIN.

The calculation procedure is shown, and Table B3 represents the calibration constants for each channel.

X - gas concentration [vol%]
E - voltage from gas analyzer
k_1 - calibration constant
k_0 - offset at zero

$$X = k_0 + k_1 \cdot E \qquad [vol\%]$$

Table B III Calibration constants for gas analyzers.

Channel No.	Gas analyzer	Calibration factor	Offset
		k	b
191	A.a.0006	2.5965	-5.1515
192	A.a.0003	7.9279	-16.1727
193	A.a.0313	0.7183	-1.4621

B.3.5 LIGHT EXTINCTION BY SMOKE IN THE EXHAUST PIPE; C_{186}

The light extinction is measured by an optical device, of the MAURER ME-82 type, which measures the light extinction at an interval of wavelengths, as a fraction of the initial beam of light. The receiver is equipped with a filter adjusted to the sensitivity to the human eye.

I - transmitted intensity
I_0 - initial transmitted intensity
f - fraction

$f_{186} = E_{186} = I/I_0$

B.3.6 SOOT PRODUCTION RATE BY OPTICAL DENSITY; C_{247}.

Particulate generation method is coupled with use of a monochromatic extinction measurement of smoke in the exhaust pipe. When a monochromatic beam of light passes through smoke, the fraction of light transmitted can be expressed with the following notations:

I - transmitted intensity
I_0 - initial transmitted intensity
τ_λ - extinction coefficient of smoke
L - optical path length

$I/I_0 = e^{(-\tau\lambda L)}$

This quantity is measured directly by the optical measuring device at channel 186.

$\tau_\lambda = - \ln(I/I_0) / L = - \ln(E_{186}) / L \qquad [m^{-1}]$

The particulate mass concentration of soot can be estimated with an average variation

about ± 20 %. ref./14/. The term is written as follows:

$\bar{c}$ - average coefficient of particulate extinction
λ - wavelength [μm]
ρ_s - density of soot [g/m^3]

$$\dot{V}_{pipe} = c_e \cdot A_e \cdot v_{241}$$

c_e - calibration factor for the measured velocity
A_e - cross area of exhaust pipe

$$\dot{m}_{274} = \frac{\rho_s \cdot \lambda \cdot \tau_\lambda}{\bar{c}} \cdot \dot{V}_{pipe} \quad [g/s]$$

ρ_s	$= 1.1 \cdot 10^6$	[g/m^3]
λ	$= 0.555$	[μm]
$\bar{c}$	$= 7.0$	
L	$= 1.0$	[m]
c_e	$= 0.93$	
A_e	$= 0.785$	[m^2]

B.3.7 WATER PRESSURE AND MASS RATE, C_{200} AND C_{201}.

Water flow into the spray system is measured by the pressure at the floor level. Water flow out of the model compartment is measured by collecting the run-off water in a reservoir, placed upon a weighing platform. The weight is logged continuously.

A special subroutine called CAL200 is created to calibrate the water flow.First step is to calculate the pressure at C_{200} by linear interpolation.

P_{atm} - atmospheric pressure the actual day of the experiment
P_{200} - pressure
E_{200} - voltage from pressure transmitter
k_0 - offset at zero
k_1 - calibration constant

$$P_{200} = k_0 + k_1 \cdot E_{200} \qquad [Pa]$$

$$k_0 = 0.2680 \cdot P_{atm}$$
$$k_1 = -1.503 \cdot P_{atm}$$

This pressure is averaged over the period when water is on in the experiment, and is written to an information file during the execution of the calibration program M5. To find the pressure at the level of the nozzle, the water gauge from the floor level to the nozzle is subtracted from the logged value. For ceiling mounted nozzles this difference is about 2 [m], corresponding to a pressure difference of ≈0.2 [bar].

For each test the correlation between the measured water pressure and the mass rate is established by the subroutine. The water is allowed to flow for 10 minutes after the fire has been extinguished, and the correlation between the water pressure and the mass rate is established by linear regression analysis for all data in a period 1 minute after FIROFF to WATEROFF. FIROFF is defined as the time when the propane flow, C_{214}, is reduced to zero. WATEROFF is the time when the water pressure at the floor level is reduced to approximately zero, after the experiment.

The water flow out of the model compartment is logged by a weighing cell, which is calibrated by linear interpolation.

m_{201} - mass of the water reservoir
k_0 - offset at zero load of water reservoir
k_1 - calibration constant of weighing cell
E_{201} - Voltage from weighing cell

$$m_{201} = k_0 + k_1 \cdot E_{201} \qquad [kg]$$

k_0 = -27.3061
k_1 = 319.0746

The flow of water is then calculated as the weight difference from one time step to another, divided by the length of the time step. This is done by the subroutine CALDIF.

The water flow out of the model compartment has a time delay compared to the flow in. This time delay is found to be 61 [s], from various experiments. The flow of water into the model is shifted in time, to compensate this time delay. This is done by a subroutine TIMELAG.

The water flow into the model is then calculated from the pressure P_{200}, by the correlation found by the regression analysis, and is written to C_{200}. To restore the pressure at C_{200} the raw data file has to be used.

B.3.8 PROPANE CONSUMPTION , C_{202}.

To get a reliable calibration of propane consumption, the supply tank was weighed by a weighing cell in some of the experiments. The calibration of the weighing cell is done by linear interpolation, but is not included in the program M5.

m_{202} - mass of the propane tank
k_0 - offset at zero load of weighing cell
k_1 - calibration constant of weighing cell
E_{202} - Voltage from weighing cell

$$m_{202} = k_0 + k_1 \cdot E_{202} \qquad [kg]$$

k_0 = -12.6569
k_1 = 200.7987

The flow of propane is then calculated as the weight difference from one time step to another, divided by the length of the time step. This is done by the subroutine CALDIF.

B.3.9 PROPANE FLOW MEASURED BY FLOWMETERS

C_{211}, the propane temperature, $[T_{211}]$, is converted from voltage measured by a PT 100 resistance thermometer, by linear interpolation by the subroutine CALLIN.

T_{211} - propane temperature [K]
k_0 - offset at calibration temperature
k_1 - calibration constant
E_{211} - Voltage from the thermometer

$T_{211} = k_0 + k_1 \cdot E_{211}$ [K]

$k_0 = 80.0$
$k_1 = 243.0$

The propane pressure in the flowline is measured by a pressure transmitter. The conversion from voltage to pressure is done by linear interpolation, by the subroutine CALLIN.

P_{atm} - atmospheric pressure measured the day of the experiment
P_{212} - propane pressure
k_0 - offset at zero
k_1 - calibration constant
E_{212} - Voltage from thermometer

$P_{212} = (k_0 + k_1 \cdot E_{212}) P_{atm}$ [K]

The pressure transmitter was recalibrated 1989-09-04, and different values for the calibration is valid for experiments before and after that date.

Before 1989-09-04

$k_0 = 0.0$
$k_1 = 7.09$

After 1989-09-04

$k_0 = 0.00306$
$k_1 = 4.498$

The flow of propane is measured by two parallel flowmeters, which are part of the fixed propane supply system of the laboratory. The conversion from voltage to mass flow is done by a procedure described by the producer of the equipment, and by calibration from total propane consumption measured by weighing cell. The calibration factor a is given by the producer, and the factor c is found by laboratory calibration.

$\dot{m}_{213} = a \cdot c \cdot [(P_{212}/T_{211})]^{1/2} \cdot (E_{213} - b)$

$a = 0.919 \cdot 1.868 \cdot 10^{-2}$
$b = E_{213}$ at the first time step of the measurement
$c = 0.8929$

$\dot{m}_{214} = a \cdot c \cdot [(P_{212}/T_{211})]^{1/2} \cdot (E_{214} - b)$

$a = 0.9509 \cdot 9.334 \cdot 10^{-2}$

b = E_{214} at the first time step of the measurement
c = 0.8929

B.3.10 HEAT FLUX DENSITY BY MEDTHERM FLUXMETERS

Heat flux density is measured in 5 positions by total fluxmeters of the MEDTHERM 64-10-18 type. The fluxmeters are cooled by circulation of water at an inlet temperature about 30 [°C]. The conversion from measured voltage to heat flux density is done by linear interpolation by the subroutine CALLIN.

$\dot{q}$ - heat flux density
k_0 - offset at zero heat flux
k_1 - calibration constant
E - Voltage from heat flux meter

$$\dot{q} = k_0 + k_1 \cdot E \qquad [kg]$$

The calibration is done in a calibration furnace with a black body radiation source at a temperature range from ambient to 1100 [°C]. The calibration factors are given in Table B4.

Table B IV Calibration factors for the MEDTHERM heat flux meters

Channel No.	Heat flux meter	Calibration factor	Offset
		k_1	k_0
215	HF 1	$1.1959 \cdot 10^7$	$-3.1702 \cdot 10^3$
216	HF 2	$1.1749 \cdot 10^7$	$-4.1157 \cdot 10^3$
235	HF 3	$1.2089 \cdot 10^7$	$-3.4415 \cdot 10^3$
236	HF 4	$1.2040 \cdot 10^7$	$-1.6059 \cdot 10^3$
240	HF 5	$1.2090 \cdot 10^7$	$-1.0236 \cdot 10^3$

B.3.11 HEAT FLUX MEASUREMENTS BY STEEL CALORIMETERS

The total heat flux measurements have been done by steel calorimeters specially made for this type of fire loads. Two of the calorimeters are located close to a MEDTHERM heat flux meter, central at the south wall of the model compartment. One calorimeter is located central at the rear wall, close to the flames from the propane burner.

The calorimeters are steel bars, with 20 mm diameter, 354 mm long, insulated with gypsum, placed in a pipe with inner diameter ≈ 60 mm. The steel bars are instrumented with 10 thermocouples, spaced with 10 mm at one end, increased to 50 and 100 mm towards the other end.

The measurement principle is to measure temperature differences in a steel bar, where the heat conduction is one dimensional. From the basic equations for heat transfer, the heat flux can be determined when the thermal properties of the materials are known. Two types of steel have been used, one normal construction steel, and a stainless steel. Thermal properties for the steel types are based on universal data, temperature dependent,/15/. The specific conductivity of the two types of steel is quite different, but the specific heat capacity is quite similar.

The subroutine TEMPRO contains an algorithm used to solve the one dimensional heat conduction problem :

The steel bar is divided into control volumes representing the parts between two thermocouples.This is shown in Figure B 6.

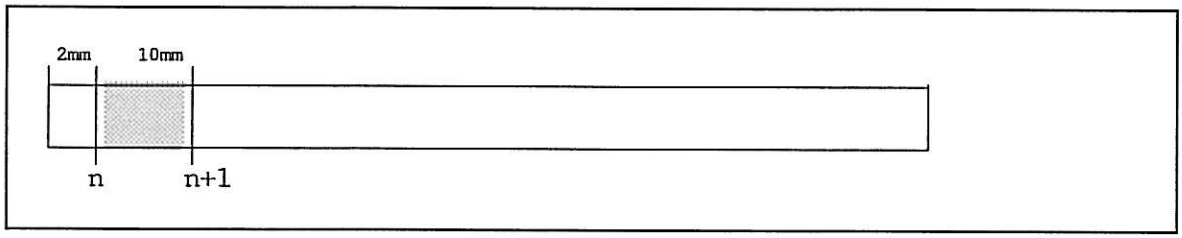

Figure B.6. A steel calorimeter, with indications of location of two thermocouples. The marked area represents the control volume. The steel bar is insulated and supported in a steel pipe of 60 [mm] diameter.

The heat balance for this control volume is calculated for each time step. In the fire tests the logging interval was 10 s. The heat input to the control volume will partly increase the internal heat, and partly be conducted to the next control volume.These two parts are calculated individually for each time step, and added.

$$\dot{q}''_t = \dot{q}''_{cond} + \dot{q}''_{acc}$$

The equation for the i'th time step is:

$$\dot{q}''_{t,i} = k/L \cdot (T_{n+1} - T_n)_i + L \cdot \rho_s \cdot c_p \cdot \Delta T_m / \Delta t$$

$$\Delta T_m/\Delta t = \{\cdot [(T_{n+1} + T_n)_{i+1} - (T_{n+1} + T_n)_{i-1}]\}/2 \cdot \Delta t$$

where

$\dot{q}''_{t,i}$ is the total heat flux density for the i'th time step [kW/m^2]
k is the thermal conductivity [kJ/m K]
L is the distance between thermocouple n and n+1 [m]

T_n	is the temperature of thermocouple n	
T_{n+1}	is the temperature of thermocouple n+1	
ρ_s	is the density of the steel	[kg/m^3]
c_p	is the specific heat capacity of the steel	[kJ/kg K]
ΔT_m	is the mean temperature difference of the control volume in the time from (i-1)'th to (i+1)'th time step	
Δt	is the time step	[s]

subscript:

i	is the time step number
n	is the thermocouple number

The thermal properties of steels used in the calorimeters are shown in Table B 4 and B 5, and in Figure B 7 and B 8. The resulting heat flux density represents the heat flow through the steel bar. Since the surface temperature of the steel bar is measured, an estimate of the total heat flux density can be found, assuming a surface emissivity.

Table B 4 Thermal properties of stainless steel, AISI 304, /15/.

Temp. [K]	k [W/m K]	c_p [kJ/kg K]
273.15	14.7	0.494
373.15	16.6	0.510
473.15	18.0	0.536
573.15	19.4	0.552
673.15	20.8	0.569
773.15	22.1	0.594
873.15	23.5	0.653
973.15	24.9	0.628
1073.15	26.3	0.644
1173.15	27.7	0.644
1273.15	29.1	0.653
1373.15	30.5	0.661
1473.15	31.9	0.669
1573.15	33.3	0.678
1673.15	34.8	0.678

ρ_s = 8000 [kg/m^3] at 288 [K]

Table B 5 Thermal properties of construction steel, St 37.2, DIN 17100 (approximated by AISI 1026) /15/.

Temp. [K]	k [W/m K]	c_p [kJ/kg K]
273.15	51.8	0.469
373.15	51.0	0.485
473.15	48.6	0.519
573.15	44.4	0.552
673.15	42.6	0.594
773.15	39.3	0.661
873.15	35.6	0.745
973.15	31.8	0.845
1073.15	28.5	1.431
1173.15	25.9	0.954
1273.15	26.4	0.644
1373.15	27.2	0.644
1473.15	28.5	0.644
1573.15	29.7	0.661
1673.15	29.7	0.686

ρ_s = 7860 [kg/m^3] at 288 [K]

The heat flux measured by the calorimeters is the net heat flux absorbed by the surface of the probes. Since the conductivity of the stainless steel is less than the construction steel, the surface temperature of the stainless steel probe will be higher. The net heat flux to this calorimeter will the be less, since both convective and radiative heat flux are reduced with increased surface temperature, provided the same initial environment.

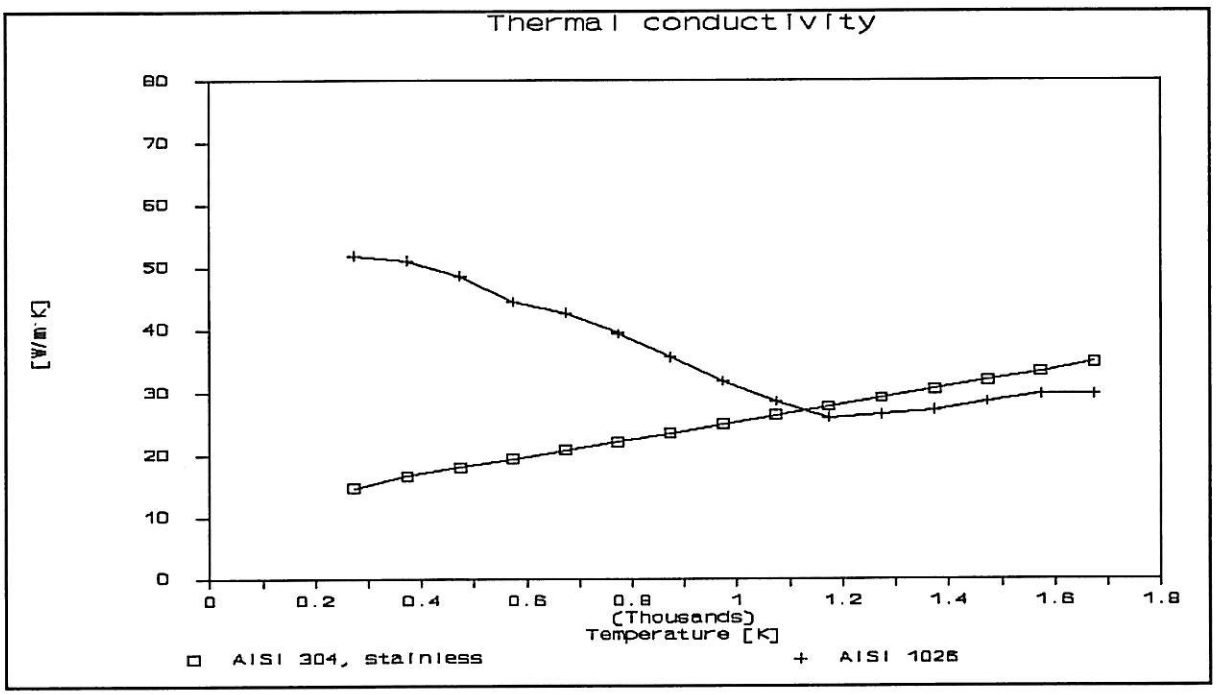

Figure B 7 *Thermal conductivity for the steels used in calorimeters, /15/*

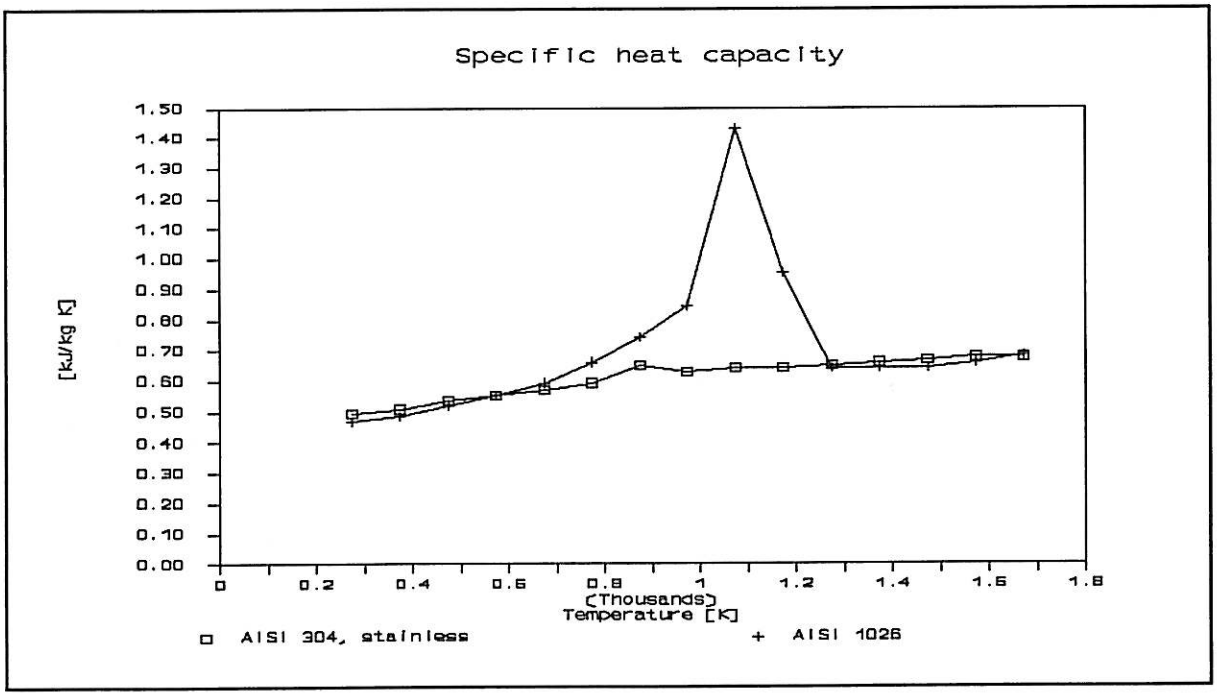

Figure B 8 *Specific heat capacity for the steels used in calorimeters, /15/*

As shown in Figures B 7 and B 8, the thermal conductivity of the two types of steel differ much both in trend and quantity. There is also a step in the specific heat capacity of the construction steel, starting at about 800 [K]. The thermal data for stainless steel are more steady in the temperature regions measured by the calorimeters in the tests, and are the most reliable.

B.3.12 THE HEAT RELEASE RATE FROM THE FIRE; C_{242}

The heat release is calculated by two different methods. C_{242} is using the oxygen consumption method and $C_{244}$is using the fuel supply rate. The heat release represented by C_{242} is measured in the exhaust pipe. The oxygen consumption technic is using a volume flow. This flow is here the exhaust pipe flow. The volume flow estimation is based on the velocity calculated at C_{241}. The velocity profile is approached by across measuring the velocities normal to the exhaust pipe. The calibration is done with air at ambient condition and the profile is assumed to keep the same shape with exhaust gases. The coefficient c_e for the mean velocity and the central velocity in the exhaust pipe is estimated to 0.93.

The temperature profile is measured by four thermocouples, each representing a concentric circle. The mean temperature T_e is expressed by:

$$T_e = (0.149 \cdot T_{046} + 0.304 \cdot T_{047} + 0.283 \cdot T_{048} + 0.049 \cdot T_{049}) / A_e$$

V_0 represent the volume flow in the exhaust pipe normalized to the ambient temperature T_0 = 20 [°C].

$$V_0 = c_e A_e v_{241} \cdot (T_0/T_e) \quad [m^3/s]$$

T_0 = 298.0 [K]
c_e = 0.93

A_e - cross section area of exhaust pipe = 0.785 $[m^2]$

The expression for the heat release Q_e (exhaust) is now available with the following parameters given, ref /14/.

α	-	expansion factor due to chemical reaction of the air that is depleted of it's oxygen
E^1	-	heat release per unit volume of oxygen consumed
x^{O2}	=	X_{183} / 100 - volume fraction of oxygen
x^{CO2}	=	X_{184} / 100 - volume fraction of carbon dioxide
Q_e	-	heat release rate [J/s]

$$Q_e = E^1 V_0 \left[\frac{\alpha - 1}{x_0^{O2}} + \frac{\left(1 - \frac{x^{O2}}{1 - x^{CO2}}\right)}{\left(x_0^{O2} - \frac{x^{O2}}{1 - x^{CO2}}\right)} \right]^{-1}$$

$E^1 = 17.2 \cdot 10^6$ [J/m^3]
$\alpha = 1.1$

B.3.13 THE FUEL SUPPLY RATE; C_{243}.

C_{243} is calculated as the sum of the mass flow of both propane supply branches, C_{213} and C_{214}.

$\dot{m}_{243} = \dot{m}_{213} + \dot{m}_{214}$

B.3.14 THE HEAT RELEASE RATE BY FUEL; C_{244}.

The heat release based on fuel supply rate is simply done by multiplication of the fuel supply rate by the specific heat of combustion of propane,

$Q_{244} = \Delta H_c \cdot \dot{m}_{243}$ [W]

ΔH_c - Heat of combustion = 46330 [J/g]

B.3.15 TOTAL HEAT RELEASED BASED ON THE OXYGEN CONSUMPTION TECHNIQUE; C_{245}.

Channel 245 is a time integration of the heat release rate at each time step, presented at channel 242.

N - actual number of time step to reach elapsed time.

$$Q_{N,245} = \sum^{i=1,N} (Q_{i,242} \cdot \Delta t) \quad [J]$$

B.3.16 TOTAL HEAT RELEASED BY THE FUEL; C_{246}.

Channel 246 is a time integration of the heat release rate at each time step, presented at C_{244}.

N - actual number of time step to reach elapsed time.

$$Q_{N,246} = \sum_{i=1,N} (Q_{i,244} \cdot \Delta t) \quad [J]$$

B.3.17 MASS FLOW AT THE OUTLET OPENING; C_{248}.

The outlet opening is instrumented by three bidirectional probes with connected thermocouples to estimate the mass flow. The velocities are already calculated at channels 194 - 196. At channel 248 each probe represents distinctive parts of the outlet area. When the mean flow is calculated, it is based on the weighed average. The orifice factor is estimated by comparison of the forced air inlet and the outlet response/2/. The factor is influenced by the actual location of the probes at the outlet. The outlet mass flow is calculated by the subroutine VELCAL which calculates the mass flow through three parts of the opening. The velocity is measured by the corresponding bi-directional probe, calibrated by the subroutine PROBE. The actual gas density at the probe is separately calculated by ideal gas law, using the measured temperature at the probe. The subroutine VELCAL is prepared to take evaporated water into account, but this is disregarded in these experiments.
The area of the three parts of the outlet opening is:

North :	0.256	[m^2]
Centre:	0.171	[m^2]
South :	0.265	[m^2]

The orifice factor found by earlier tests with cold air, is 0.8, /1/.

B.3.18 HEAT RELEASE RATE AT THE OUTLET; OPENING C_{249}.

The heat release rate at the outlet opening is based on the oxygen consumption method. The gas concentrations at the outlet are measured by gas analyzers, and the gas is taken at three suction points joined together to one flowline. The heat release rate is calculated by the same formula as used at C_{242}, ref./13/.

B.3.19 THE AVERAGE GAS TEMPERATURE; C_{250}.

The average gas temperature is the mean value of all the thermocouples in the gas phase within the compartment. The calculation does not concern whether thermocouples are located in the flames, hot gas layer or in colder inflowing air.

$$C_{250} = \frac{\sum_{j=1,9} C_j + \sum_{j=61,100} C_j}{(9 + 40)} \qquad [°C]$$

B.3.20 HEAT FLUX TO THE FLOOR, C_{256}.

The heat flux to the floor is based on the heat absorbed by the corrugated steel plates only. Control of temperature rise of the materials below the plates show that there is only a small error introduced by this simplification. The algorithm for calculation is to divide the plates into 15 section of equal area. The temperature of one area is represented by one thermocouple in the middle of the area. The floor is assumed to be symmetrically exposed, and the temperatures in one half of the floor represents the other half. The calculated heat transferred to the floor is done by the subroutine HEFLOO.

$\dot{q}_{floor}$ - heat flux to the floor
m_{floor} - mass of the steel plates
cp_{steel} - specific heat capacity of the steel plates
ΔT_{mean} - mean temperature difference from one time step to another
Δt - time step length

$$\dot{q}_{floor} = (m_{floor} \cdot cp_{steel} \cdot \Delta T_{mean})/\Delta t \qquad [W]$$

$$\Delta T_{mean} = [2 \cdot \sum_{j=141}^{146} (T_{i,j} - T_{i-1,j}) + \sum_{j=147}^{149} (T_{i,j} - T_{i-1,j})]/15$$

m_{floor} = 90 [kg]
cp_{steel} = 476 [kJ/kg]
Δt = 10 [s]
i = time step number
j = channel number

B.3.21 HEAT TO THE CEILING, C_{257}

The heat transfer to the ceiling is represented by measurements by two calorimeters, one of the MEDTHERM type and a steel calorimeter. The ceiling is divided into two sectors, one which is affected by flame impingement, and the rest. The heat flux is calculated for each sector separately, and then added. This is done by the subroutine HECEIL.
The sector not impinged by flames is represented by the heat flux probe positioned in the ceiling, C_{240}. The area of this section is estimated to be 90% of the total area, A_1. The heat flux probe located at the rear wall, C_{279}, represents the rest of the ceiling, 10% of the total area.

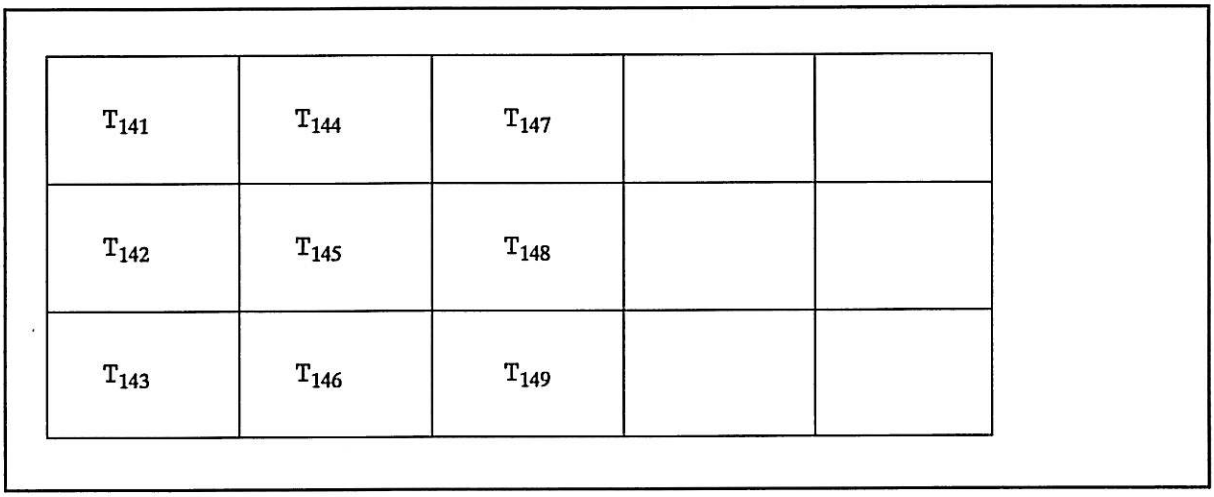

Figure B 9 *Distribution of the temperature measurements at the floor of the model compartment.*

$$\dot{q}_{257} = 0.9 \cdot A_4 \cdot C_{240} + 0.1 \cdot A_4 \cdot C_{279} \qquad [W]$$

$\dot{q}_{257}$- heat transferred to the ceiling
A_1 - area of the ceiling, 11.76 [m^2].

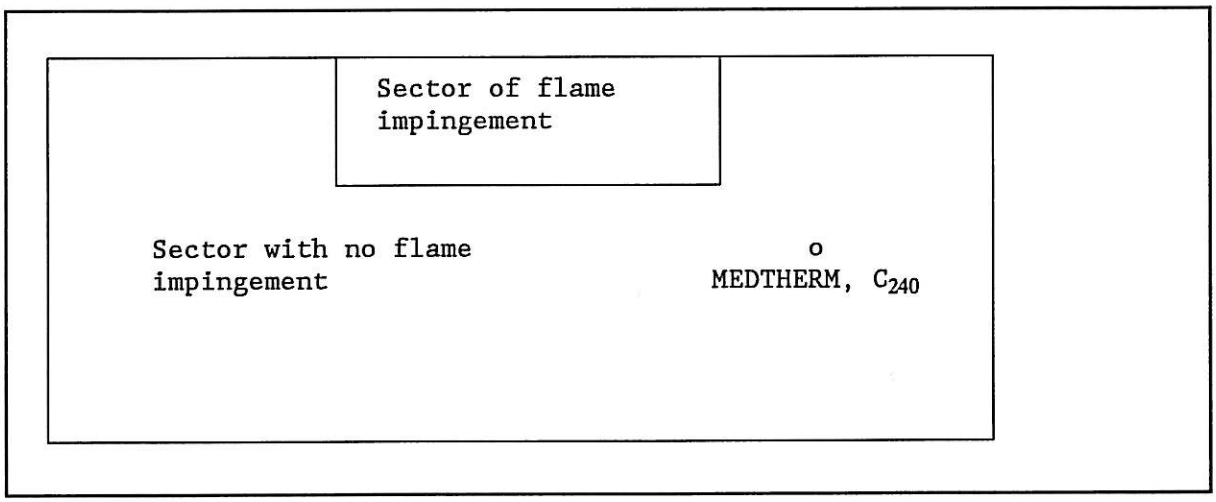

Figure B 10 *Plan view of the ceiling of the model compartment, with the position of the heat flux meter indicated.*

B.3.22 HEAT TO THE WALLS, C_{258}

The heat transfer to the walls is measured by 4 calorimeters of the MEDTHERM type, and one steel calorimeter. The heat to the north wall is assumed equal to the south wall, due to symmetry. The heat flux is calculated for each wall separately, and then added. This procedure is done by the subroutine HEWALL.

South wall = north wall

The upper part of the wall is represented by the heat flux probe positioned central in the wall, C_{215}. The area of this section is estimated to be 80% of the total area, A_1. The heat flux probe located 0.25 [m] above the floor level, C_{216}, represents the lower part of the wall, 20% of the total area. The total area A_1 is 5.64 [m^2].

$\dot{q}_1$ - heat transferred to the south wall
A_1 - area of the south wall, 5.64 [m^2].

$$\dot{q}_1 = 0.8 \cdot A_1 \cdot C_{215} + 0.2 \cdot A_1 \cdot C_{216} \qquad [W]$$

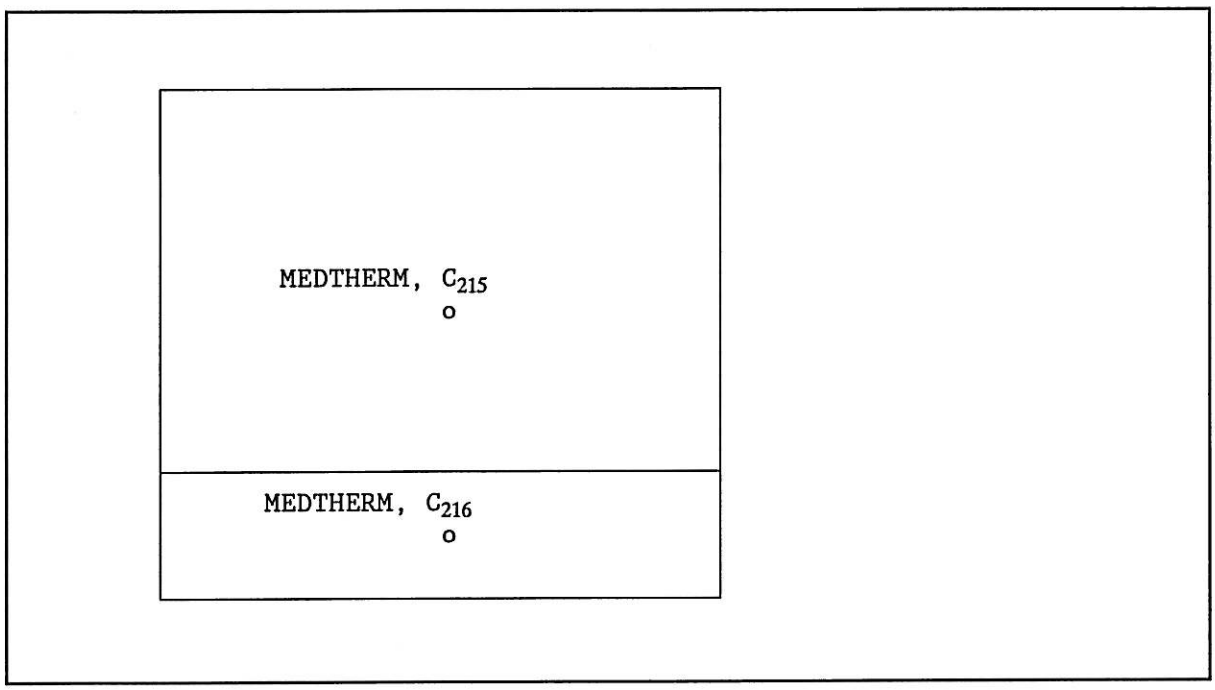

Figure B 11 Plan view of the south wall, with the heat flux meters located.

Front wall

The heat transferred to the front wall is measured by two heat flux meters, of the type MEDTHERM.

The front wall is divided into 3 sections of equal area. The central part is represented by the heat flux density measured by C_{235}, and the two parts on the sides are represented by C_{236}.

$\dot{q}_2$ - heat transferred to the front wall
A_2 - area of the front wall, 10.20 [m^2].

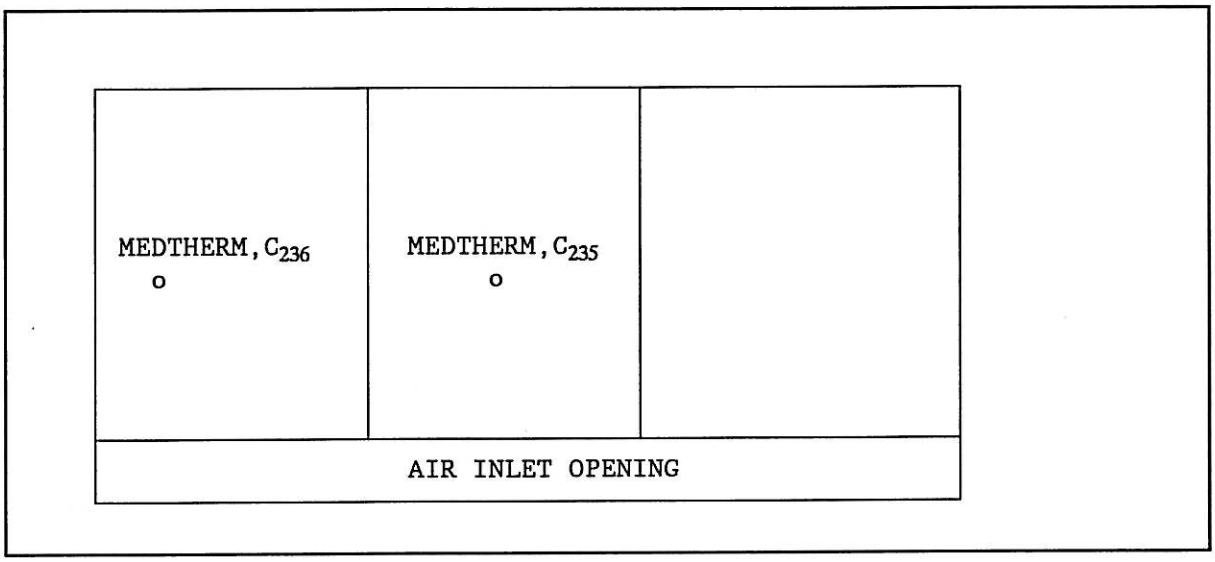

Figure B 12 Plan view of the front wall, seen from inside. The positions of the heat flux meters are indicated.

$$\dot{q}_2 = A_2/3 \cdot C_{235} + 2/3 \cdot A_2 \cdot C_{236} \qquad [W]$$

Rear wall

The heat transferred to the rear wall is represented by the heat flux meters at the south wall, and by the steel calorimeter located central at the rear wall.
The rear wall is divided into 3 sections. The central part is represented by the heat flux density measured by C_{279},and the two parts on the sides are represented by $C_{215}$and C_{216}.

$\dot{q}_3$ - heat transferred to the rear wall
A_3 - area of the rear wall, 9.44 [m^2], divided into a central part of 2.7 [m^2], and two side areas of 3.37 [m^2] each.

$$\dot{q}_3 = (0.8 \cdot C_{215} + 0.2 \cdot C_{216}) \cdot 2 \cdot 3.37 + C_{279} \cdot 2.7 \qquad [W]$$

Total heat transferred to the walls: $\dot{q}_{258} = \dot{q}_1 + \dot{q}_2 + \dot{q}_3$

B.3.23 HEAT TO THE RUN OFF WATER, C_{259}

The heat transferred to the run off water is calculated by the mass flux multiplied with the temperature difference and the specific heat capacity of water. This is done by the subroutine HEWATER.

$\dot{q}_{water}$ - heat transferred to the run off water

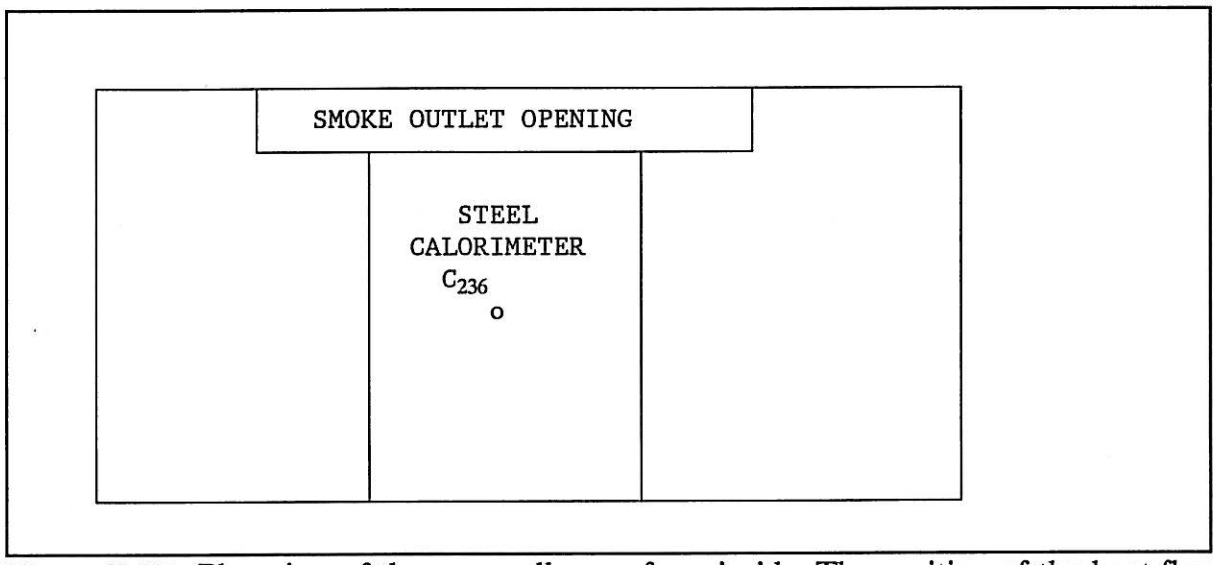

Figure B 13 Plan view of the rear wall, seen from inside. The position of the heat flux meter is indicated.

m_{water} - mass flux of water out of the model compartment
cp_{water} - specific heat capacity
ΔT_{water} - temperature difference

$$\dot{q}_{water} = m_{water} \cdot cp_{water} \cdot \Delta T_{water}$$

$m_{water} = C_{201}$ [g/s]
$cp_{water} = 4.185$ [J/(g·°C)]
$\Delta T_{water} = C_{225} - C_{224}$ [°C]

B.3.24 VENTILATED HEAT, C_{260}

The heat transferred to the ambient through to outlet opening is calculated assuming ideal gas. The smoke is assumed to have the properties of air. The amount of water in the smoke after activation of the spray is neglected, since the most important characteristics of the fire is measured before spray action. The calculation of the heat flow through ventilation is done by the subroutine HEVENT.
The mass flow at the outlet is calculated as a sum of weighted flows at three sections represented by velocity and temperature. The temperature of the inlet air is also weighted in the same way.

The formula is:

$$\dot{q}_{260} = m_{248} \cdot c_{pair} \cdot \{(A_{1out} \cdot T_{221} + A_{2out} \cdot T_{222} + A_{3out} \cdot T_{223})/A_{out} - (A_{1in} \cdot T_{55} + A_{2in} \cdot T_{56} + A_{3in} \cdot T_{57})/A_{in}\}$$

$$c_{pair} = 1.0 \quad [J/(g \cdot °C)]$$

$A_{1out} = 0.256 \ [m^2]$
$A_{2out} = 0.171 \ [m^2]$
$A_{3out} = 0.256 \ [m^2]$
$A_{out} = 0.683 \ [m^2]$
$A_{1in} = A_{2in} = A_{3in}$
$A_{in} = A_{1in} + A_{2in} + A_{3in}$

B.3.25 CALCULATION OF EVAPORATED WATER, C_{276}

The mass rate of water evaporated is calculated as the difference between the water flow into the system and the run off water.

$\dot{m}_{276} = \dot{m}_{200} - \dot{m}_{201}$

Some of the water will be accumulated in the model itself, since the water which hits the walls may flow outside the steel plates of the floor. This amount of water will be registered as evaporated water, even if it is not true. However, when the water spray is introduced into a preheated compartment, most of the water will evaporate immideately, and the remaining water will run off and will be collected. The calculation of evaporated water accounts for droplets leaving the outlet opening without being evaporated. The water mass flow is then relevant, but the heat balance may suffer from the inaccuracy.

B.3.26 CALCULATION OF SPRAY HEAT ABSORBTION RATIO, C_{280}

The final calculation done by the program M5 is to compute the ratio between the heat absorbed by the walls, the floor, the ceiling and the ventilated air, versus the heat release rate of the fire, characterized by the fuel consumption rate. The calculation is done by the subroutine SHAR.

$$1 - SHAR = C_{280} = (C_{256} + C_{257} + C_{258} + C_{260})/C_{244}$$

The value of 1-SHAR appeared to be less than zero before the spray was activated, which means that some of the assumptions made was incorrect. Analysis of the heat transfer shows a very high sensitivity on the heat flux to the walls. The assumption made that the heat flux density to the wall sections is evenly distributed with the value measured by the heat flux probes seem to be the reason for over estimating the heat flux to the walls. The value of SHAR was therefor post calculated by means of spread sheet operation, and the heat transferred to the walls was reduced to 60% of its originally calculated value. The SHAR then came out to be close to zero just before spray activation in almost all experiments.

The formula for SHAR presented in the report is:

$$SHAR = 1 - C_{280corr} = 1 - (C_{256} + C_{257} + 0.6 \cdot C_{258} + C_{260})/C_{244}$$